

Supporting Information

Structures and Absolute Configurations of Phomalones from Coral-associated fungus *Parengyodontium album* sp. SCSIO 40430

Lu Wang,^{‡a,b} Yanbing Huang,^{‡a,f} Liping Zhang,^{a,c} Zhiwen Liu,^{a,c} Wei Liu,^{a,c} Huixin Xu,^{a,b} Qingbo Zhang,^{a,c} Haibo Zhang,^{a,c} Yan Yan,^{a,b,c} Zhiyong Liu,^c Tianyu Zhang,^e Wenjun Zhang,^{*a,b,c} Changsheng Zhang^{*a,b,c,d}

^aKey Laboratory of Tropical Marine Bio-resources and Ecology, Guangdong Key Laboratory of Marine Materia Medica, Innovation Academy of South China Sea Ecology and Environmental Engineering, South China Sea Institute of Oceanology, Chinese Academy of Sciences, Guangzhou 510301, China.

^bUniversity of Chinese Academy of Sciences, Beijing 100049, China.

^cSouthern Marine Science and Engineering Guangdong Laboratory (Guangzhou), Guangzhou 511458, China.

^dSanya Institute of Oceanology, SCSIO, Yazhou Scientific Bay, Sanya 572000, China.

^eTuberculosis Research Laboratory, State Key Laboratory of Respiratory Disease, Guangzhou Institutes of Biomedicine and Health, Chinese Academy of Sciences, Guangzhou 510530, China; Guangdong-Hong Kong-Macao Joint Laboratory of Respiratory Infectious Disease, Guangzhou 510530, China;

^fGuangxi Key Laboratory of Marine Natural Products and Combinatorial Biosynthesis Chemistry, Beibu Gulf Marine Research Center, Guangxi Academy of Sciences, Nanning 530007, China;

[‡] These authors contributed equally to this work.

Electronic Supplementary Information (ESI) available: [details of any supplementary information available should be included here]. See DOI: 10.1039/x0xx00000x

*Corresponding author: wzhang@scsio.ac.cn or czhang@scsio.ac.cn

EXPERIMENTAL SECTION.....	S4
General Experimental Procedures.....	S4
Screening and Fermentation.....	S4
Extraction and Isolation.....	S4
The Quantum Chemical Electrostatic Circular dichroism (ECD) Calculation.....	S8
X-ray Crystallographic Analysis.....	S8
Chiral HPLC Analysis.....	S9
Mosher's MTPA Esters 5b.....	S9
Biological Assays.....	S9
Table S1. The ¹ H and ¹³ C NMR Data for 1-4	S11
Table S2. Crystal data and structure refinement for 2	S12
Table S3. Crystal data and structure refinement for 3	S13
Table S4. Crystal data and structure refinement for 4	S14
Table S5. $\Delta\delta^{SR}$ (ppm) data for the <i>S</i> - and <i>R</i> -MTPA- 5b Mosher esters in methanol- <i>d</i> ₄	S15
Table S6. Crystal data and structure refinement for 7	S16
Table S7. Crystal data and structure refinement for 8	S17
Table S8. The ¹ H (500 MHz) and ¹³ C (125 MHz) NMR Data for 12-15 . ⁵⁻⁷	S18
Table S9. The ¹ H (500 MHz) and ¹³ C (125 MHz) NMR Data for 16⁷ in DMSO- <i>d</i> ₆	S19
Figure S1. Spectroscopic data for 1	S20
Figure S2. Chiral-phase HPLC analyses of compound 1	S26
Figure S3. Spectroscopic data for 2	S27
Figure S4. Chiral-phase HPLC analyses of compound 2	S33
Figure S5. Spectroscopic data for 3	S34
Figure S6. Chiral-phase HPLC analyses of compound 3	S40
Figure S7. Spectroscopic data for 4	S41
Figure S8. Chiral-phase HPLC analyses of compound 4	S47
Figure S9. Spectroscopic data for 5	S48
Figure S10. Chiral-phase HPLC analyses of compound 5	S54
Figure S11. Spectroscopic data for <i>S</i> - and <i>R</i> -MTPA esters of 5b	S55
Figure S12. Spectroscopic data for 6	S57

Figure S13. Chiral-phase HPLC analyses of compound 6	S63
Figure S14. Spectroscopic data for 7	S64
Figure S15. Chiral-phase HPLC analyses of compound 7	S70
Figure S16. Spectroscopic data for 8	S71
Figure S17. Spectroscopic data for 8Ac	S77
Figure S18. Chiral-phase HPLC analyses of compound 8Ac	S80
Figure S19. Spectroscopic data for 9	S81
Figure S20. Spectroscopic data for 10 and 11	S87
Figure S21. Spectroscopic data for 12	S93
Figure S22. Spectroscopic data for 13	S95
Figure S23. Spectroscopic data for 14	S97
Figure S24. Spectroscopic data for 15	S99
Figure S25. Spectroscopic data for 16	S101
Figure S26. Spontaneous reaction observed from 13 to 1	S103

EXPERIMENTAL SECTION

General Experimental Procedures. Optical rotations were measured with a MCP 500 polarimeter (Anton Paar, Austria). Ultra Violet (UV) spectra were recorded on UV-2600 spectrophotometer (Shimadzu, Japan). Electronic Circular Dichroism (ECD) spectra were recorded on a Chirascan circular dichroism spectrometer (Applied Photophysics, Ltd., Surrey, UK), and Infra Red (IR) spectra were recorded on Affinity-1 FT-IR spectrometer (Shimadzu). ^1H , ^{13}C , and 2D NMR spectra were recorded on a Bruker AVANCE-500 MHz NMR spectrometer or a Bruker AVANCE-700 MHz NMR spectrometer (Bruker Biospin GmbH), with TMS as an internal standard. Mass spectrometric data were obtained on a Maxis quadrupole-time-of-flight mass spectrometry (Bruker Maxis 4G). Materials for column chromatography (CC) were silica gel (100–200 mesh; 300–400 mesh; Jiangyou Silica gel development, Inc.), Sephadex LH-20 (40–70 μm ; Amersham Pharmacia Biotech AB), and YMC*GEL ODS-A (12 nm S-50 μm ; YMC Company Ltd.). Medium pressure liquid chromatography (MPLC) was performed on CHEETAH flash system (Bonna-Agela technologies Inc.). Semipreparative HPLC was performed on a Hitachi HPLC station (Hitachi-L2130) with Diode Array Detector (Hitachi L-2455) using a Phenomenex ODS column (250 \times 10.0 mm, 5 μm ; Phenomenex, USA); flow rate 2.5 mL min $^{-1}$. Single-crystal data were collected on an XtaLAB PRO MM007HF diffractometer (Rigaku) using Cu $K\alpha$ radiation. All chemicals and solvents were of analytical or chromatographic grade.

Screening and Fermentation. The isolation of strain *Parengyodontium album* sp. SCSIO 40430 has been previously described.¹ *Parengyodontium album* sp. SCSIO 40430 was grown and maintained on the PDA containing 3% natural sea salt. A few loops of cells of *Parengyodontium album* sp. SCSIO 40430 were inoculated into 50 mL of seed medium (Potato Dextrose Broth 24 g/L, natural sea salt 3%, pH 7.0-7.3) in a 250 mL Erlenmeyer flask. The cultivation was carried out on a rotary shaker (200 rpm) at 28 °C for 3-5 days. After growing to logarithmic growth phase, 20 mL of seed cultures was transferred to 200 mL fermentation medium (Potato Dextrose Broth 24 g/L, natural sea salt 3%, pH 7.0-7.3) in a 1L Erlenmeyer flask. The cultivation was carried out on a rotary shaker (200 rpm) at 28 °C for another 7 days.

Extraction and Isolation. The fermentation broth was collected and separated into mycelium and supernatants. The mycelium was extracted three times with 2 L of acetone. The acetone fractions were

concentrated under vacuum to afford an aqueous residue, which was extracted with 2L butanone to obtain extract A. The supernatants was extracted with 4L butanone and was concentrated under vacuum to obtain extract B. A crude extract (15.0 g) was obtained after combining extract A and B. The crude extract was subjected to column chromatography (CC) over silica gel (100-200 mesh), eluting with a gradient of CHCl₃/MeOH (100:0→0:100) to give five fractions (Fr.1-Fr.5). Fr.3 (1.08 g) was subjected to column chromatography (CC) over silica gel (100-200 mesh), eluting with a gradient of petroleum benzin/EtOAc (100:0→0:100) to yield ten fractions (Fr.3-1-Fr.3-10). Fr.3-2 was further purified by semipreparative HPLC using a Phenomenex ODS column (250 × 10.0 mm i.d., 5 μm; Phenomenex) to yield **2** (8.08 mg). Fr.3-5 was separated by Sephadex LH-20 CC (2.5 × 100 cm) and eluted with CHCl₃/MeOH (1:1) to give six subfractions (Fr3-5-1 to Fr3-5-6). Fr3-5-2 was purified by semipreparative HPLC using a Phenomenex ODS column to yield **1** (2.01 mg), **17** (20.2 mg), **12** (4.9 mg), **6** (2.8 mg), and **8** (37.9 mg). Fr.1 was subjected to column chromatography (CC) over silica gel (100-200 mesh), eluting with a gradient of MeOH/H₂O (100:0→0:100) to give five fractions (Fr.1-1-Fr.1-5). Fr.1-1 was purified by semipreparative HPLC using a Phenomenex ODS column to yield **3** (4.01 mg), and **15** (2.1 mg). Fr.1-2 was purified by semipreparative HPLC using a Phenomenex ODS column to yield **4** (5.22 mg) and **9** (2.02 mg). Fr.1-2 also was separated by Sephadex LH-20 CC and eluted with CHCl₃/MeOH (1:1) to give seven subfractions (Fr.1-2-1 to Fr.1-2-7). Fr.1-2-7 was purified by semipreparative HPLC using a Phenomenex ODS column to yield **13** (2.7 mg), **16** (3.1 mg), and **5** (2.9 mg). Fr.6 was separated by Sephadex LH-20 CC and eluted with CHCl₃/MeOH (1:1) to give three subfractions (Fr.6-1 to Fr.6-3). Fr.6-3 was purified by semipreparative HPLC using a Phenomenex ODS column to yield **7** (1.3 mg), and **14** (2.0 mg). Fr.1-4 was purified by preparative HPLC (LC3000) with column (250 mm × 21.1 mm i.d., 5 μm) to yield **10**, **11** (2.5 mg) and **18** (2.0 mg).

(+/-)-8-ethyl-7-hydroxy-5-methoxy-2-methylchroman-4-one (I) Scalemic Mixture: Colorless powder; UV (MeOH) λ_{max} (log ε) 288 nm (3.88), 211 nm (4.01); IR (film) ν_{max} 3332, 2947, 1647, 1506, 1018 cm⁻¹; ¹H NMR (500MHz, CD₃OD) and ¹³C NMR (125 MHz, CD₃OD) data, see Table 1; HRMS (ESI-TOF) *m/z* [M + H]⁺ calcd for C₁₃H₁₇O₄, 237.1121, found 237.1124; *m/z* [M + Na]⁺ calcd for C₁₃H₁₆NaO₄, 259.0941, found 259.0946.

(-)-8-ethyl-7-hydroxy-5-methoxy-2-methylchroman-4-one (1a): [α]_{25D}-26 (c 0.1, MeOH); ECD (c

1.40×10^{-3} M, MeOH) λ_{\max} ($\Delta\epsilon$) 331 (-1.86), 286 (2.61), and 219 (-3.65) nm;

(+)-8-ethyl-7-hydroxy-5-methoxy-2-methylchroman-4-one (**1b**): $[\alpha]_{25D}^{25}$ (c 0.1, MeOH); ECD (c 1.40×10^{-3} M, MeOH) λ_{\max} ($\Delta\epsilon$) 331 (1.64), 287 (-2.89), and 217 (3.29) nm;

(+/-)-8-Ethyl-5,7-dihydroxy-2-methylchroman-4-one (**2**) *Racemic Mixture*: colorless needle; UV (MeOH) λ_{\max} ($\log \epsilon$) 292 nm (4.05), 213 nm (4.12), 202 nm (4.09); IR (film) ν_{\max} 3342, 2947, 1637, 1256, 1018 cm^{-1} ; ^1H NMR (500 MHz, CD_3OD) and ^{13}C NMR (125 MHz, CD_3OD) data, see Table 1; HRMS (ESI-TOF) m/z $[\text{M} + \text{H}]^+$ calcd for $\text{C}_{12}\text{H}_{15}\text{O}_4$, 223.0973, found 223.0962.

(-)-8-Ethyl-5,7-dihydroxy-2-methylchroman-4-one (**2a**): $[\alpha]_{25D}^{25}$ -56 (c 0.2, MeOH); ECD (c 1.49×10^{-3} M, MeOH) λ_{\max} ($\Delta\epsilon$) 309 (-1.23), 288 (2.53), and 215 (-4.50) nm.

(+)-8-Ethyl-5,7-dihydroxy-2-methylchroman-4-one (**2b**): $[\alpha]_{25D}^{25}$ 56 (c 0.2, MeOH); ECD (c 1.49×10^{-3} M, MeOH) λ_{\max} ($\Delta\epsilon$) 310(0.98), 288 (-3.33), and 215 (4.63) nm;

(+/-)-parenmycin A (**3**) *Racemic Mixture*: off-white powder; UV (MeOH) λ_{\max} ($\log \epsilon$) 292 nm (3.61), 213 nm (3.69), 203 nm (3.69); IR (film) ν_{\max} 3381, 2918, 1647, 1508, 1016 cm^{-1} ; ^1H NMR (500MHz, CD_3OD) and ^{13}C NMR (125 MHz, CD_3OD) data, see Table 1; HRMS (ESI-TOF) m/z $[\text{M} - \text{H}]^-$ calcd for $\text{C}_{12}\text{H}_{13}\text{O}_4$, 221.0819, found 221.0815; m/z $[\text{M} + \text{Cl}]^-$ calcd for $\text{C}_{12}\text{H}_{14}\text{ClO}_4$, 257.0586, found 257.0583.

(-)-parenmycin A (**3a**): off-white powder; $[\alpha]_{25D}^{25}$ -56 (c 0.1, MeOH); ECD (c 1.13×10^{-3} M, MeOH) λ_{\max} ($\Delta\epsilon$) 309 (-1.46), 287 (4.04), and 215 (-5.35) nm;

(+)-parenmycin A (**3b**): off-white powder; $[\alpha]_{25D}^{25}$ +56 (c 0.1, MeOH); ECD (c 1.13×10^{-3} M, MeOH) λ_{\max} ($\Delta\epsilon$) 309 (1.11), 287 (-4.14), and 214 (4.95) nm;

(+/-)-LL-D253c (**4**) *Scalemic Mixture*: yellow powder; UV (MeOH) λ_{\max} ($\log \epsilon$) 289 nm (3.77), 241 nm (3.72), 213 nm (3.90), 202 nm (3.91); IR (film) ν_{\max} 3363, 2945, 1647, 1456, 1020 cm^{-1} ; ^1H NMR (500 MHz, CD_3OD) and ^{13}C NMR (125 MHz, CDCl_3) data, see Table 1; HRMS (ESI-TOF) m/z $[\text{M} + \text{H}]^+$ calcd for $\text{C}_{13}\text{H}_{15}\text{O}_4$, 235.0965, found 235.0964; $[\text{M} + \text{Na}]^+$ calcd for $\text{C}_{13}\text{H}_{14}\text{NaO}_4$, 257.0784, found 257.0790.

(-)-LL-D253c (**4a**): $[\alpha]_{25D}^{25}$ -33 (c 0.1, MeOH); ECD (c 1.41×10^{-3} M, MeOH) λ_{\max} ($\Delta\epsilon$) 324 (-1.38), 287 (3.35), and 215 (-3.52) nm;

(+)-LL-D253c (**4b**): $[\alpha]_{25D}^{25}$ +33 (c 0.1, MeOH); ECD (c 1.41×10^{-3} M, MeOH) λ_{\max} ($\Delta\epsilon$) 322 (1.44), 288 (-3.38), and 215 (3.94) nm;

(+/-)-*Parentmycin B (5) Scalemic Mixture*: yellow oil; UV (MeOH) λ_{\max} (log ϵ) 296nm (4.02), 238 nm (3.77), 212 nm (4.02), 204 nm (4.02); IR (film) ν_{\max} 3390, 2947, 1647, 1456, 1020 cm^{-1} ; ^1H NMR (500MHz, CD_3OD) and ^{13}C NMR (125 MHz, CD_3OD) data, see Table 2; HRMS (ESI-TOF) m/z $[\text{M} - \text{H}]^-$ calcd for $\text{C}_{13}\text{H}_{15}\text{O}_5$, 251.0925, found 251.0925; m/z $[\text{M} + \text{Cl}]^-$ calcd for $\text{C}_{13}\text{H}_{16}\text{ClO}_5$, 287.0692, found 287.0692.

(-)-*Parentmycin B (5a)*: $[\alpha]_{\text{D}}^{25} -17$ (c 0.1, MeOH).

(+)-*Parentmycin B (5b)*: $[\alpha]_{\text{D}}^{25} +17$ (0.1, MeOH).

(+/-)-*Parentmycin C (6) Racemic Mixture*: yellow oil; UV (MeOH) λ_{\max} (log ϵ) 294 nm (3.44), 202 nm (3.71); IR (film) ν_{\max} 3354, 2945, 1653, 1458, 1020 cm^{-1} ; ^1H NMR (500MHz, CD_3OD) and ^{13}C NMR (125 MHz, CD_3OD) data, see Table 2; HRMS (ESI-TOF) m/z $[\text{M} - \text{H}]^-$ calcd for $\text{C}_{13}\text{H}_{17}\text{O}_5$, 253.1081, found 253.1085; $[\text{M} + \text{Cl}]^-$ calcd for $\text{C}_{13}\text{H}_{18}\text{ClO}_5$, 289.0848, found 289.0847.

(-)-*Parentmycin C (6a)*: $[\alpha]_{\text{D}}^{25} -14$ (c 0.13, MeOH).

(+)-*Parentmycin C (6b)*: $[\alpha]_{\text{D}}^{25} +14$ (c 0.13, MeOH).

(+/-)- *1-(2,4-dihydroxy-3-[2-hydroxyethyl]-6-methoxyphenyl)-3-hydroxybutan-1-one (7) Scalemic Mixture*: off-white solid; UV (MeOH) λ_{\max} (log ϵ) 293 nm (3.69), 202 nm (3.91); IR (film) ν_{\max} 3336, 2945, 1653, 1506, 1020 cm^{-1} ; ^1H NMR (500MHz, $\text{DMSO}-d_6$) and ^{13}C NMR (125 MHz, $\text{DMSO}-d_6$) data, see Tables 2; HRMS (ESI-TOF) m/z $[\text{M} - \text{H}]^-$ calcd for $\text{C}_{13}\text{H}_{17}\text{O}_5$, 269.1031, found 269.1032; $[\text{M} + \text{Cl}]^-$ calcd for $\text{C}_{13}\text{H}_{18}\text{ClO}_6$, 305.0797, found 305.0804.

(-) - **(7a)**: $[\alpha]_{\text{D}}^{25} -14$ (c 0.13, MeOH);

(+) - **(7b)**: $[\alpha]_{\text{D}}^{25} +14$ (c 0.13, MeOH);

(+/-)-*parenamide D (8) Racemic Mixture*: off-white solid; UV (MeOH) λ_{\max} (log ϵ) 324 nm (3.71), 296 nm (4.24), 235 nm (3.82), 210 nm (4.28); IR (film) ν_{\max} 3329, 2972, 1600 cm^{-1} ; ^1H NMR (500MHz, $\text{DMSO}-d_6$) and ^{13}C NMR (125 MHz, $\text{DMSO}-d_6$) data, see Tables 1 and 2; HRMS (ESI-TOF) m/z $[\text{M} - \text{H}]^-$ calcd for $\text{C}_{13}\text{H}_{15}\text{O}_5$, 251.0925, found 251.0932; $[\text{M} + \text{Cl}]^-$ calcd for $\text{C}_{13}\text{H}_{16}\text{ClO}_5$, 287.0692, found 287.0694.

(+)-*acetyl-parenamide D (8a)*: off-white solid; $[\alpha]_{\text{D}}^{25} +108$ (c 0.1, MeOH); ECD (c 1.02×10^{-3} M, MeOH) λ_{\max} ($\Delta\epsilon$) 326 (10.5), 280 (-7.5), and 237 (-9.4) nm; MS (ESI-TOF) m/z $[\text{M} + \text{H}]^+$ found 295.7.

Parenamide E (9) off-white powder; UV (MeOH) λ_{\max} (log ϵ) 310 nm (3.28), 296 nm (3.30), 256 nm (3.89), 226 nm (3.72), 203 nm (3.85); IR (film) ν_{\max} 3197, 2986, 1653 cm^{-1} ; ^1H NMR (500MHz,

CD₃OD) and ¹³C NMR (125 MHz, CD₃OD) data, see Tables 1 and 2; HRMS (ESI-TOF) *m/z* [M + H]⁺ calcd for C₁₃H₁₃O₄, 233.0808, found 233.0810; *m/z* [M + Na]⁺ calcd for C₁₃H₁₂NaO₄, 255.0628, found 255.0630.

Parenamide FIG (10/11): off-white powder; UV (MeOH) λ_{max} (log ε) 323 nm (3.23), 298 nm (3.40), 260 nm (4.00), 253 nm (4.00), 231 nm (3.89), 208 nm (4.05)⁻¹; IR (film) ν_{max} 3360, 2918, 2848, 1660 cm⁻¹; ¹H NMR (500MHz, CD₃OD) and ¹³C NMR (125 MHz, CD₃OD) data, see Tables 1 and 2; HRMS (ESI-TOF) *m/z* [M + H]⁺ calcd for C₁₄H₁₇O₄ 249.1121, found 249.1124.

The Quantum Chemical Electrostatic Circular dichroism (ECD) Calculation. Quantum chemical calculation methods for electrostatic circular dichroism (ECD) were used to support or establish the C-11 absolute configuration of compound **1**, and C-10 absolute configuration of compound **8**. The compounds were charged using the Gasteiger-Huckel method and the preliminary conformational search was performed with the SYBYL 8.0 software package using the MMFF94s force field. The geometry optimizations were then performed by using DFT at the B3LYP/6-31+G (d) level as implemented in the Gaussian 09 program package. The stable conformers obtained were subsequently submitted to CD calculations by time dependent (TD) DFT calculations (B3LYP/6-31G (d)) with Gaussian 09. The overall calculated ECD curves of all the compounds were weighted by Boltzmann distribution. The ECD curves were produced by SpecDis 1.64 software.²

X-ray Crystallographic Analysis. An optically active light white crystal of **2-4**, **7**, and **8** was obtained in MeOH or CHCl₃/MeOH. Single-crystal data were collected on an XtaLAB PRO MM007HF diffractometer (Rigaku) using Cu Kα radiation (λ = 1.54184 Å). The structures were solved by direct methods (SHELXS-97) and refined using full-matrix least-squares difference Fourier techniques. Crystallographic data have been deposited in the Cambridge Crystallographic Data Center. A copy of the data can be obtained, free of charge, on application to the Director, CCDC, 12 Union Road, Cambridge CB21EZ, U.K. (fax, +44(0)-1233-336033; e-mail, deposit@ccdc.cam.ac.uk).

Crystal data of **2**: colorless (block), monoclinic, space group P2₁/c, *a* = 15.6505(4) Å, *b* = 4.35190(10) Å, *c* = 17.2668(5) Å, *V* = 1065.72(6) Å³, *Z* = 4, μ(Cu Kα) = 0.865, *T* = 99.9(5), and *F*(000) = 472, Crystal size: 0.2 × 0.05 × 0.05 mm³. 4622 reflections measured, of which 2097 unique (*R*int (*R* factor for symmetry-equivalent intensities) = 0.0236) were used in all calculations. CCDC no. 2072125.

Crystal data of **3**: colorless (block), monoclinic, space group $P2_1/c$, $a = 5.1015(3) \text{ \AA}$, $b = 21.7906(18) \text{ \AA}$, $c = 10.1611(4) \text{ \AA}$, $V = 1102.27(12) \text{ \AA}^3$, $Z = 4$, $\mu(\text{Cu K}\alpha) = 0.834$, $T = 99.9(6)$, and $F(000) = 470$, Crystal size: $0.2 \times 0.05 \times 0.05 \text{ mm}^3$. 5466 reflections measured, of which 2144 unique (Rint (R factor for symmetry-equivalent intensities) = 0.0420) were used in all calculations. CCDC no. 2072148.

Crystal data of **4**: colorless (block), monoclinic, space group $P2_1/c$, $a = 12.1797(3) \text{ \AA}$, $b = 5.27290(10) \text{ \AA}$, $c = 17.2041(4) \text{ \AA}$, $V = 1090.63(4) \text{ \AA}^3$, $Z = 4$, $\mu(\text{Cu K}\alpha) = 0.878$, $T = 99.98(16)$, and $F(000) = 496$, Crystal size: $0.3 \times 0.1 \times 0.05 \text{ mm}^3$. 6947 reflections measured, of which 2311 unique (Rint (R factor for symmetry-equivalent intensities) = 0.0222) were used in all calculations. CCDC no. 2072134.

Crystal data of **7**: colorless (block), monoclinic, space group $C2/c$, $a = 23.3741(4) \text{ \AA}$, $b = 13.2115(2) \text{ \AA}$, $c = 17.7270(3) \text{ \AA}$, $V = 5377.60(15) \text{ \AA}^3$, $Z = 8$, $\mu(\text{Cu K}\alpha) = 0.939$, $T = 99.9(6)$, and $F(000) = 2384$, Crystal size: $0.1 \times 0.05 \times 0.05 \text{ mm}^3$. 29267 reflections measured, of which 5403 unique (Rint (R factor for symmetry-equivalent intensities) = 0.0311) were used in all calculations. CCDC no. 2072139.

Crystal data of **8**: colorless (block), triclinic, space group $P-1$, $a = 10.3819(6) \text{ \AA}$, $b = 12.0675(7) \text{ \AA}$, $c = 12.3012(6) \text{ \AA}$, $V = 1445.20(14) \text{ \AA}^3$, $Z = 1$, $\mu(\text{Cu K}\alpha) = 0.874$, $T = 99.9(6)$, and $F(000) = 596$, Crystal size: $0.02 \times 0.02 \times 0.02 \text{ mm}^3$. 10544 reflections measured, of which 10544 unique (Rint (R factor for symmetry-equivalent intensities) = 0.0633) were used in all calculations. CCDC no. 2072145.

Chiral HPLC Analysis. All compounds contained two enantiomers was dissolved in MeOH (1 mL) and filtered. Chiral HPLC analysis was carried out on an Agilent 1260 system (binary pump, column oven, autosampler, DAD), using chiral column chromatography and a mixture of MeCN/H₂O as eluent, applying a total flow rate of 0.5 mL/min.

Mosher's MTPA Esters 5b. Compound **5b** (2 mg) was divided into two equal portions, and each was dissolved in 300 μL of pyridine in separate NMR tubes. To each 1 mg DMAP, and 10 μL of (*R*)-MTPA-Cl or 10 μL (*S*)-MTPA-Cl was added. After 24 h, LC-MS analysis indicated that equal amounts of mono-Mosher's ester products were formed. The reactions were terminated and the products were purified by semi-preparative HPLC.

ESIMS: mono-10-(*S*)-MTPA ester **5b-1** m/z 469.4 $[\text{M} + \text{H}]^+$; mono-10-(*R*)-MTPA ester **5b-2** m/z $[\text{M} + \text{H}]^+$ 469.4; The ¹H NMR spectra for Mosher esters **5b-1/5b-2** were recorded.

Biological Assays. Antimicrobial activities of compounds **1-18** were measured against the eight indicator strains *Staphylococcus aureus* ATCC 29213, *Vibrio* XSBZ 14, *Pseudomonas aeruginosa*

ATCC 161028, *Pseudomonas aeruginosa* ATCC 27853, *Acinetobacter baumannii* ATCC 19606, *Bacillus thuringensis*, *Bacillus subtilis*, Methicillin-resistant *Staphylococcus aureus* MRSA ATCC 43300, and the autoluminescent *Mycobacterium tuberculosis* H37Ra (AIRa) by detecting relative light unit using the broth microdilution method.^{3,4} The indicator strains were grown for 12 h on a rotary shaker at 37 °C. Cultures were diluted with sterilized medium to achieve an optical absorbance of 0.04–0.06 at 600 nm, then diluted 1000-fold before being added into 96-well micro titer plates. Three replicates of each compound were tested in dilution series ranging from 64 to 0.25 µg mL⁻¹. The lowest concentrations that completely inhibited the visible growth of the tested strains were recorded after 16 h cultivation from two independent experiments. For AIRa, Compounds **1-18** were dissolved in dimethyl sulfoxide (DMSO) and then serially diluted to final concentrations (µg/mL) of 0.0078–128 for testing with 7H9 broth (added with 0.2% glycerol and 10% v/v oleic acid albumin dextrose catalase). The antitubercular assays were performed in triplicate. DMSO was used as a negative control, and rifampin was used as a positive control.

Table S1. The ^1H and ^{13}C NMR Data for **1-4**.

	1^a		2^a		3^a		4^a	
	δ_{C} , type	δ_{H} , mult. (<i>J</i> in Hz)	δ_{C} , type	δ_{H} , mult. (<i>J</i> in Hz)	δ_{C} , type	δ_{H} , mult. (<i>J</i> in Hz)	δ_{C} , type	δ_{H} , mult. (<i>J</i> in Hz)
1	163.8, C		164.3, C		165.9, C		163.2, C	
2	93.3, CH	6.10, s	93.7, CH	5.80, s	111.7, C		87.7, CH	6.05, s
3	164.2, C		161.0, C		162.5, C		167.1, C	
4	112.0, C		110.1, C		95.2, CH	5.90, s	105.1, C	
5	161.7, C		160.9, C		162.4, C		159.5, C	
6	105.7, C		101.5, C		103.1, C		105.6, C	
7	20.9, CH ₂	2.58, m ^b	14.5, CH ₂	2.43, q (7.5)	16.1, CH ₂	2.55, q (7.4)	26.3, CH ₂	2.61, m ^b
8	14.1, CH ₃	1.04, t (7.5)	12.3, CH ₃	0.96, t (7.5)	13.8, CH ₃	1.06, t (7.4)	73.1, CH ₂	4.67, m
9	193.2, C		196.5, C		198.0, C		189.5, C	
10	46.4, CH ₂	2.58, m ^b	42.7, CH ₂	2.58, dd (17.0, 12.3) 2.45, dd (17.0, 3.5)	44.2, CH ₂	2.69, dd (16.6, 11.9) 2.59, m ^b	45.8, CH ₂	2.61, m ^b
11	74.9, CH	4.49, m	73.7, CH	4.40, m	75.2, CH	4.47, m	73.8, CH	4.55, m
12	16.8, CH ₃	1.46, d (6.5)	19.5, CH ₃	1.34, d (6.3)	21.1, CH ₃	1.45, d (6.3)	20.8, CH ₃	1.46, d (6.3)
13	55.9, CH ₃	3.79, s					56.3, CH ₃	3.87, s

^aData were recorded on a Bruker Avance 500 MHz NMR spectrometer in methanol-*d*₄ with TMS as an internal standard, the signals were assigned with the aid of ^1H - ^1H COSY, HSQC, and HMBC data. ^bOverlapping signals.

Table S2. Crystal data and structure refinement for **2**.

Identification code	SH31-1
Empirical formula	C ₁₂ H ₁₄ O ₄
Formula weight	222.23
Temperature/K	99.9(5)
Crystal system	monoclinic
Space group	P2 ₁ /c
a/Å	15.6505(4)
b/Å	4.35190(10)
c/Å	17.2668(5)
α /°	90
β /°	115.015(4)
γ /°	90
Volume/Å ³	1065.72(6)
Z	4
ρ_{calc} /cm ³	1.385
μ /mm ⁻¹	0.865
F(000)	472.0
Crystal size/mm ³	0.2 × 0.05 × 0.05
Radiation	CuK α (λ = 1.54184)
2 Θ range for data collection/°	10.35 to 148.036
Index ranges	-19 ≤ h ≤ 18, -5 ≤ k ≤ 3, -21 ≤ l ≤ 19
Reflections collected	4622
Independent reflections	2097 [R _{int} = 0.0236, R _{sigma} = 0.0384]
Data/restraints/parameters	2097/0/151
Goodness-of-fit on F ²	1.077
Final R indexes [I ≥ 2 σ (I)]	R ₁ = 0.0475, wR ₂ = 0.1307
Final R indexes [all data]	R ₁ = 0.0554, wR ₂ = 0.1367
Largest diff. peak/hole / e Å ⁻³	0.87/-0.27

Table S3. Crystal data and structure refinement for **3**.

Identification code	zhangwenjun_SH31-18_collect
Empirical formula	C _{11.92} H _{13.91} O ₄
Formula weight	221.21
Temperature/K	99.9(6)
Crystal system	monoclinic
Space group	P2 ₁ /c
a/Å	5.1015(3)
b/Å	21.7906(18)
c/Å	10.1611(4)
α /°	90
β /°	102.619(5)
γ /°	90
Volume/Å ³	1102.27(12)
Z	4
$\rho_{\text{calc}}/\text{g}/\text{cm}^3$	1.333
μ/mm^{-1}	0.834
F(000)	470.0
Crystal size/mm ³	0.2 × 0.05 × 0.05
Radiation	CuK α (λ = 1.54184)
2 Θ range for data collection/°	9.8 to 147.998
Index ranges	-3 ≤ h ≤ 6, -26 ≤ k ≤ 13, -12 ≤ l ≤ 11
Reflections collected	5466
Independent reflections	2144 [R _{int} = 0.0420, R _{sigma} = 0.0525]
Data/restraints/parameters	2144/0/160
Goodness-of-fit on F ²	1.101
Final R indexes [I ≥ 2 σ (I)]	R ₁ = 0.0575, wR ₂ = 0.1707
Final R indexes [all data]	R ₁ = 0.0666, wR ₂ = 0.1771
Largest diff. peak/hole / e Å ⁻³	0.29/-0.25

Table S4. Crystal data and structure refinement for **4**.

Identification code	huangyanbing_SH31-Fr1-M2_collect SH31-5
Empirical formula	C ₁₃ H ₁₄ O ₄
Formula weight	234.24
Temperature/K	99.98(16)
Crystal system	monoclinic
Space group	P2 ₁ /c
a/Å	12.1797(3)
b/Å	5.27290(10)
c/Å	17.2041(4)
α/°	90
β/°	99.215(2)
γ/°	90
Volume/Å ³	1090.63(4)
Z	4
ρ _{calc} /cm ³	1.427
μ/mm ⁻¹	0.878
F(000)	496.0
Crystal size/mm ³	0.3 × 0.1 × 0.05
Radiation	CuKα (λ = 1.54184)
2θ range for data collection/°	7.354 to 158.34
Index ranges	-15 ≤ h ≤ 15, -6 ≤ k ≤ 4, -19 ≤ l ≤ 21
Reflections collected	6947
Independent reflections	2311 [R _{int} = 0.0222, R _{sigma} = 0.0187]
Data/restraints/parameters	2311/2/177
Goodness-of-fit on F ²	1.125
Final R indexes [I ≥ 2σ (I)]	R ₁ = 0.0487, wR ₂ = 0.1253
Final R indexes [all data]	R ₁ = 0.0502, wR ₂ = 0.1263
Largest diff. peak/hole / e Å ⁻³	0.25/-0.23

Table S5. $\Delta\delta^{SR}$ (ppm) data for the *S*- and *R*-MTPA-**5b** Mosher esters in methanol-*d*₄.

No.	<i>R</i> -MTPA (5b-2)	<i>S</i> -MTPA (5b-1)	$\Delta\delta^{SR}$ (ppm)
	δ_H	δ_H	$\Delta\delta$ ($\delta_S - \delta_R$)
4	6.07	6.11	0.04
7	3.10	3.12	0.02
8	4.69	4.70	0.01
10	3.20	3.26	0.06
	3.42	3.47	0.07
11	5.81	5.78	-0.03
12	1.46	1.36	-0.1

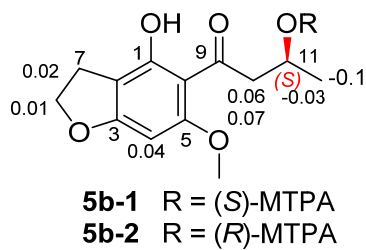


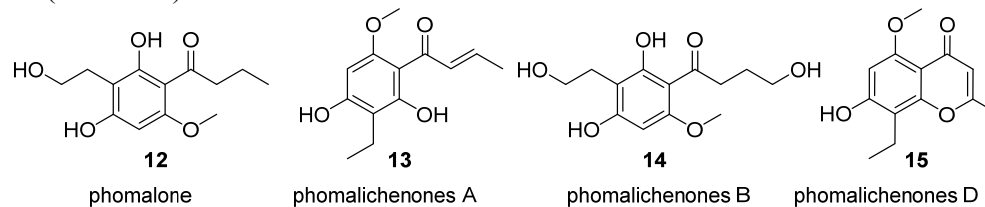
Table S6. Crystal data and structure refinement for **7**.

Identification code	zahngwenjun_SH31-10_collect
Empirical formula	C ₂₆ H ₃₈ O ₁₃
Formula weight	558.56
Temperature/K	99.9(6)
Crystal system	monoclinic
Space group	C2/c
a/Å	23.3741(4)
b/Å	13.2115(2)
c/Å	17.7270(3)
α /°	90
β /°	100.7810(10)
γ /°	90
Volume/Å ³	5377.60(15)
Z	8
ρ_{calc} /cm ³	1.380
μ /mm ⁻¹	0.939
F(000)	2384.0
Crystal size/mm ³	0.1 × 0.05 × 0.05
Radiation	CuK α (λ = 1.54184)
2 Θ range for data collection/°	7.7 to 148.318
Index ranges	-28 ≤ h ≤ 29, -16 ≤ k ≤ 16, -20 ≤ l ≤ 21
Reflections collected	29267
Independent reflections	5403 [R_{int} = 0.0311, R_{sigma} = 0.0215]
Data/restraints/parameters	5403/0/386
Goodness-of-fit on F ²	1.081
Final R indexes [$I \geq 2\sigma(I)$]	$R_1 = 0.0701$, $wR_2 = 0.1920$
Final R indexes [all data]	$R_1 = 0.0734$, $wR_2 = 0.1945$
Largest diff. peak/hole / e Å ⁻³	0.69/-0.42

Table S7. Crystal data and structure refinement for **8**.

Identification code	zhangwenjun_SH31-11_collect2_twin1_hklf4
Empirical formula	C ₅₂ H ₇₆ O ₂₆
Formula weight	1117.12
Temperature/K	99.9(6)
Crystal system	triclinic
Space group	P-1
a/Å	10.3819(6)
b/Å	12.0675(7)
c/Å	12.3012(6)
α /°	70.999(5)
β /°	84.623(5)
γ /°	83.524(5)
Volume/Å ³	1445.20(14)
Z	1
$\rho_{\text{calc}}/\text{cm}^3$	1.284
μ/mm^{-1}	0.874
F(000)	596.0
Crystal size/mm ³	0.02 × 0.02 × 0.02
Radiation	CuK α (λ = 1.54184)
2 Θ range for data collection/°	8.99 to 148.998
Index ranges	-12 ≤ h ≤ 12, -15 ≤ k ≤ 15, -15 ≤ l ≤ 15
Reflections collected	10544
Independent reflections	10544 [R _{int} = 0.0633, R _{sigma} = 0.0158]
Data/restraints/parameters	10544/0/372
Goodness-of-fit on F ²	1.073
Final R indexes [I ≥ 2 σ (I)]	R ₁ = 0.0633, wR ₂ = 0.2135
Final R indexes [all data]	R ₁ = 0.0695, wR ₂ = 0.2200
Largest diff. peak/hole / e Å ⁻³	0.39/-0.57

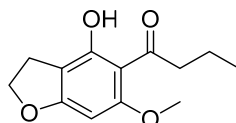
Table S8. The ^1H (500 MHz) and ^{13}C (125 MHz) NMR Data for **12-15**.⁵⁻⁷



	12^a		13^a		14^a		15^a	
	δ_{C} , type	δ_{H} , mult. (<i>J</i> in Hz)	δ_{C} , type	δ_{H} , mult. (<i>J</i> in Hz)	δ_{C} , type	δ_{H} , mult. (<i>J</i> in Hz)	δ_{C} , type	δ_{H} , mult. (<i>J</i> in Hz)
1	166.2, C		162.4, C		164.3, C		157.9, C	
2	105.8, C		91.6, CH	5.87, s	103.6, C		95.8, CH	6.47, s
3	164.4, C		166.2, C		164.3, C		159.5, C	
4	91.3, CH	6.03, s	111.6, C		90.8, CH	6.06, s	109.1, C	
5	163.1, C		163.8, C		161.0, C		156.7, C	
6	105.7, C		105.8, C		104.3, C		106.8, C	
7	26.8, CH ₂	2.85, t (8.5)	16.5, CH ₂	2.47, q (8.7)	26.2, CH ₂	2.64, t (8.7)	15.6, CH ₂	2.66, q (6.9)
8	62.1, CH ₂	3.64, t (8.3)	13.8, CH ₃	0.96, t (8.7)	59.8, CH ₂	3.38, overlapping	13.8, CH ₃	1.01, t (7.8)
9	206.9, C		194.5, C		204.7, C		175.9, C	
10	47.2, CH ₂	2.96, t (8.5)	142.3, CH	7.16, dq (14.5, 0.9)	27.8, CH ₂	1.75, m	110.5, CH	5.88, s
11	19.6, CH ₂	1.67, m	133.7, CH	6.91, dq (14.5, 6.8)	60.3, CH	3.43, overlapping	162.7, C	
12	14.4, CH ₃	0.99, t (7.5)	18.6, CH ₃	1.85, dd (6.8, 0.9)	39.9, CH ₂	2.94, t (7.7)	19.1, CH ₃	2.25, s
13	55.8, CH ₃	3.87, s	55.9, CH ₃	3.74, s	55.4, CH ₃	3.78, s	55.5, CH ₃	3.73, s

^a in methanol-*d*₄

Table S9. The ^1H (500 MHz) and ^{13}C (125 MHz) NMR Data for **16**⁷ in $\text{DMSO-}d_6$.



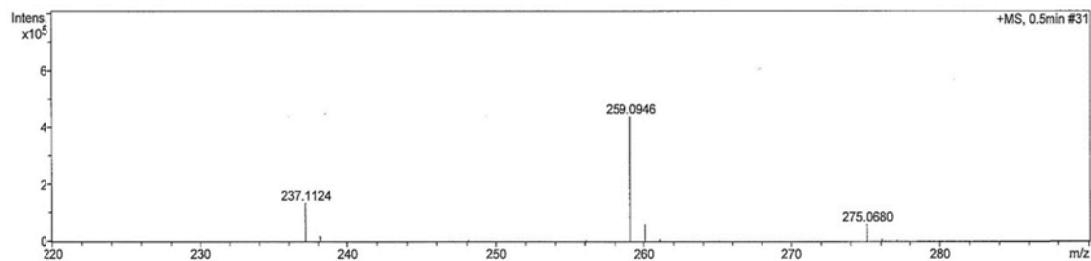
16
dihydrobenzofuran phomalone

No.	16	
	δ_{C} , type	δ_{H} , mult. (J in Hz)
1	162.8, C	
2	106.4, C	
3	168.9, C	
4	86.9, CH	6.08, s
5	165.8, C	
6	106.8, C	
7	26.7, CH_2	3.10, t (8.4)
8	74.4, CH_2	4.68, t (8.4)
9	207.3, C	
10	47.2, CH_2	2.97, t (7.4)
11	19.5, CH_2	1.71, m
12	14.4, CH_3	1.01, t (7.6)
13	56.3, CH_3	3.88, s

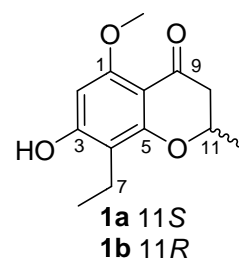
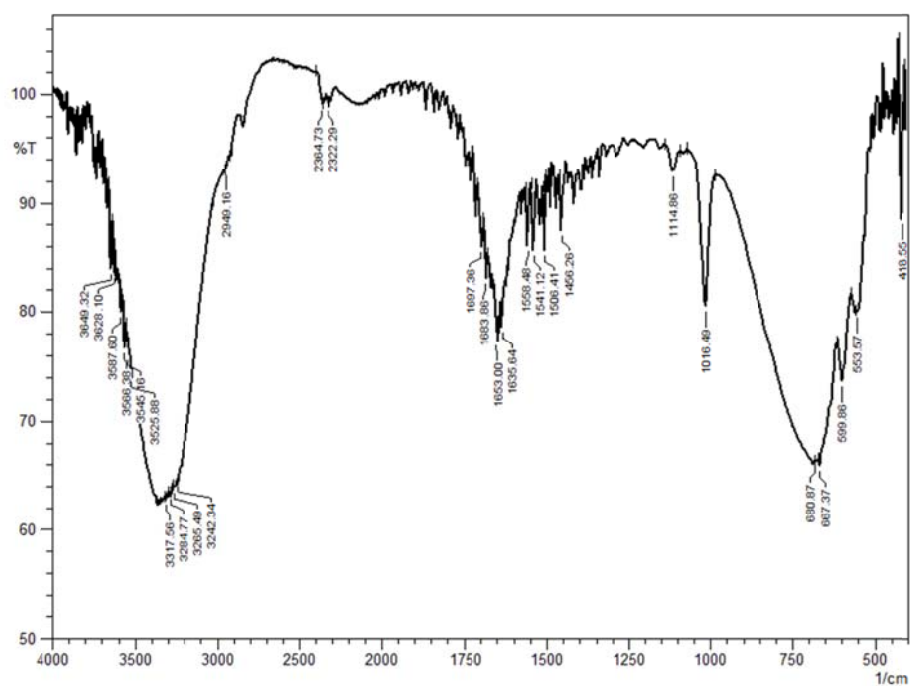
Figure S1. Spectroscopic data for **1**.

(A) HR-ESI-MS (a), IR (b), and UV (c) spectra of **1**.

(a). HR-ESI-MS



(b). IR



Chemical Formula: C₁₃H₁₆O₄
Exact Mass: 236.10

(c). UV

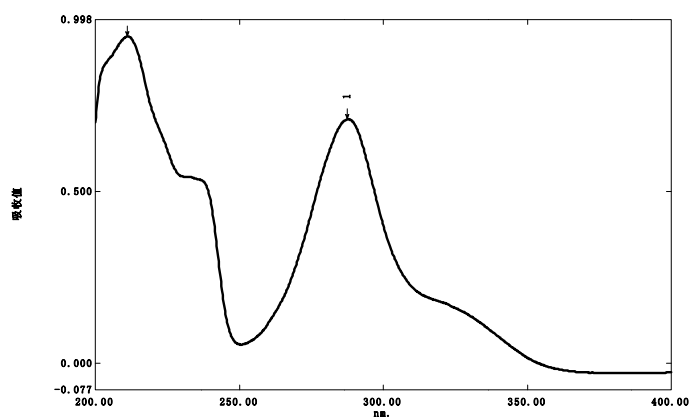


Figure S1. Spectroscopic data for **1**. (Continued)

(B) The ^1H NMR spectrum of **1** in methanol- d_4 .

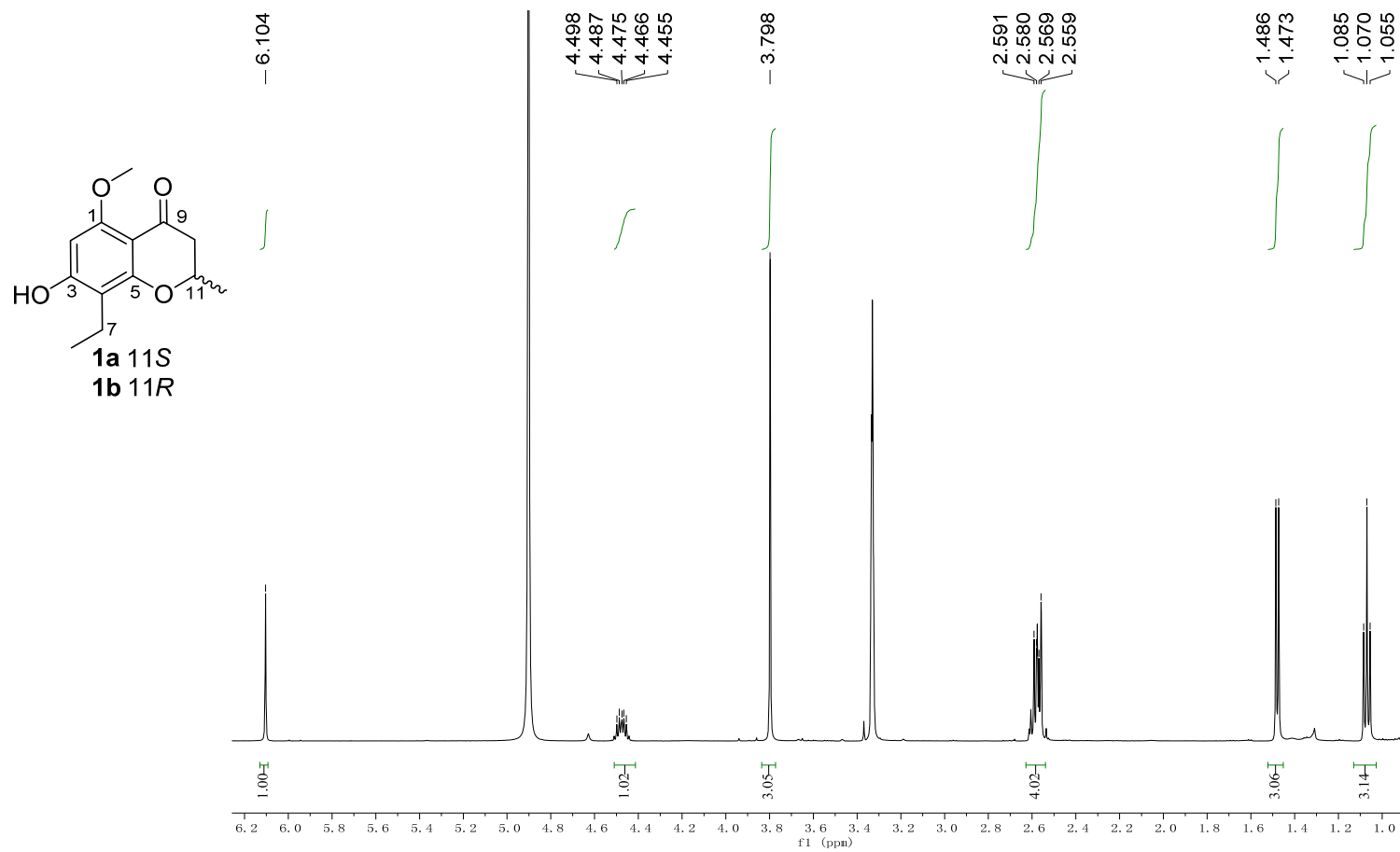


Figure S1. Spectroscopic data for **1**. (Continued)

(C) The ^{13}C and DEPT 135 NMR spectrum of **1** in methanol- d_4 .

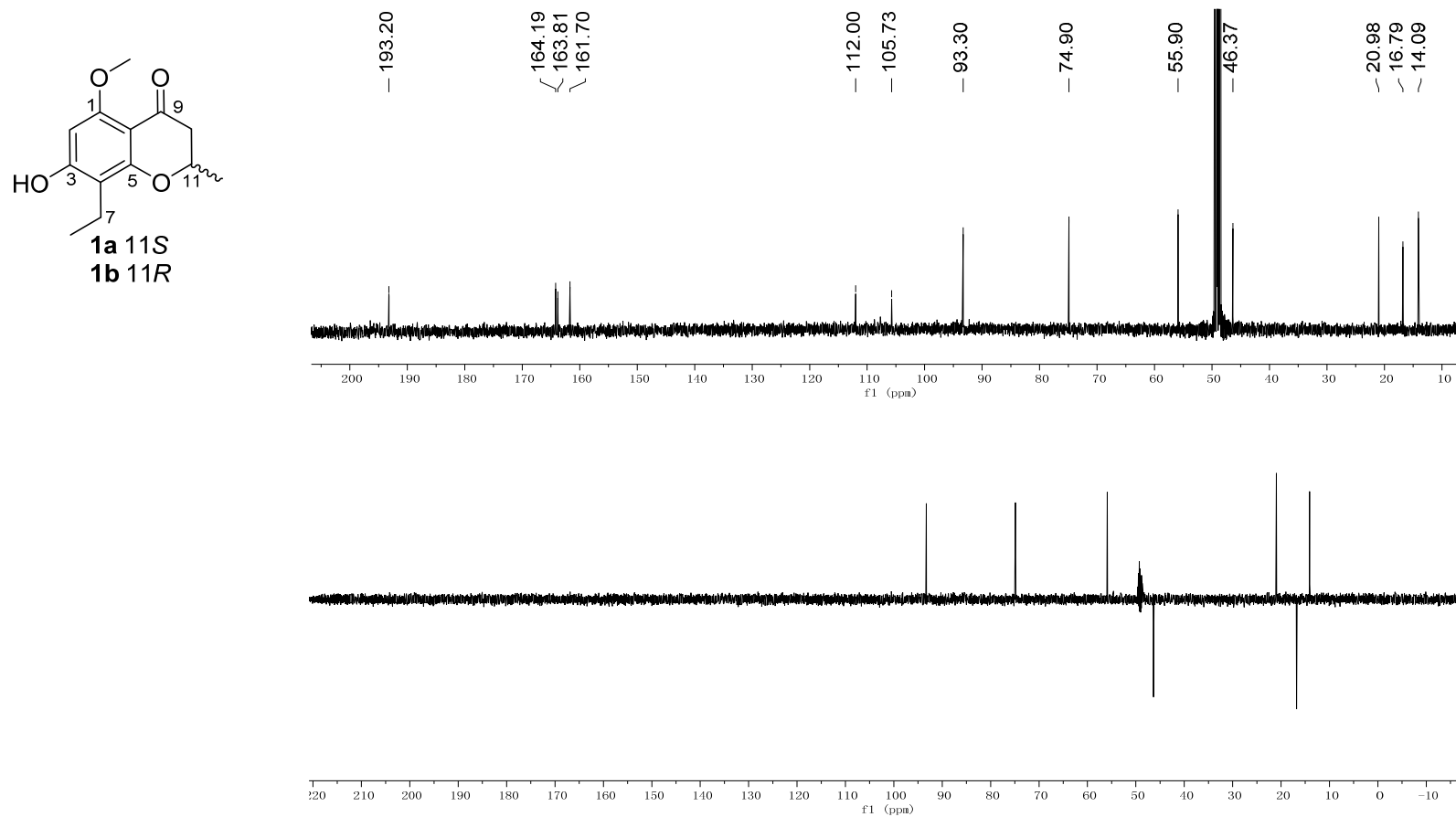


Figure S1. Spectroscopic data for **1**. (Continued)

(D) The HSQC spectrum of **1** in methanol-*d*₄.

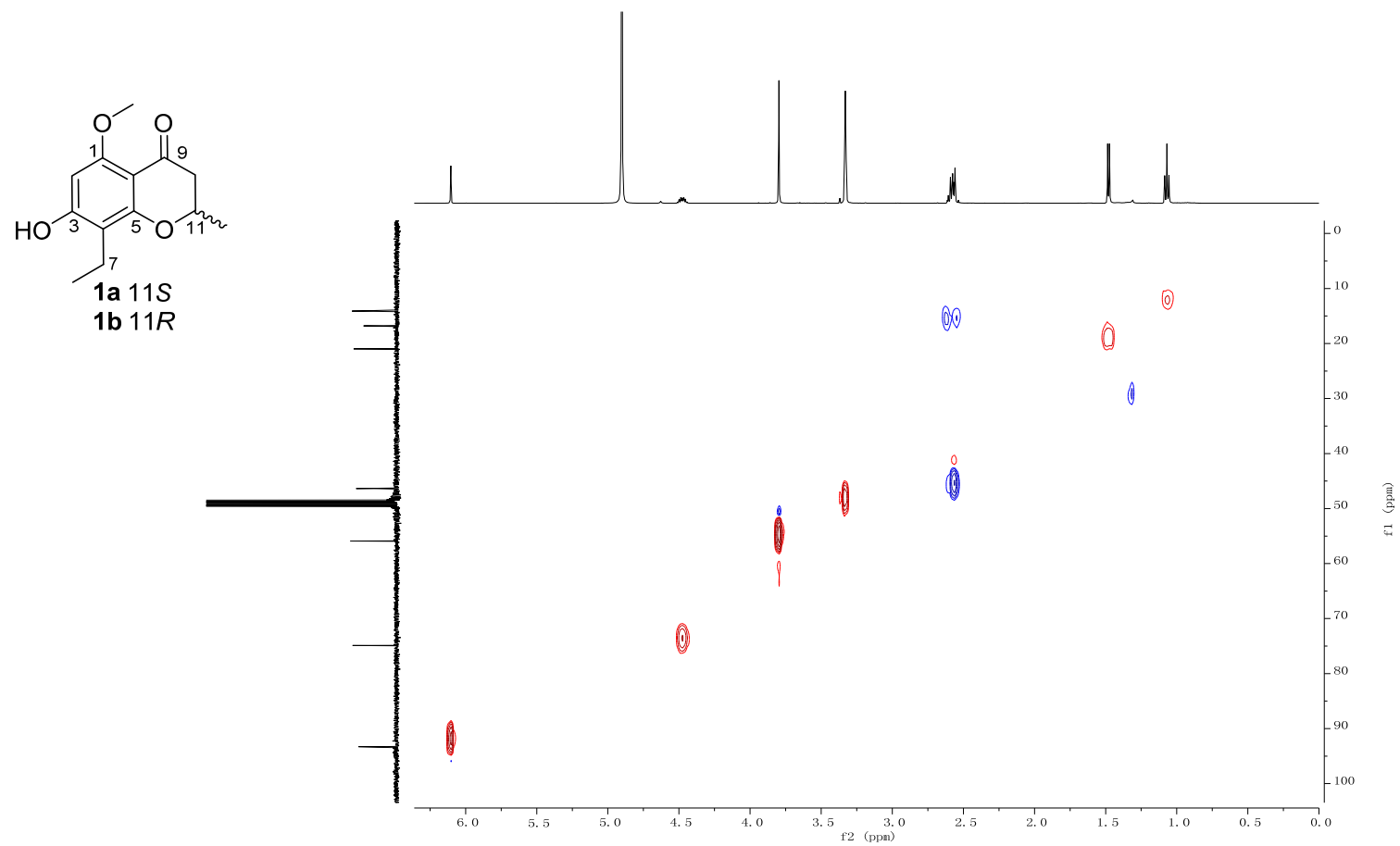


Figure S1. Spectroscopic data for **1**. (Continued)

(E) The COSY spectrum of **1** in methanol- d_4 .

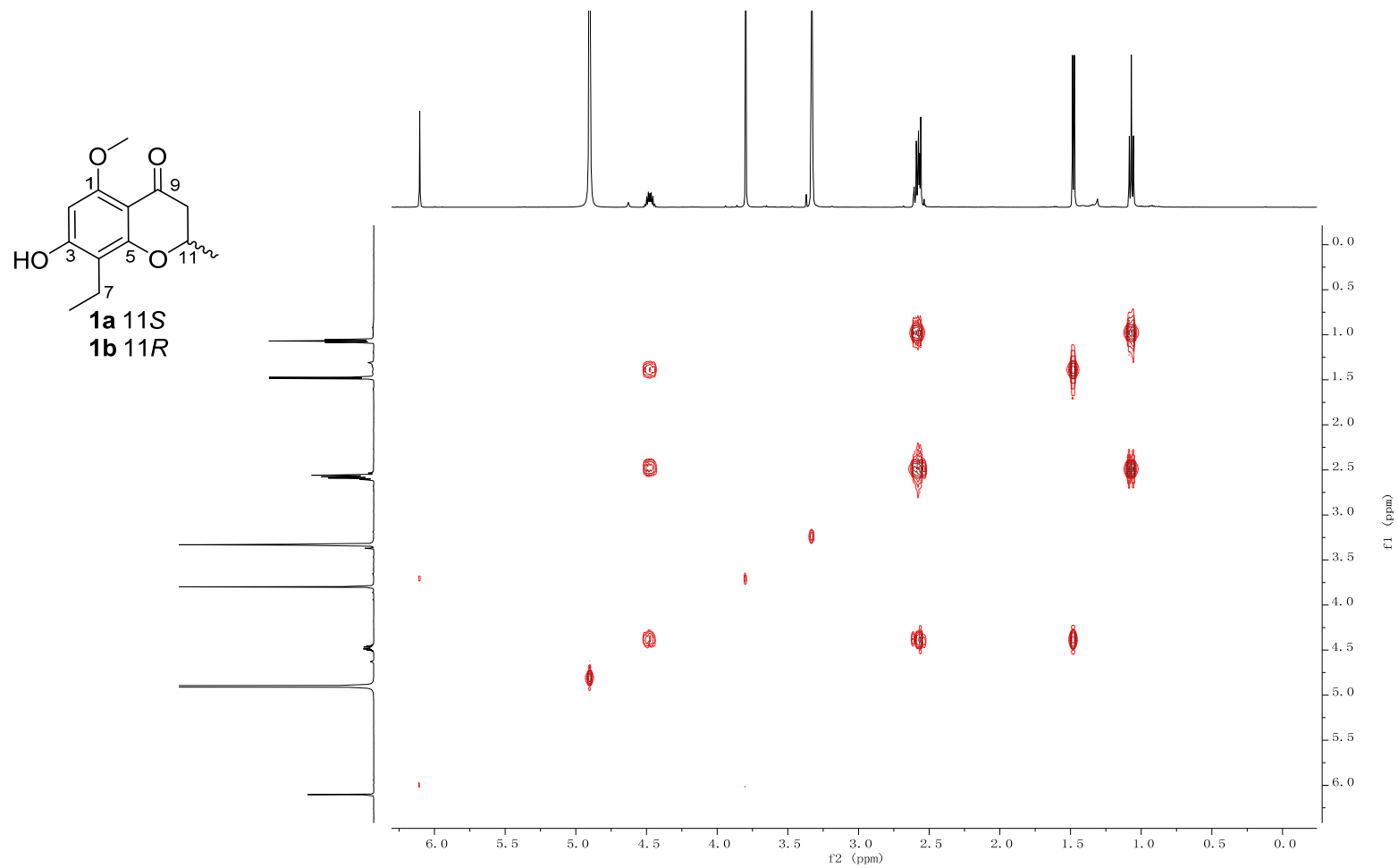


Figure S1. Spectroscopic data for **1**. (Continued)

(E) The HMBC spectrum of **1** in methanol- d_4 .

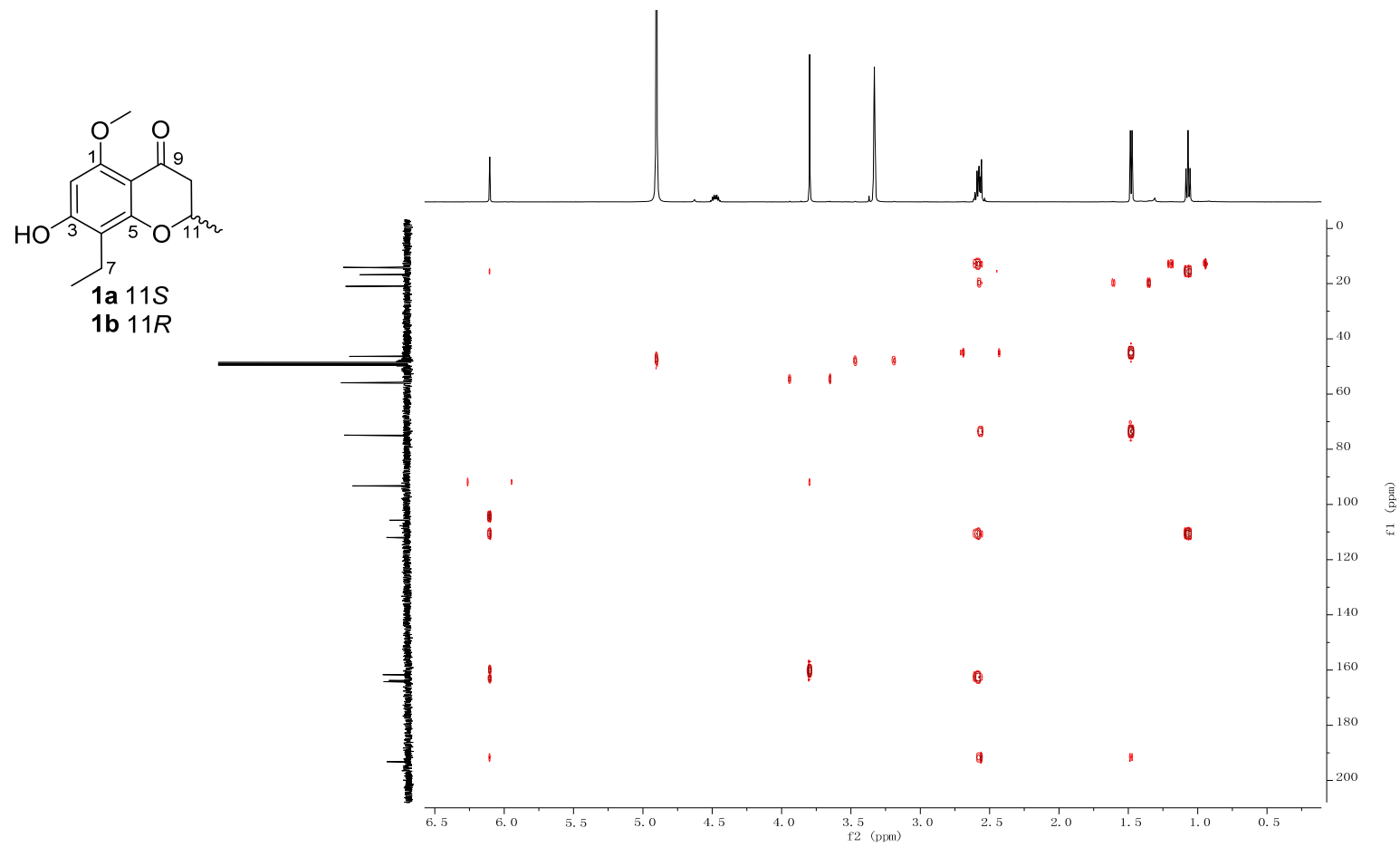
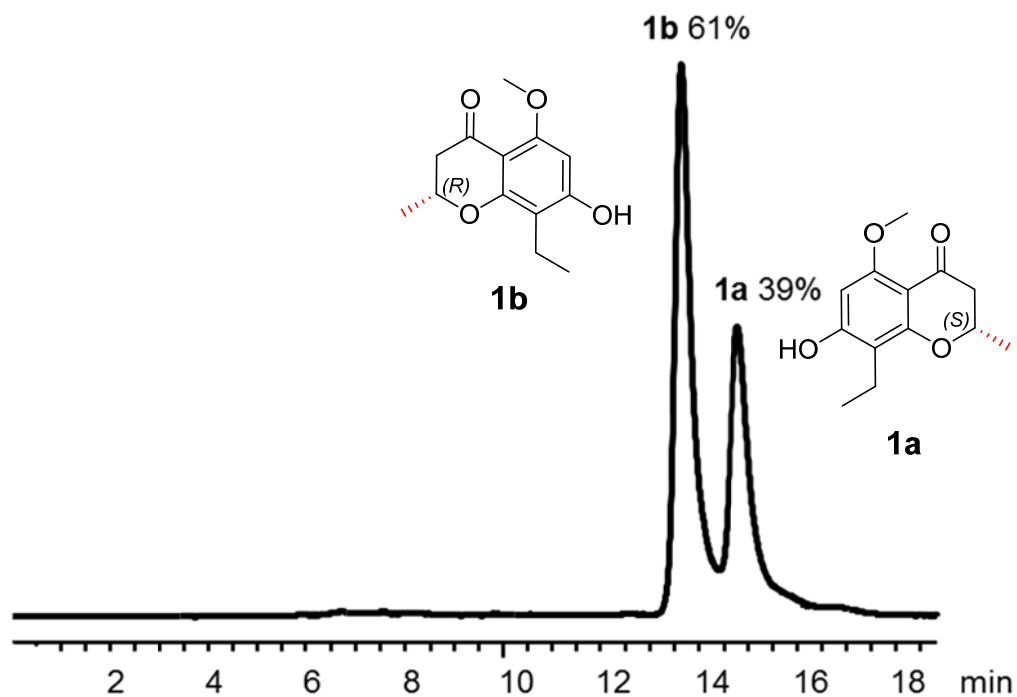


Figure S2. Chiral-phase HPLC analyses of compound **1**.



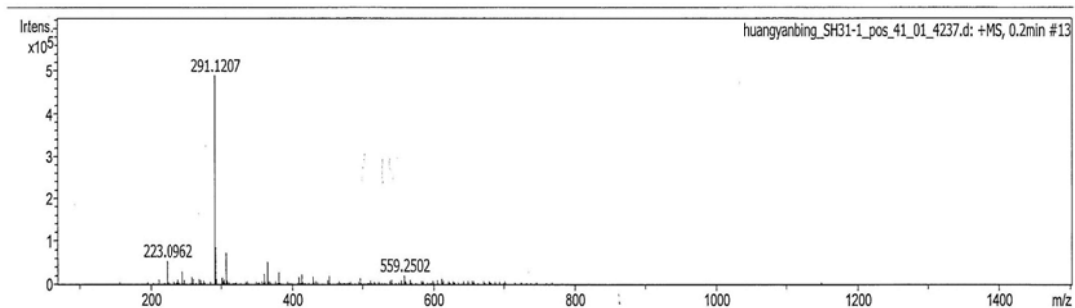
Chiral analysis of **1**, Isocratic elution: 0-20 min, A: 40%; B: 60%; Area of Peak-1 = 10848 (11*R*, t_{R1} = 13.6min), Area of Peak-2 = 6936 (11*S*, t_{R2} = 14.8min); 11*S*:11*R* = 1:1.5.

Column: Phenomenex Lux Chiral AD column, 4.6 × 250 mm, 5μM. Phenomenex instrument Co., LTD. Solvents: A, water; B, Acetonitrile,. Detection wavelength 300 nm. Flow rate 0.5 mL min⁻¹.

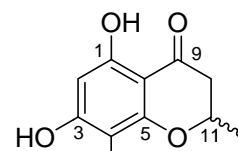
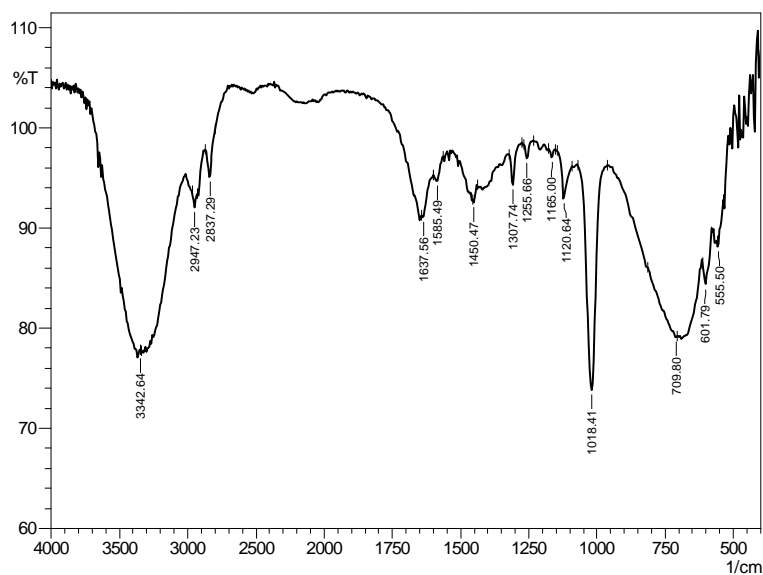
Figure S3. Spectroscopic data for **2**.

(A) HR-ESI-MS (a), IR (b), and UV (c) spectra of **2**.

(a). HR-ESI-MS



(b). IR



2a 11S

2b 11R

Chemical Formula: $C_{12}H_{14}O_4$

Exact Mass: 222.09

(c). UV

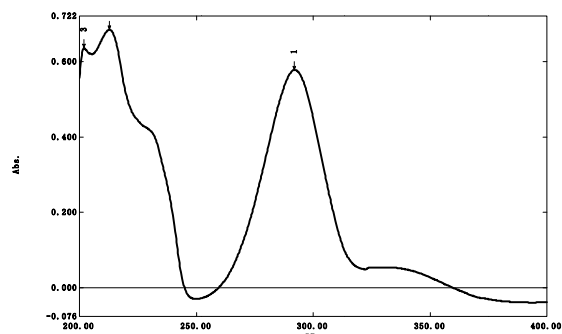


Figure S3. Spectroscopic data for **2**. (Continued)

(B) The ^1H NMR spectrum of **2** in methanol- d_4 .

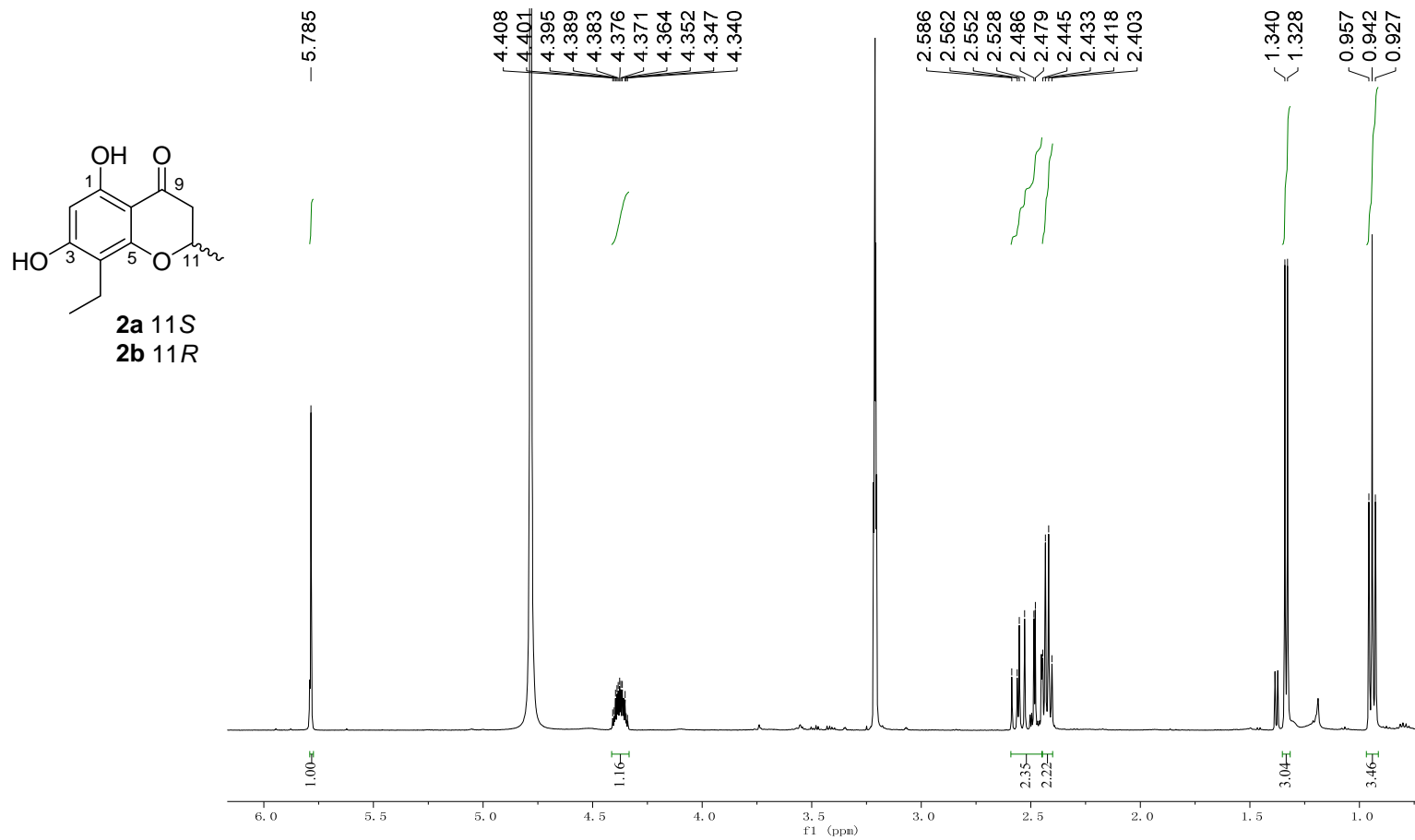


Figure S3. Spectroscopic data for **2**. (Continued)

(C) The ^{13}C spectrum of **2** in methanol- d_4 .

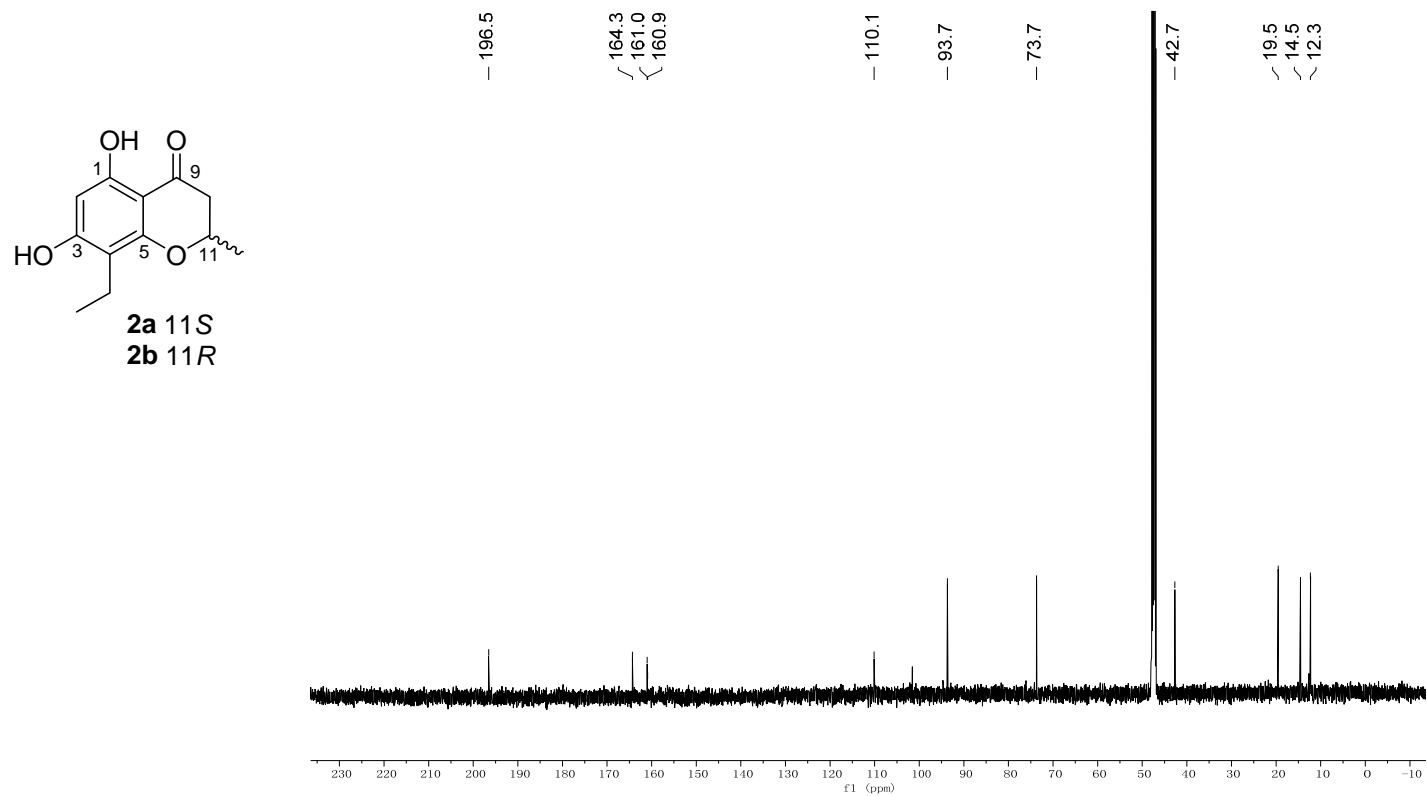


Figure S3. Spectroscopic data for **2**. (Continued)

(D) The HSQC spectrum of **2** in methanol-*d*₄.

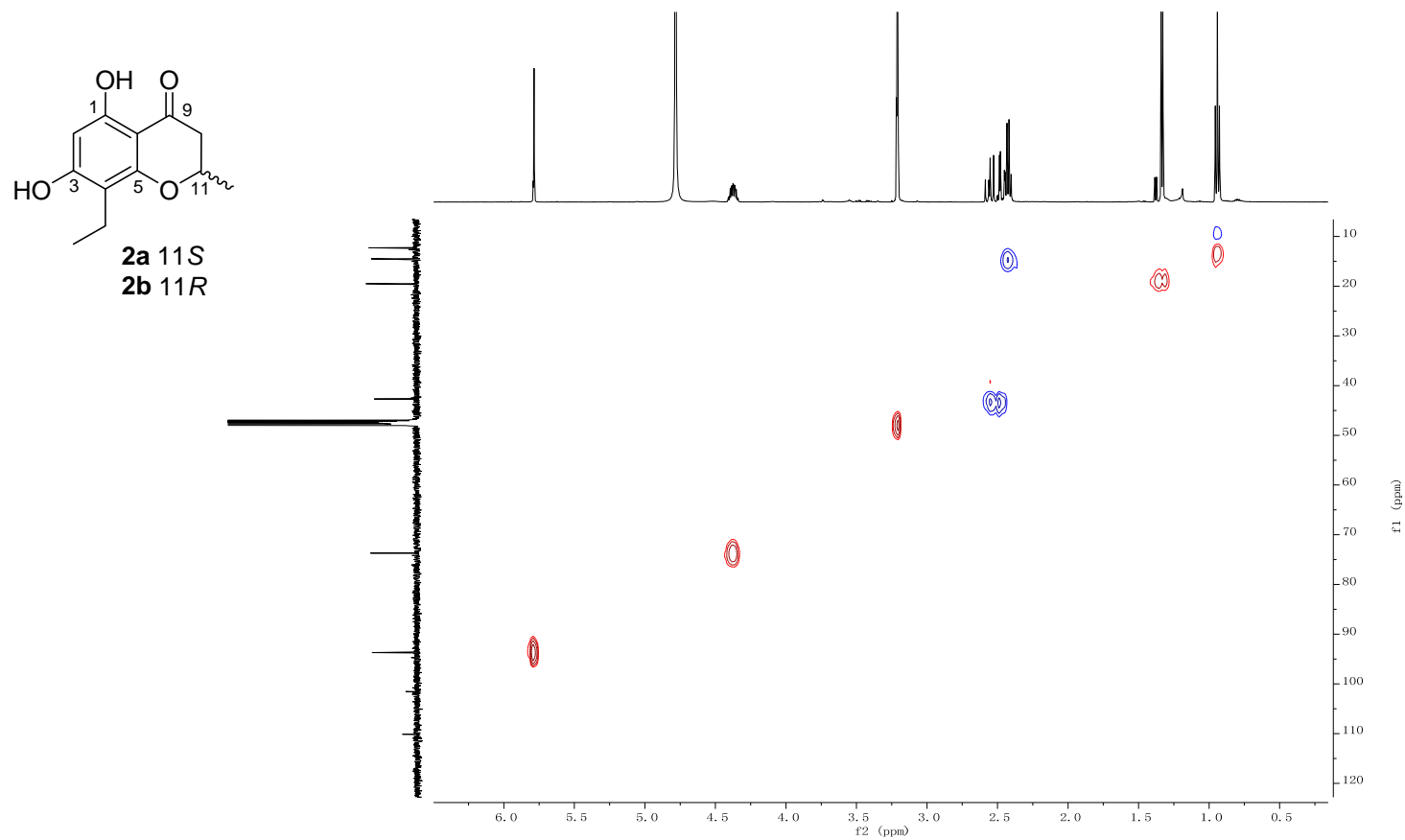


Figure S3. Spectroscopic data for **2**. (Continued)

(E) The COSY spectrum of **2** in methanol- d_4 .

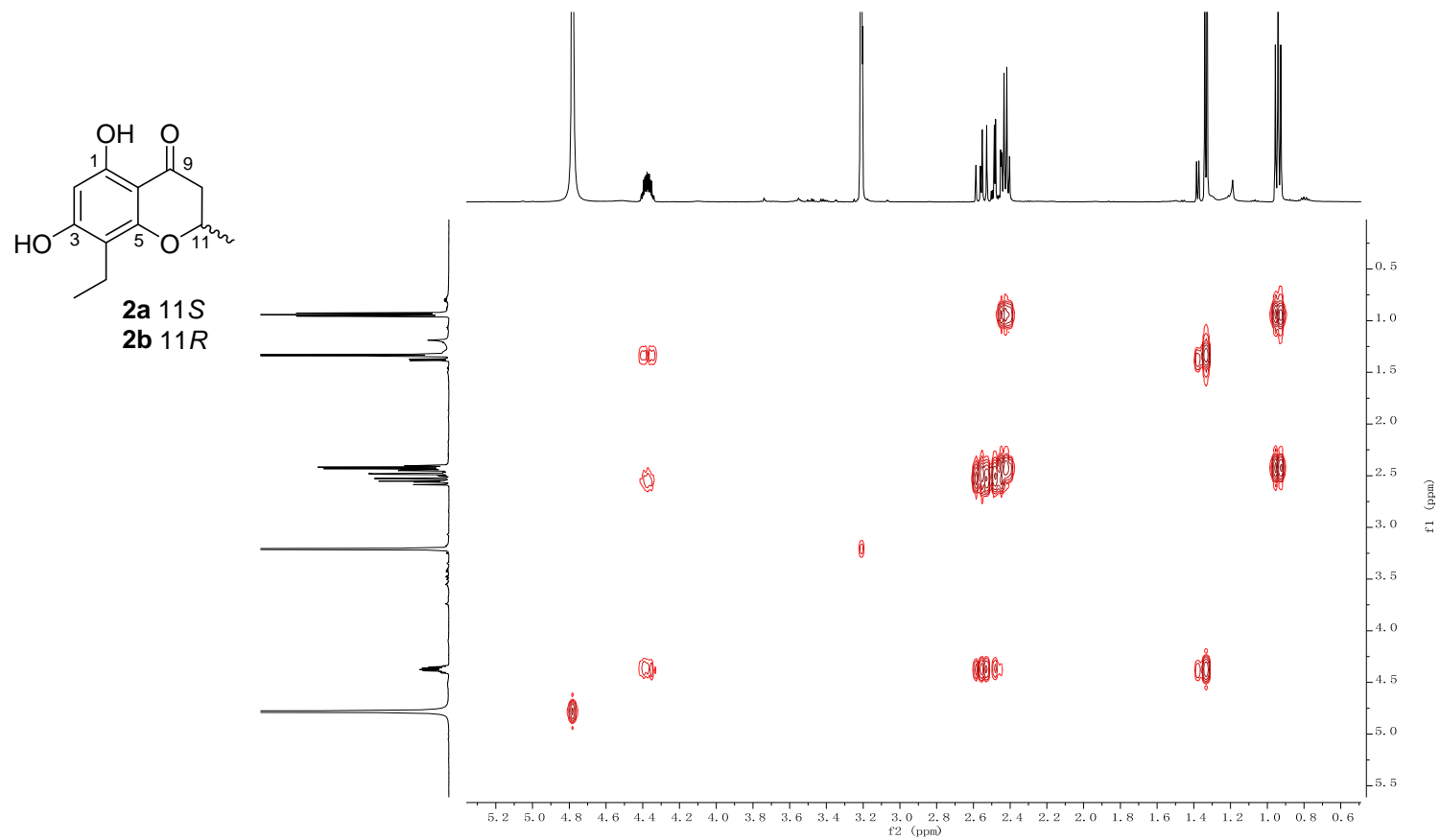


Figure S3. Spectroscopic data for **2**. (Continued)

(E) The HMBC spectrum of **2** in methanol- d_4 .

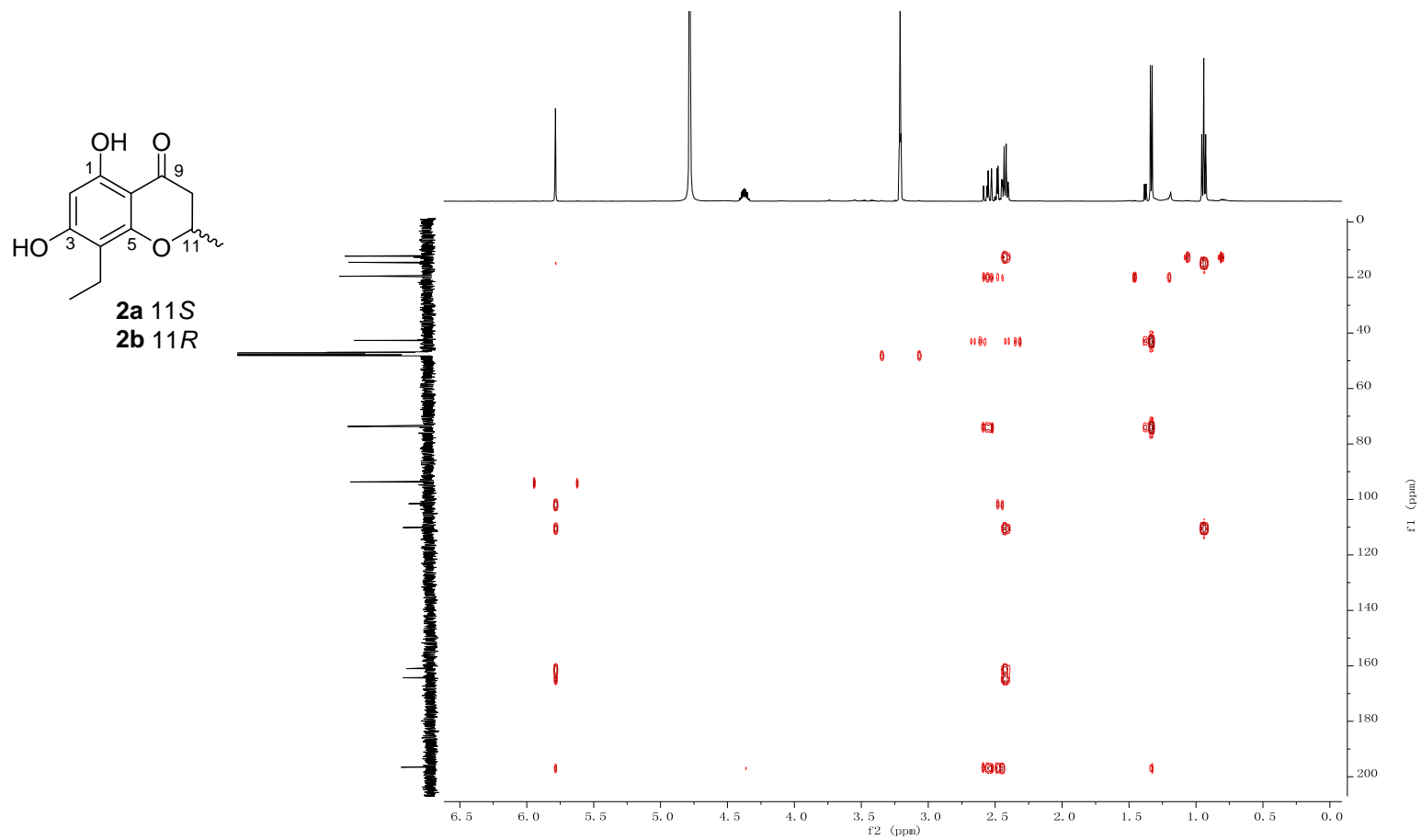
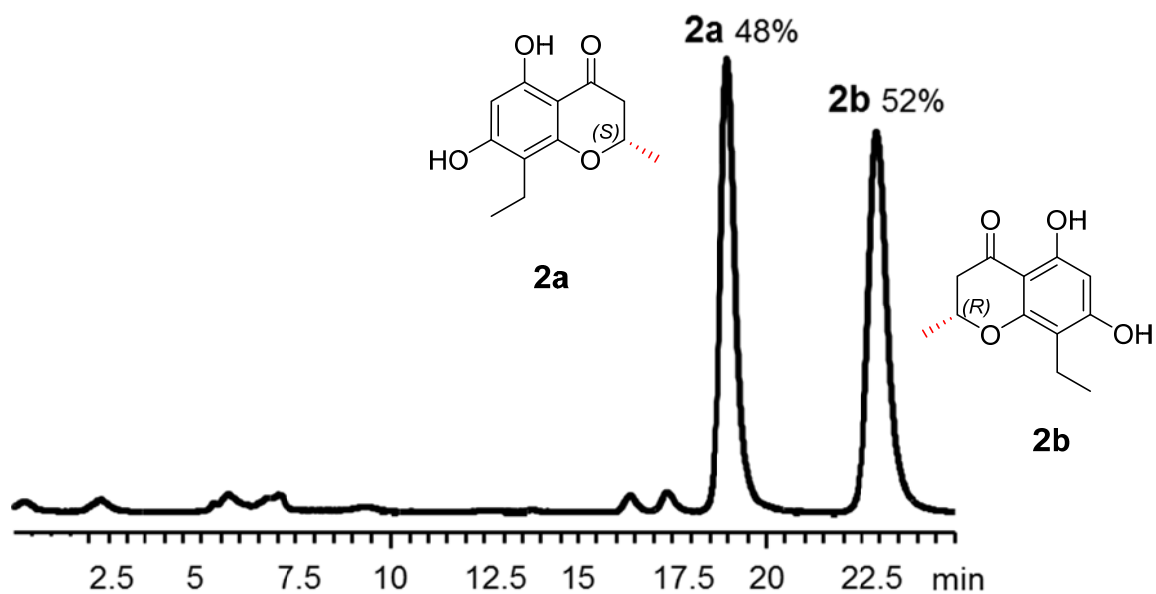


Figure S4. Chiral-phase HPLC analyses of compound **2**.

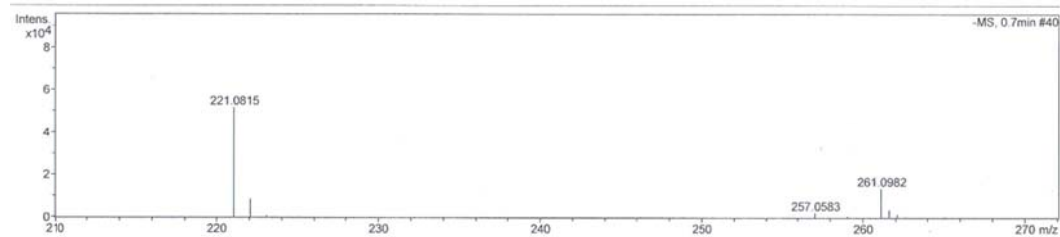


Chiral analysis of **2**, Isocratic elution: 0-25 min, A:48%; B:52%; Area of Peak-1 = 13980 (11*S*, t_{R1} = 19.0min), Area of Peak-2 = 14897 (11*R*, t_{R2} = 22.9min); 11*S*: 11*R* = 0.9:1 Column: Phenomenex Lux Chiral AD column, 4.6 × 250 mm, 5μM. Phenomenex instrument Co., LTD. Solvents: A, water; B, Acetonitrile. Detection wavelength 300 nm. Flow rate 0.5 mL min⁻¹.

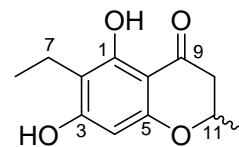
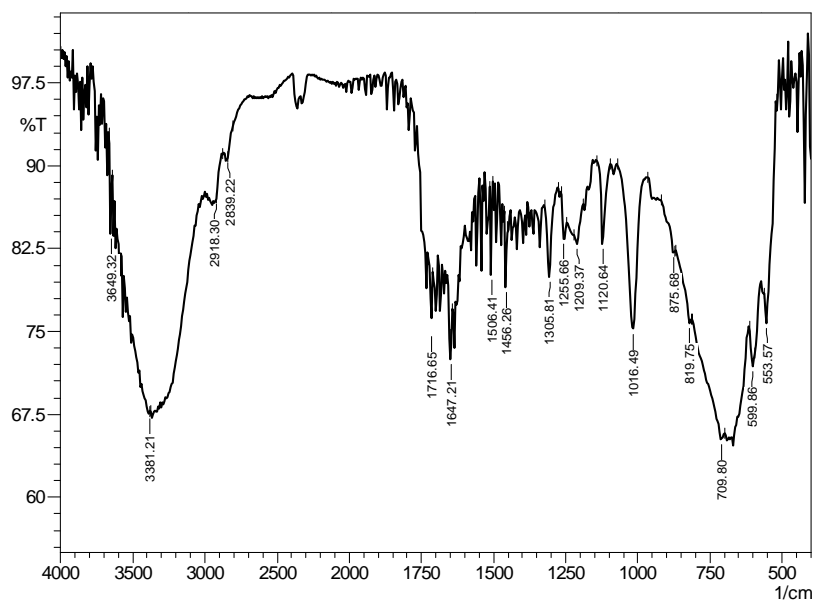
Figure S5. Spectroscopic data for **3**.

(A) HR-ESI-MS (a), IR (b), and UV (c) spectra of SH31-18 (**3**).

(a). HR-ESI-MS



(b). IR



3a 11S
3b 11R

Chemical Formula: C₁₂H₁₄O₄
Exact Mass: 222.09

(c). UV

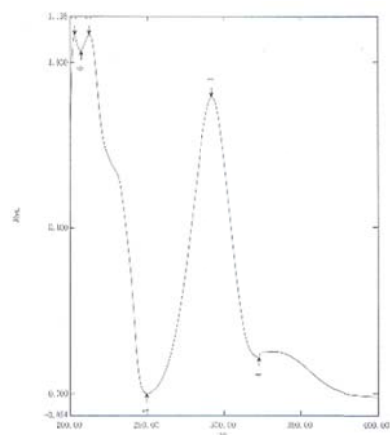


Figure S5. Spectroscopic data for **3**. (Continued)

(B) The ^1H NMR spectrum of **3** in methanol- d_4 .

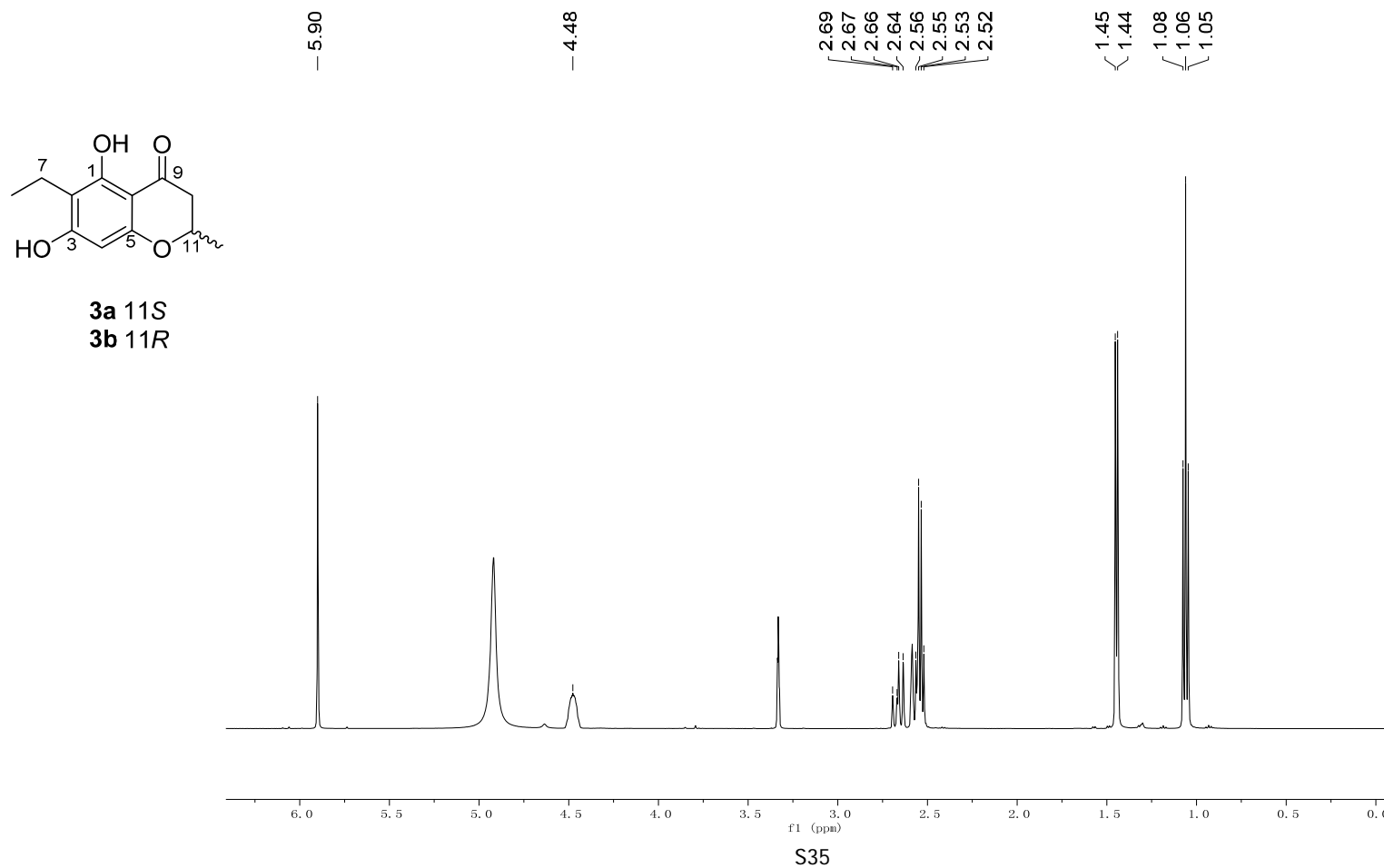


Figure S5. Spectroscopic data for **3**. (Continued)

(C) The ^{13}C and DEPT 135 NMR spectrum of **3** in methanol- d_4 .

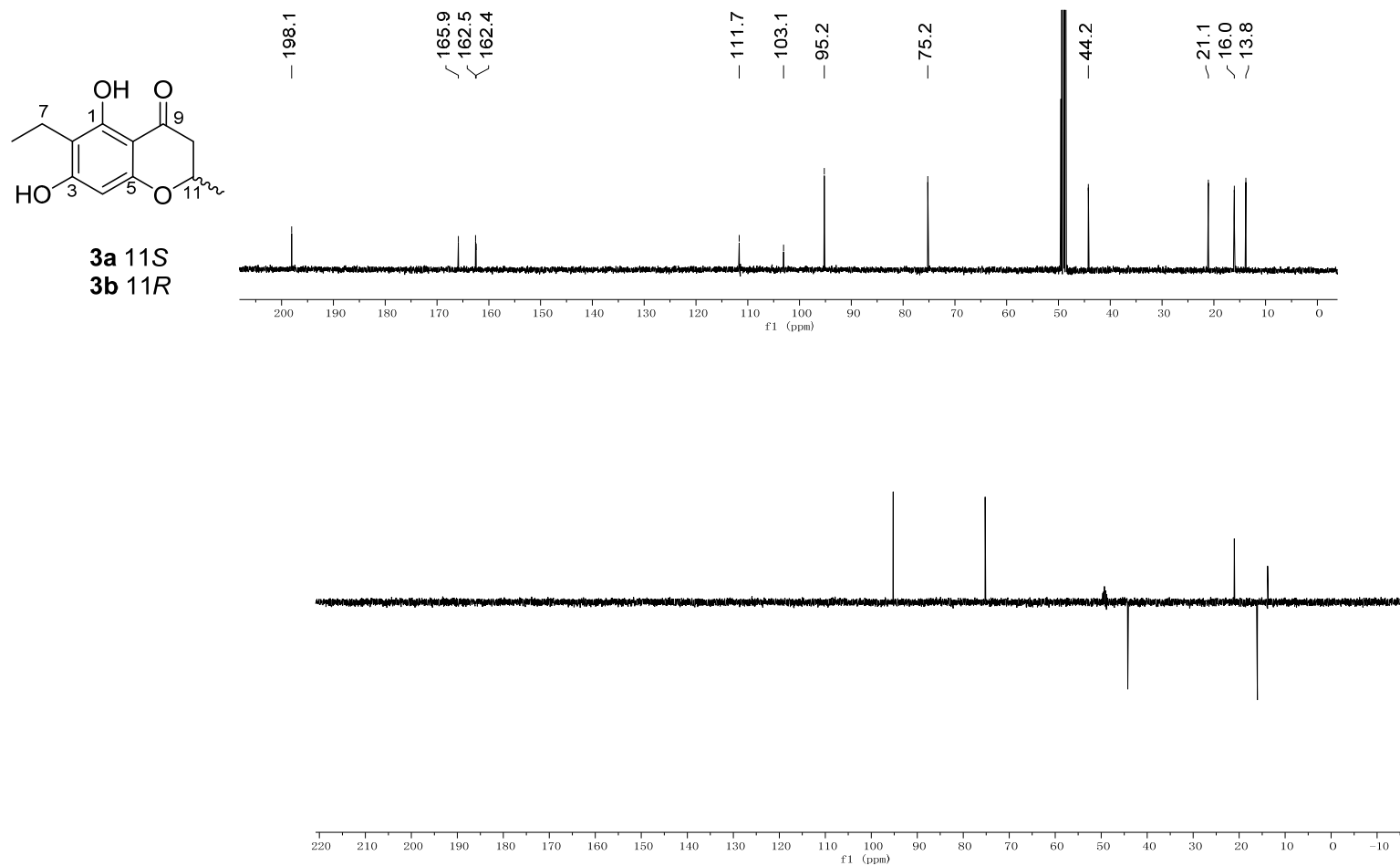


Figure S5. Spectroscopic data for **3**. (Continued)

(D) The HSQC spectrum of **3** in methanol-*d*₄.

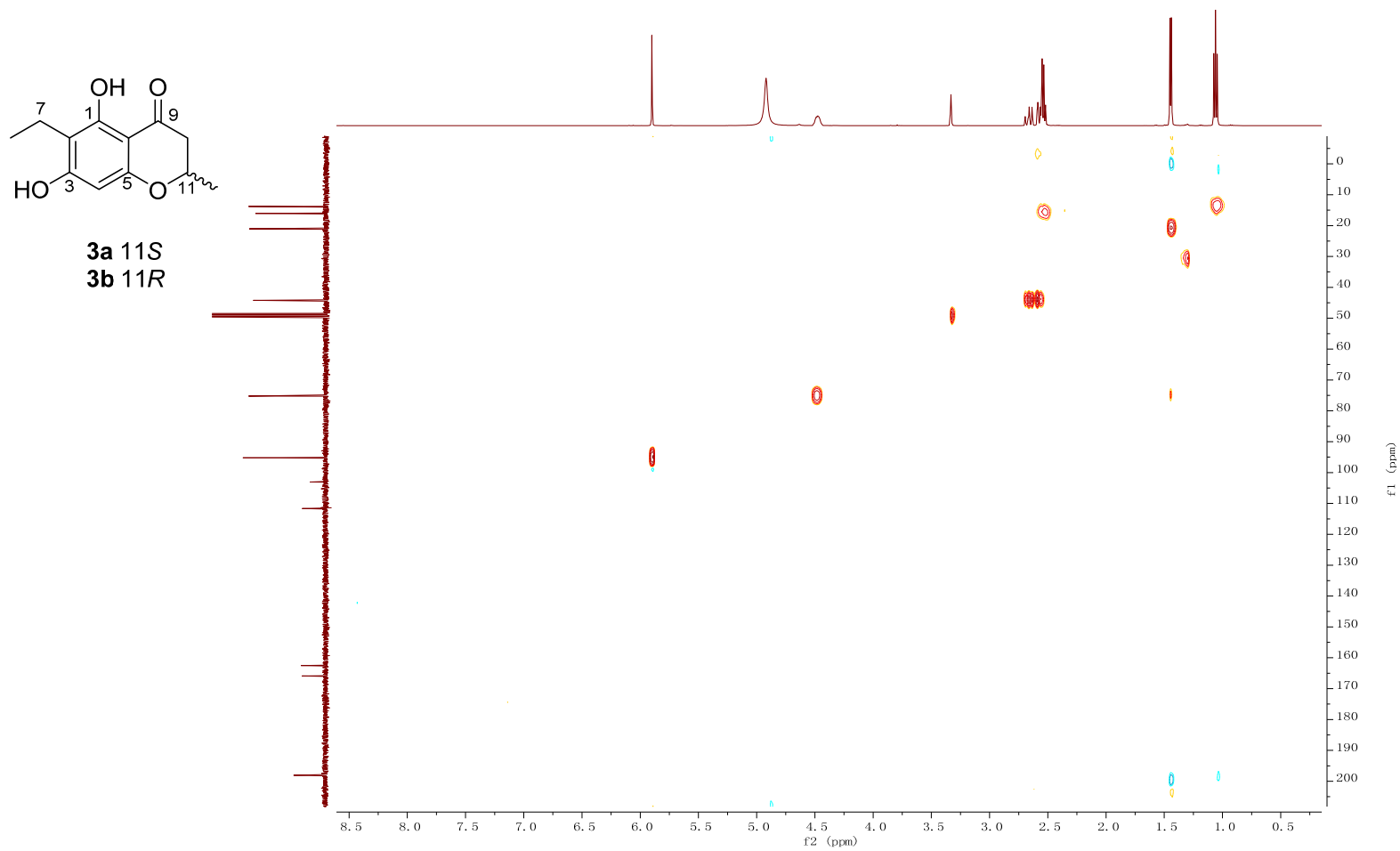


Figure S5. Spectroscopic data for **3**. (Continued)

(E) The COSY spectrum of **3** in methanol- d_4 .

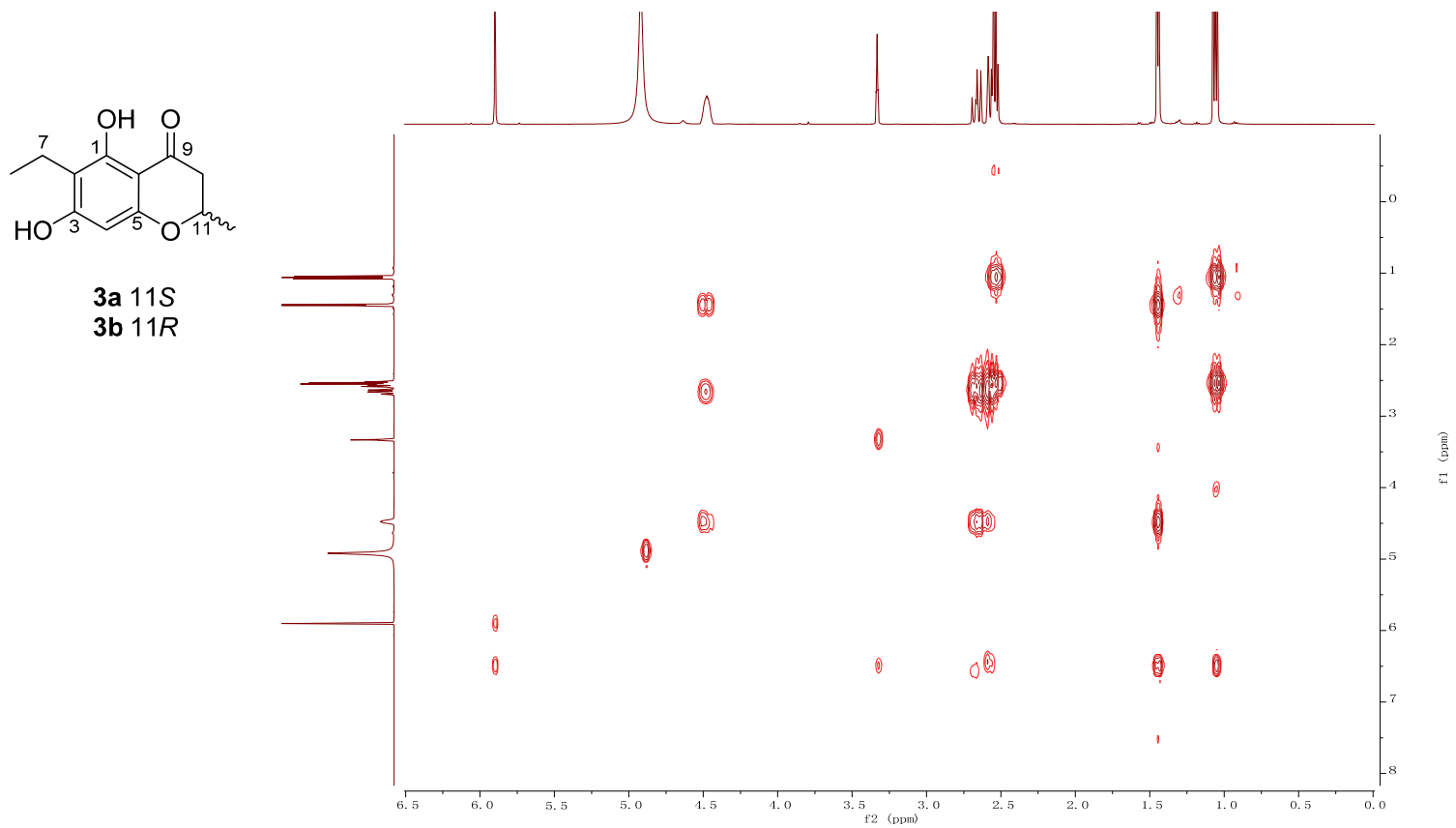


Figure S5. Spectroscopic data for **3**. (Continued)

(F) The HMBC spectrum of **3** in methanol- d_4 .

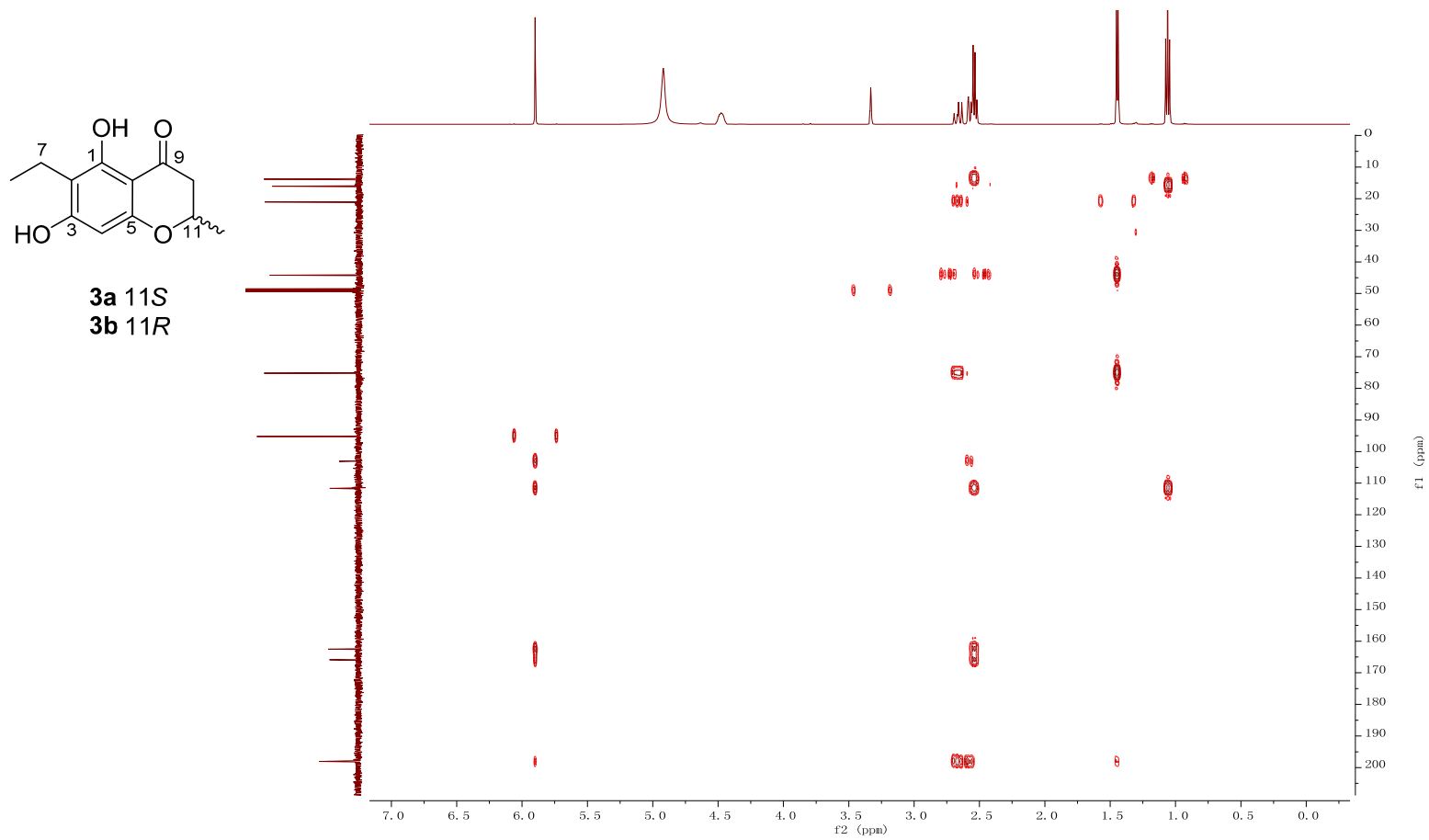
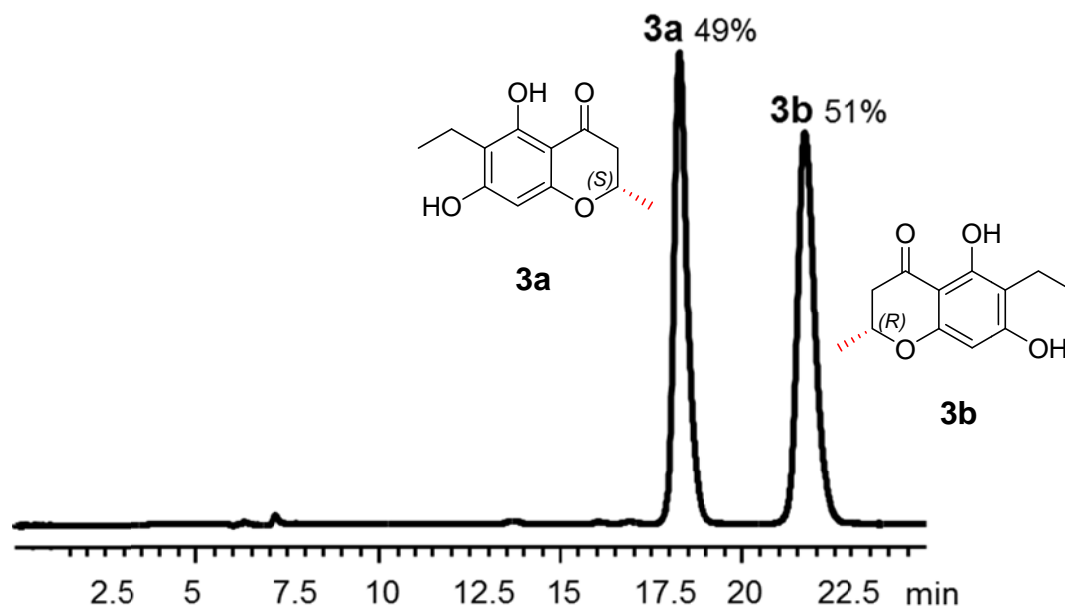


Figure S6. Chiral-phase HPLC analyses of compound **3**.

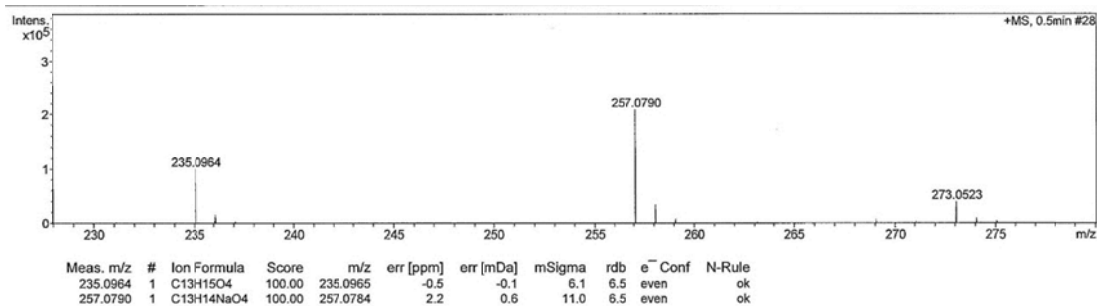


Chiral analysis of **3**, Isocratic elution: 0-25 min, A:50%:B:50%; Area of Peak-1 = 24029 (11*S*, t_{R1} = 18.3min), Area of Peak-2 = 25472 (11*R*, t_{R2} = 21.7min); 11*S*:11*R* = 1:1. Column: Phenomenex Lux Chiral AD column, 4.6 × 250 mm, 5μM. Phenomenex instrument Co., LTD. Solvents: A, water; B, Acetonitrile. Detection wavelength 300 nm. Flow rate 0.5 mL min⁻¹

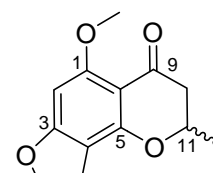
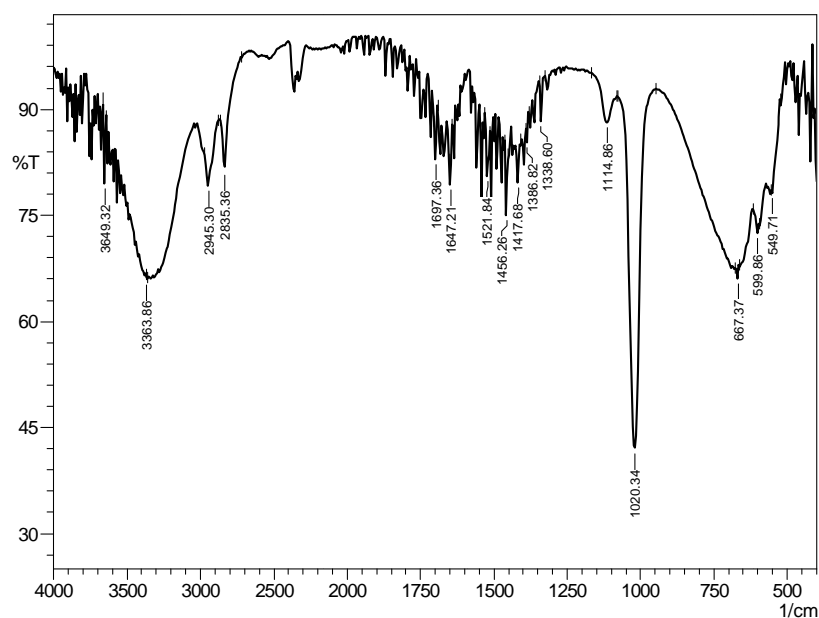
Figure S7. Spectroscopic data for **4**.

(A) HR-ESI-MS (a), IR (b), and UV (c) spectra of **4**.

(a). HR-ESI-MS



(b). IR



4a 11S
4b 11R

Chemical Formula: C₁₃H₁₄O₄
Exact Mass: 234.09

(c). UV

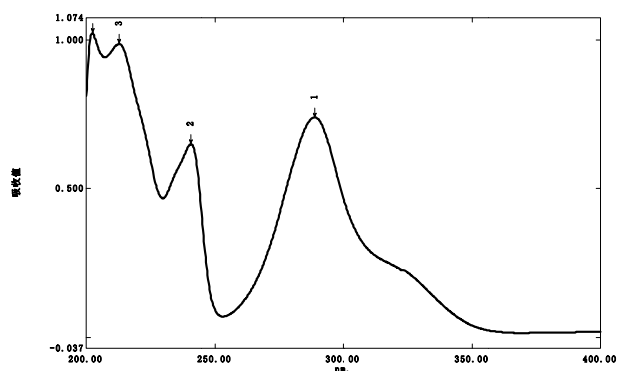


Figure S7. Spectroscopic data for **4** (Continued)

(B) The ^1H NMR spectrum of **4** in CDCl_3 .

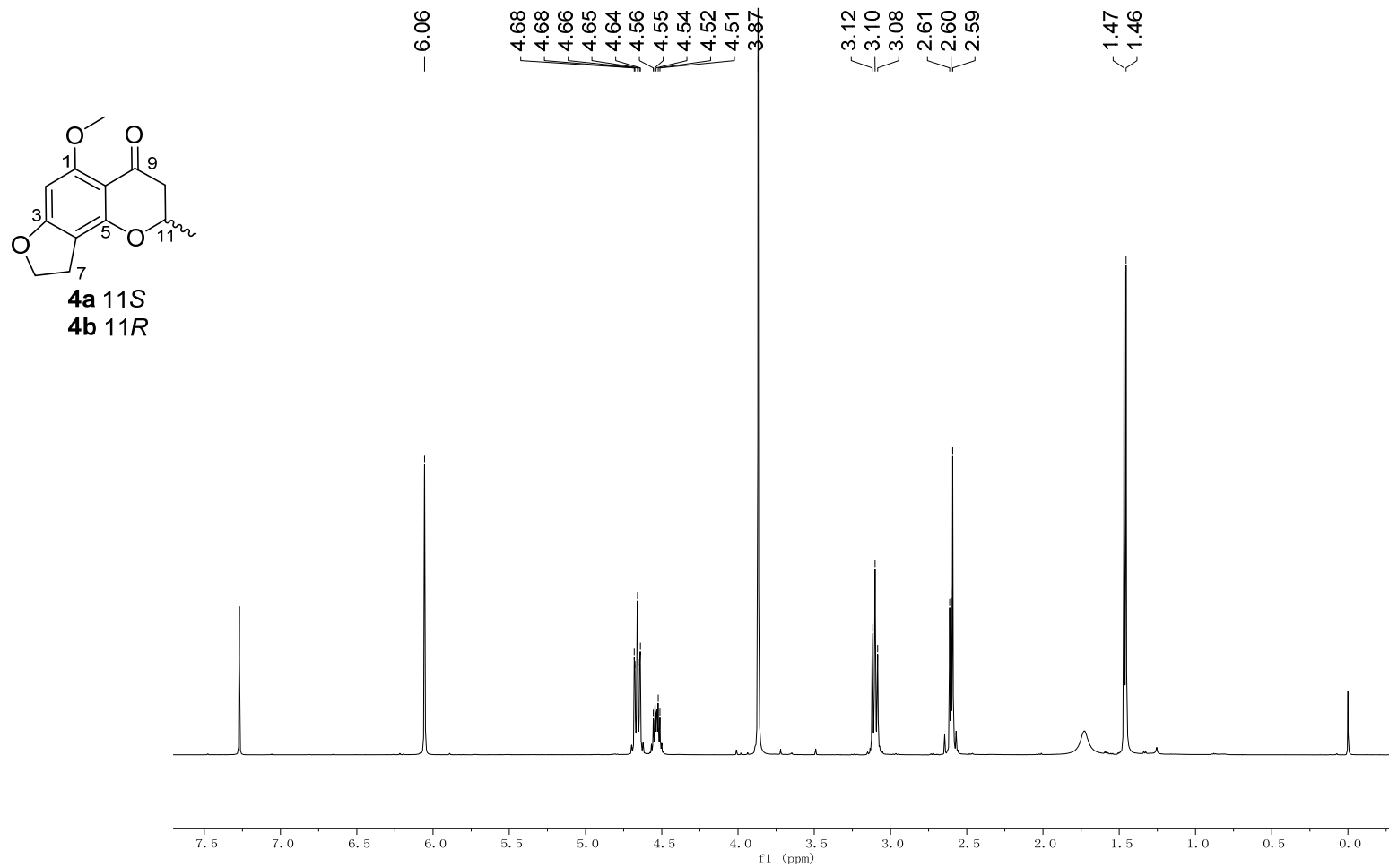


Figure S7. Spectroscopic data for **4**. (Continued)

(C) The ^{13}C and DEPT 135 NMR spectrum of **4** in CDCl_3 .

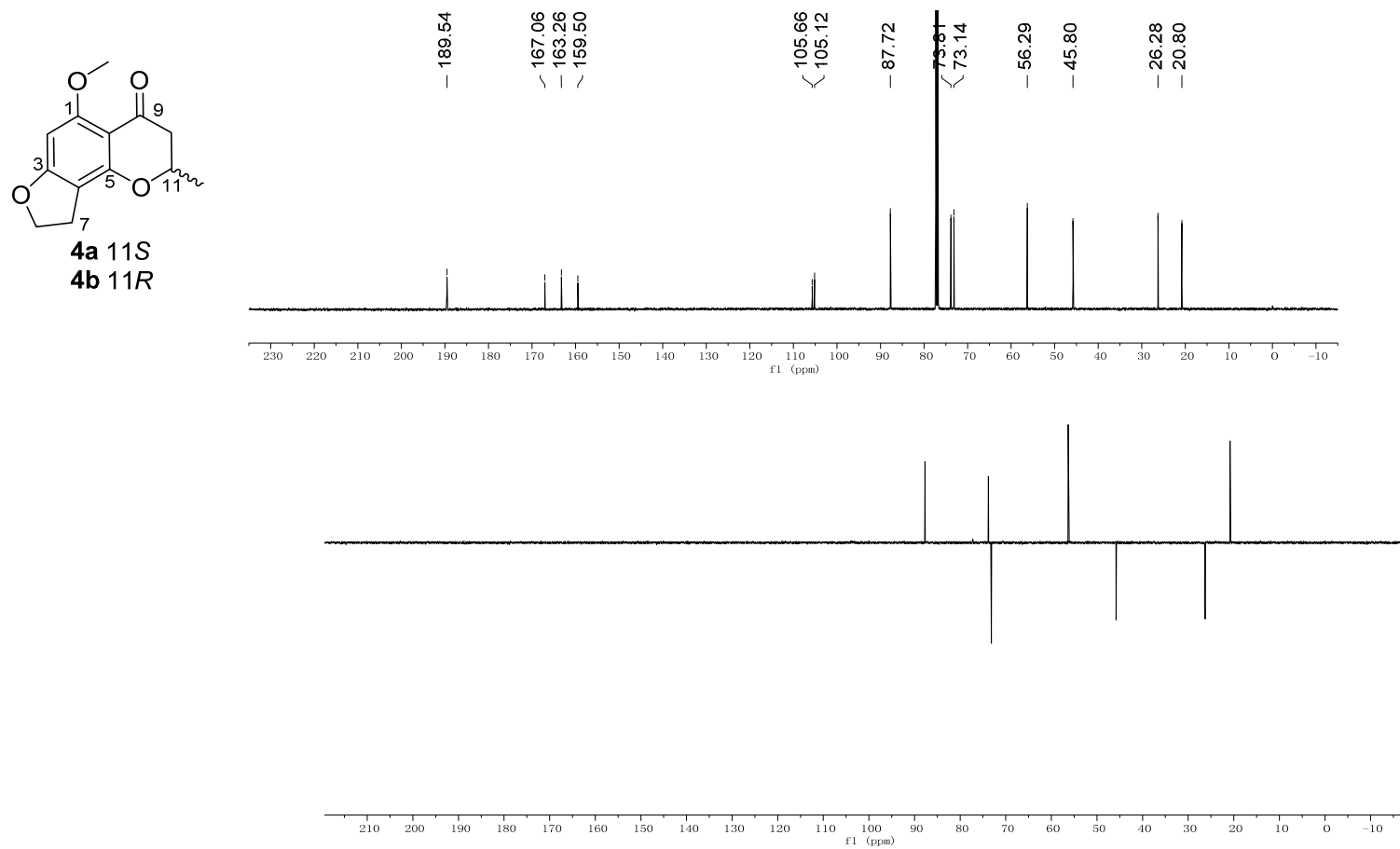


Figure S7. Spectroscopic data for **4**. (Continued)

(D) The HSQC spectrum of **4** in CDCl₃.

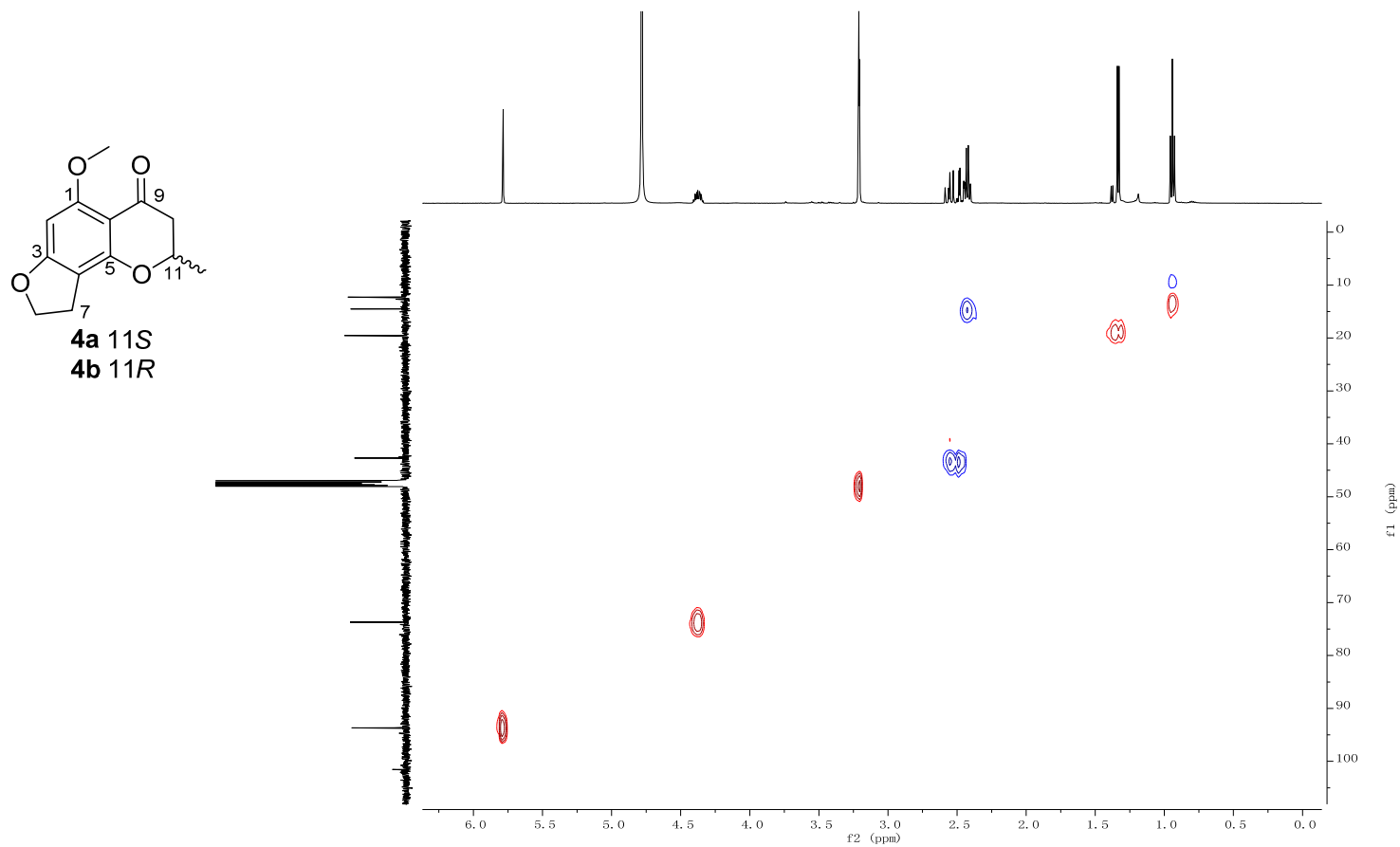


Figure S7. Spectroscopic data for **4**. (Continued)

(E) The COSY spectrum of **4** in CDCl₃.

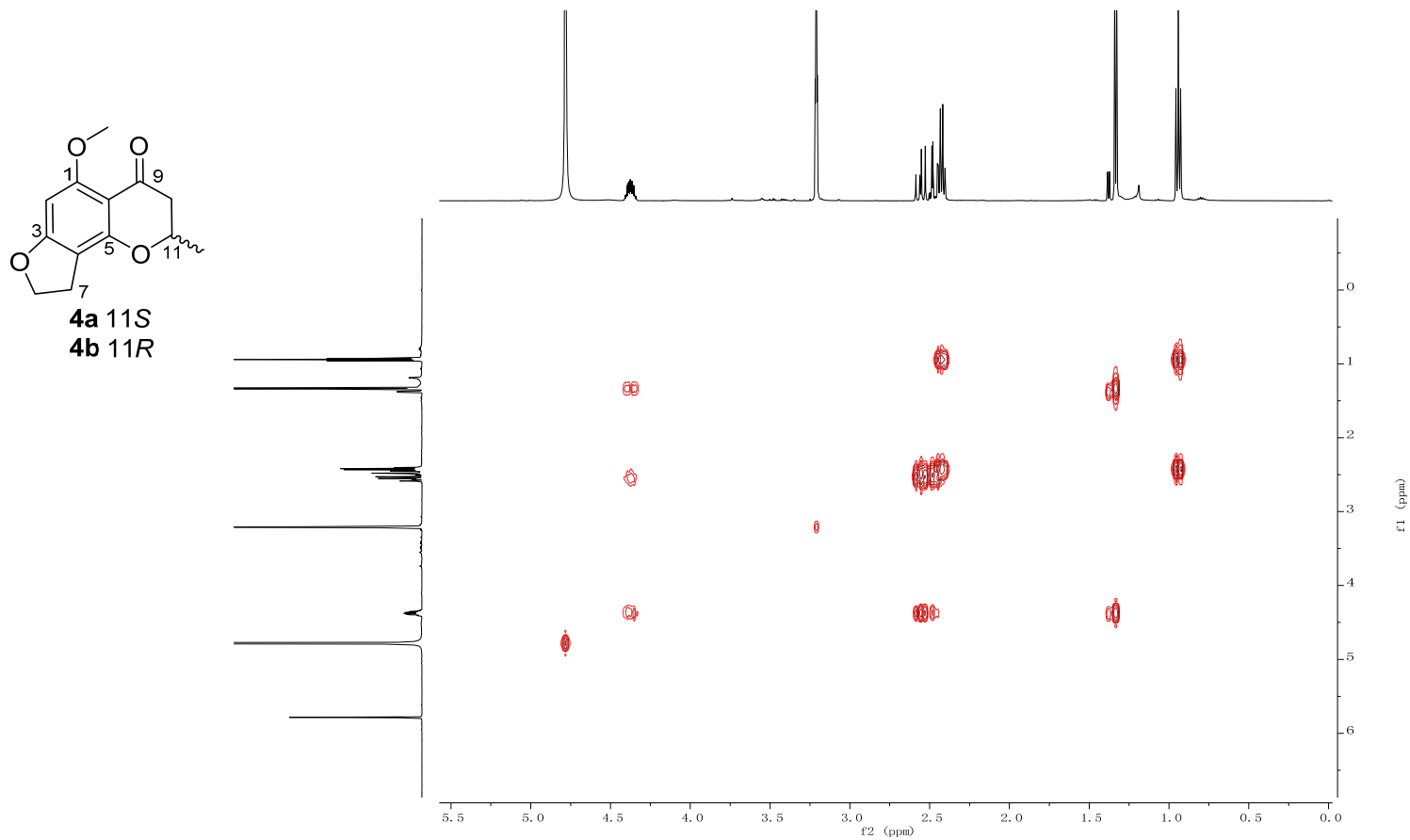


Figure S7. Spectroscopic data for **4**. (Continued)

(E) The HMBC spectrum of **4** in CDCl₃.

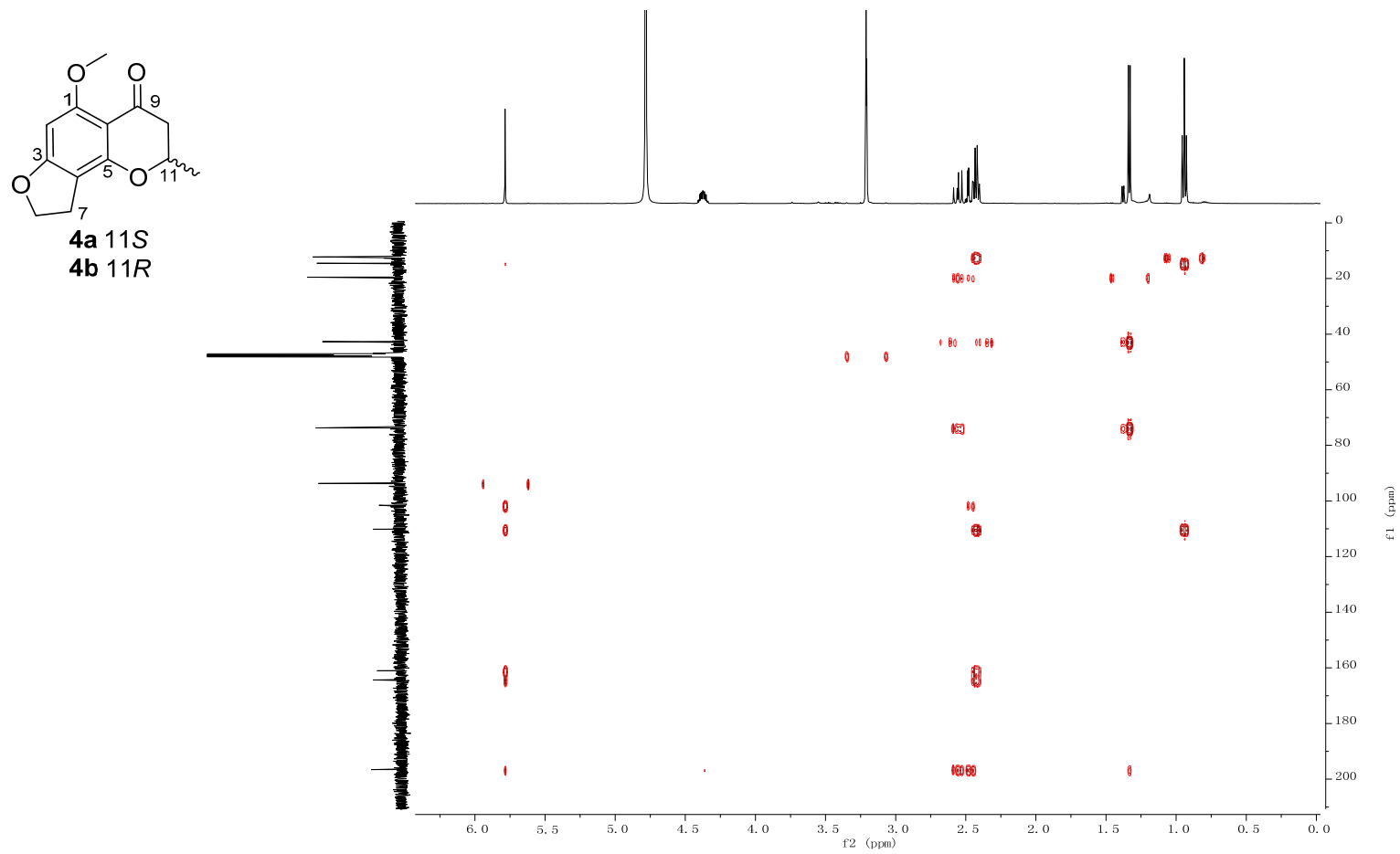
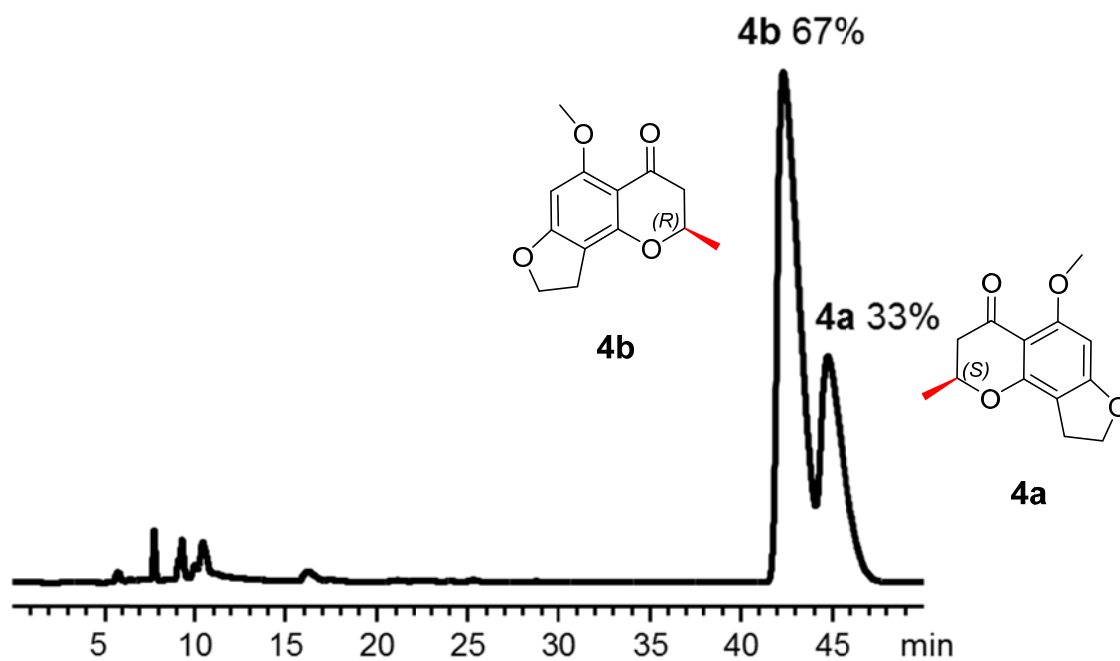


Figure S8. Chiral-phase HPLC analyses of compound **4**.



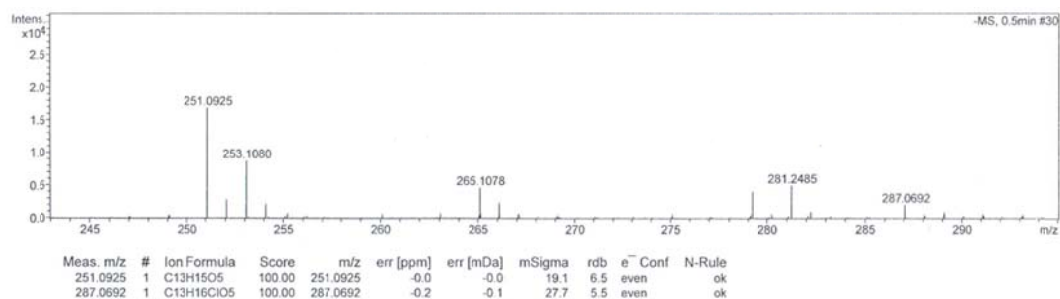
Chiral analysis of **4**, Isocratic elution: 0-50 min, A:32%; B:68%; Area of Peak-1 = 109828 (11*R*, t_{R1} = 42.3min), Area of Peak-2 = 53145 (11*S*, t_{R2} = 44.7min); 11*S* : 11*R* = 1 : 2.

Column: Phenomenex Lux Amylose-1 column, 4.6 × 250 mm, 5μM. Phenomenex instrument Co., LTD. Solvents: A, water; B, Acetonitrile. Detection wavelength 300 nm. Flow rate 0.5 mL min⁻¹.

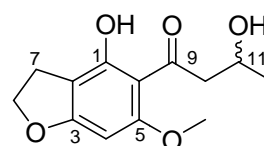
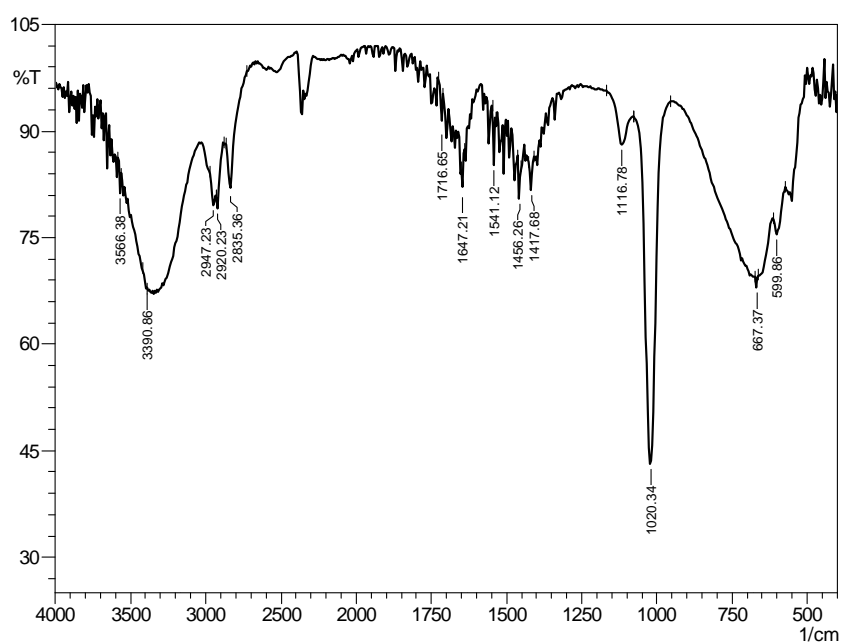
Figure S9. Spectroscopic data for **5**.

(A) HR-ESI-MS (a), IR (b), and UV (c) spectra of SH31-23 (**5**).

(a). HR-ESI-MS



(b). IR



5a 11R
5b 11S

Chemical Formula:
C₁₃H₁₆O₅
Exact Mass: 252.10

(c). UV

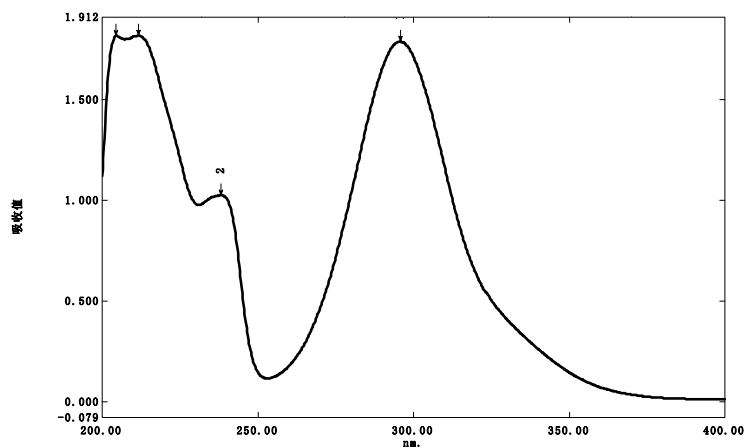


Figure S9. Spectroscopic data for **5**. (Continued)

(B) The ^1H NMR spectrum of **5** in methanol- d_4 .

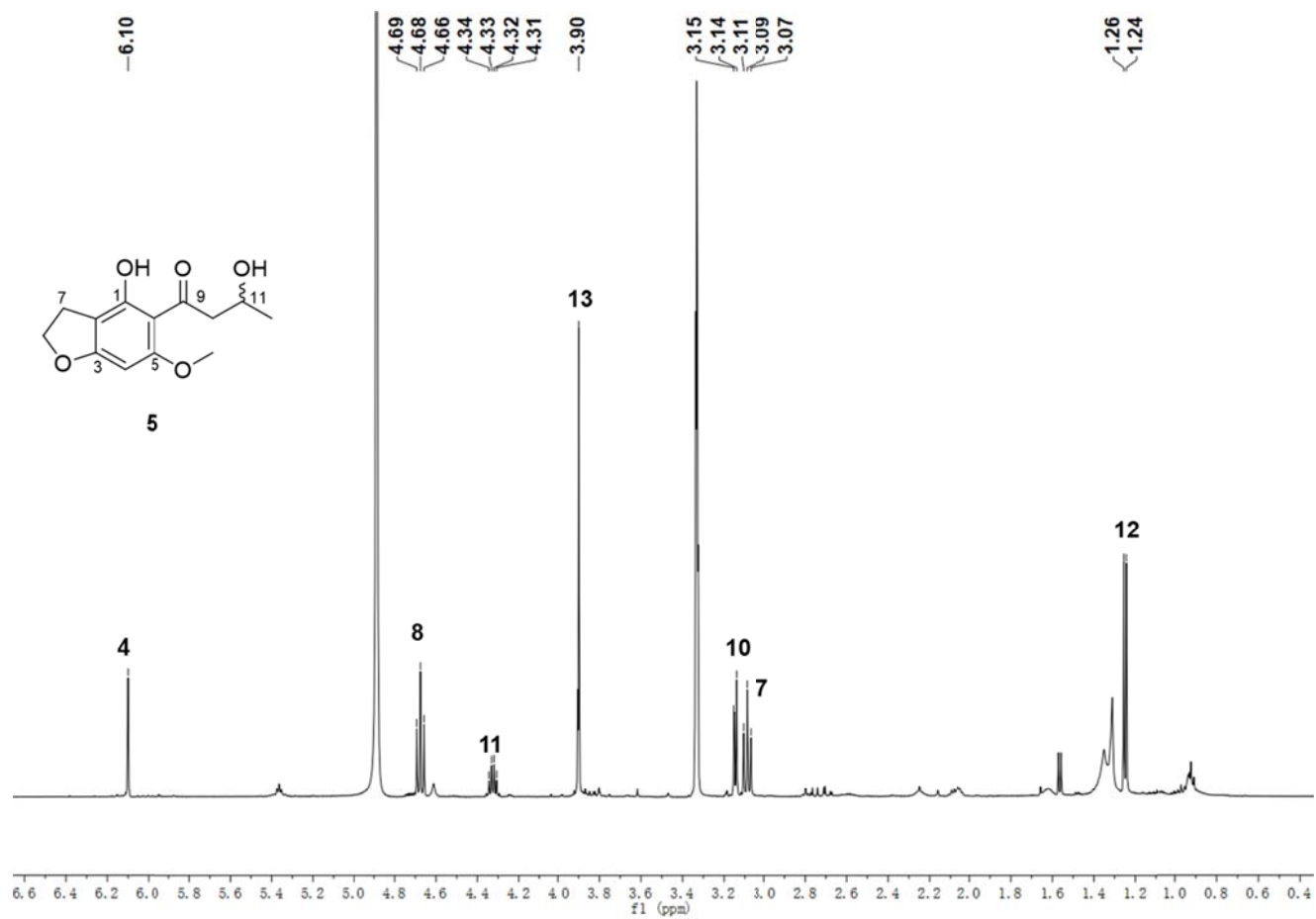


Figure S9. Spectroscopic data for **5**. (Continued)

(C) The ^{13}C and DEPT 135 NMR spectrum of **5** in methanol- d_4 .

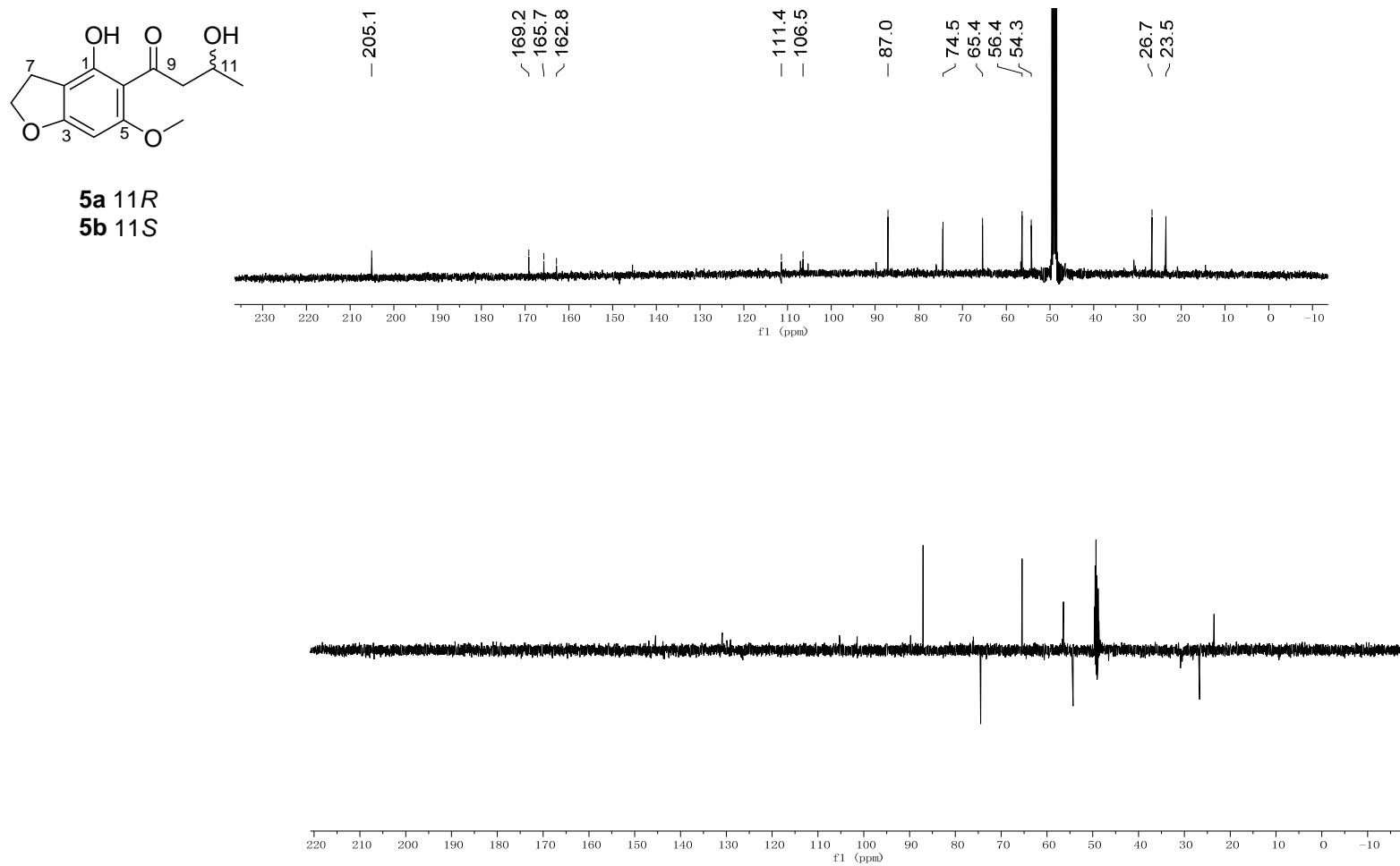


Figure S9. Spectroscopic data for **5**. (Continued)

(D) The HSQC spectrum of **5** in methanol-*d*₄.

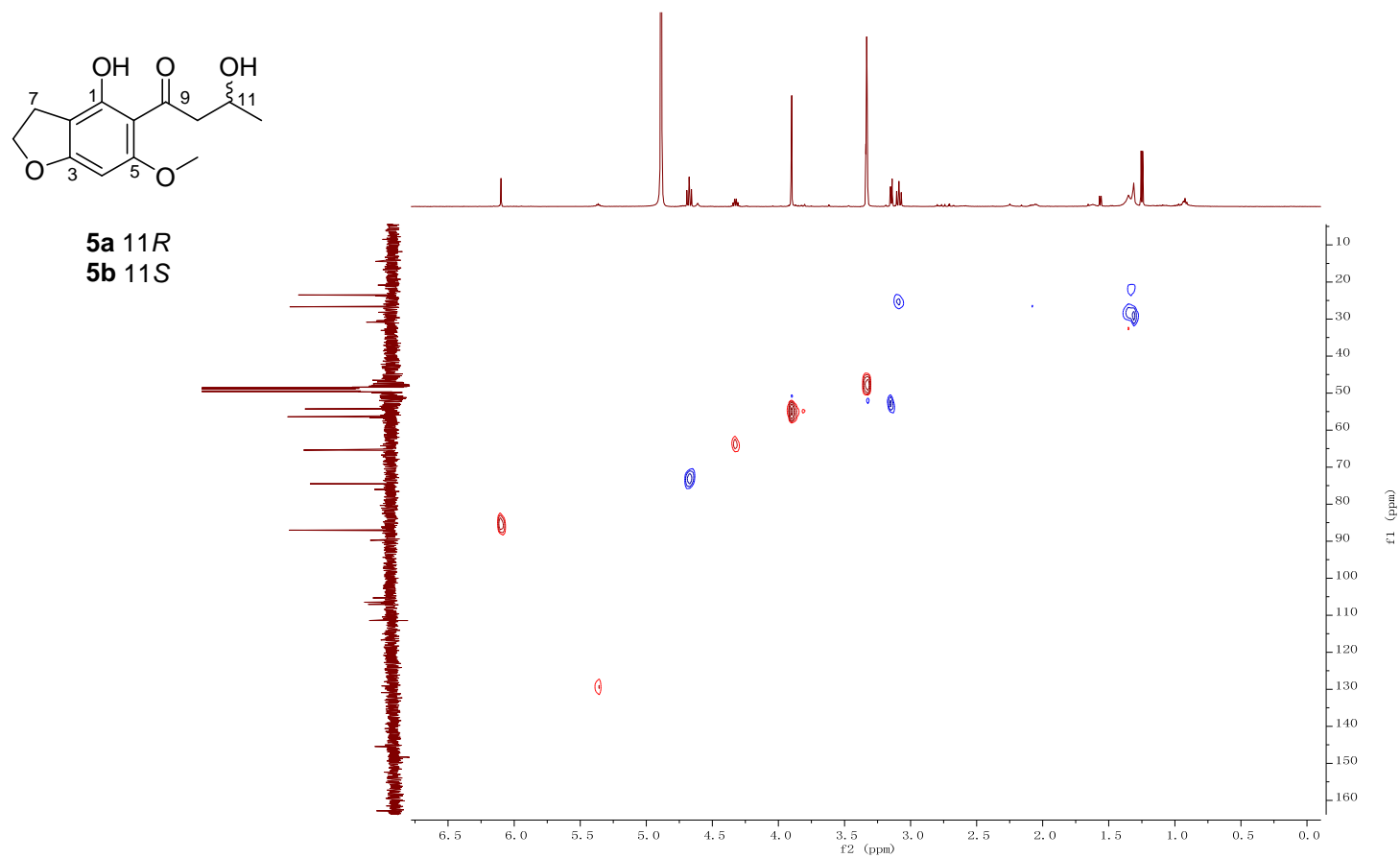


Figure S9. Spectroscopic data for **5**. (Continued)

(E) The COSY spectrum of **5** in methanol- d_4 .

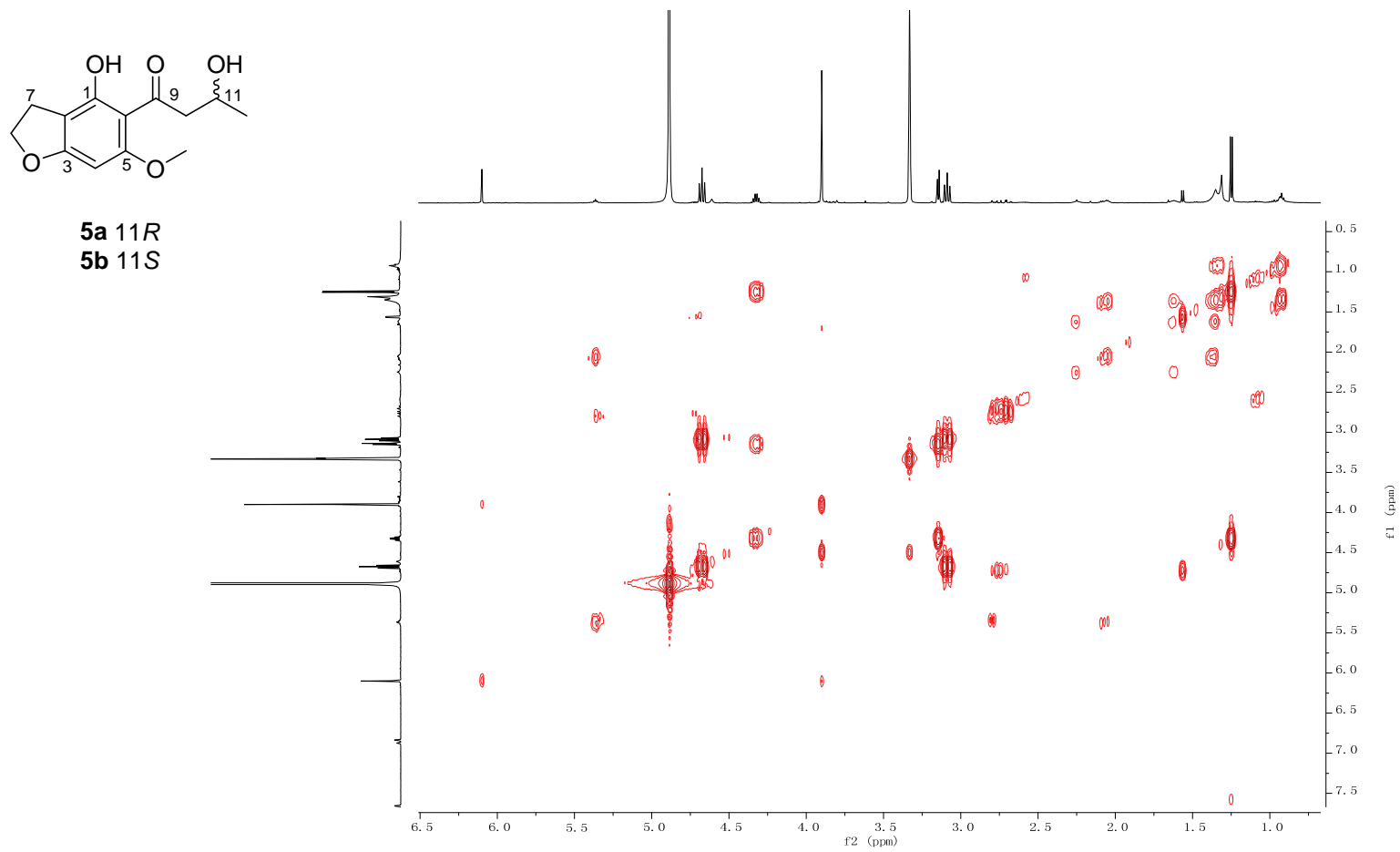


Figure S9. Spectroscopic data for **5**. (Continued)

(F) The HMBC spectrum of **5** in methanol- d_4 .

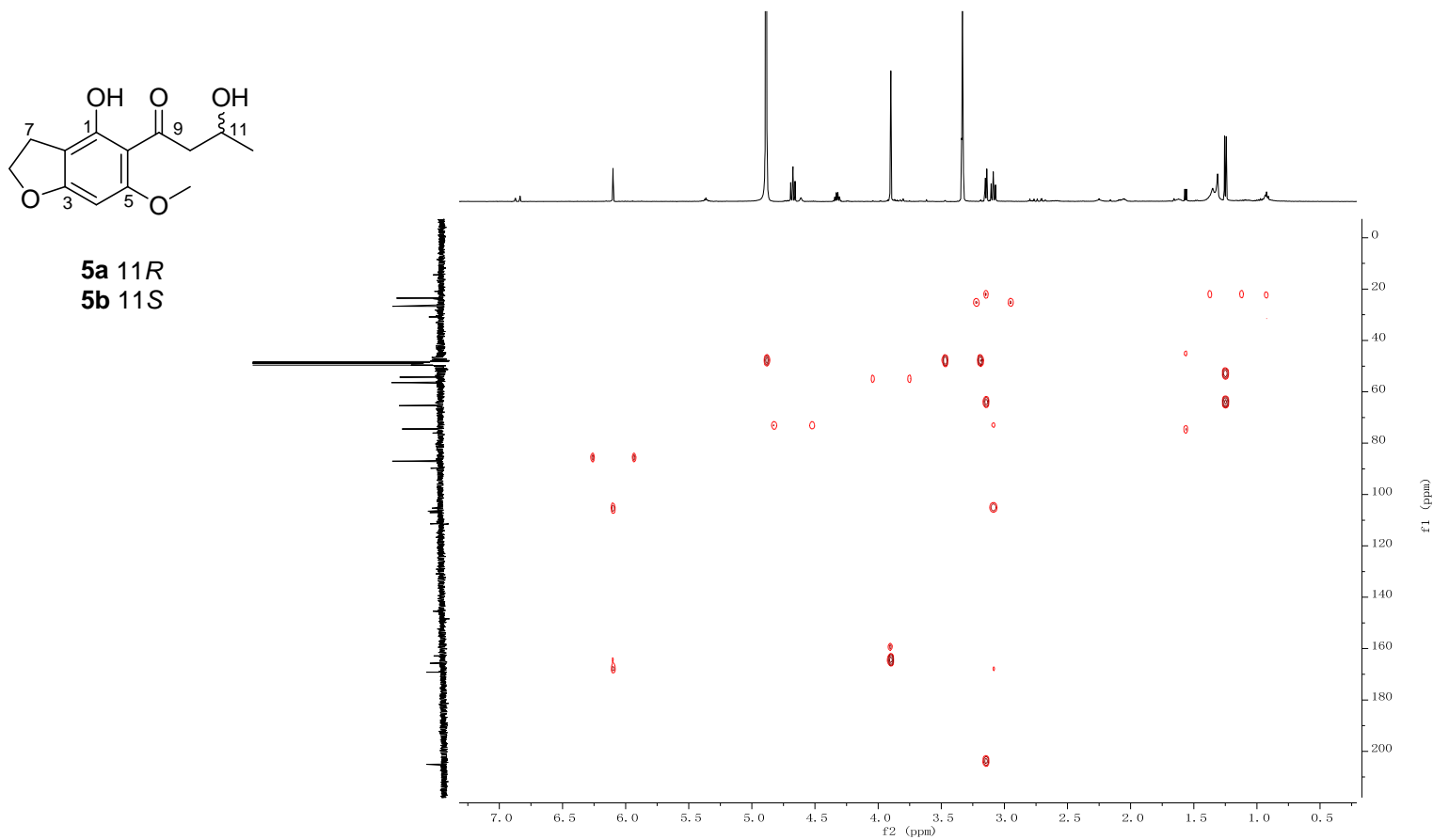
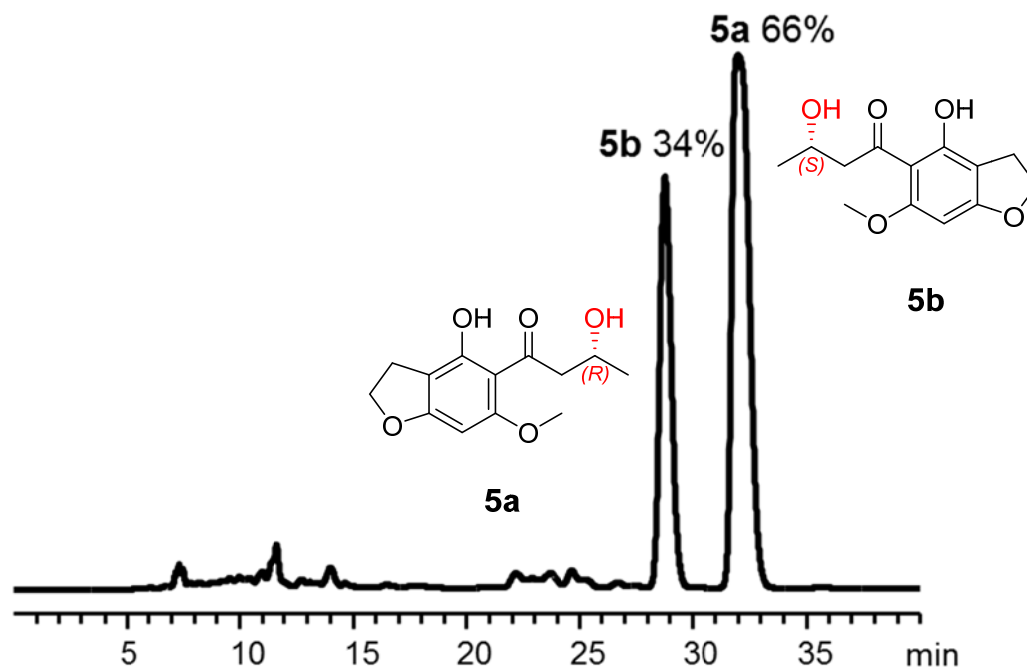


Figure S10. Chiral-phase HPLC analyses of compound **5**.



Chiral analysis of **5**, Isocratic elution: 0-40 min, A : 50%, B: 50%; Area of Peak-1 = 60123 (11*R*, t_{R1} = 28.8min), Area of Peak-2 = 116404(11*S*, t_{R2} = 32.0min); 11*R* : 11*S* = 1 : 2

Column: Phenomenex Lux Cellulose-5 column, 4.6 × 250 mm, 5μM. Phenomenex instrument Co., LTD. Solvents: A, water; B, Acetonitrile. Detection wavelength 300 nm. Flow rate 0.5 mL min⁻¹.

Figure S11. Spectroscopic data for *S*- and *R*-MTPA esters of **5b**.

A. LC-MS analysis of *S*- and *R*-MTPA esters of **5b**.

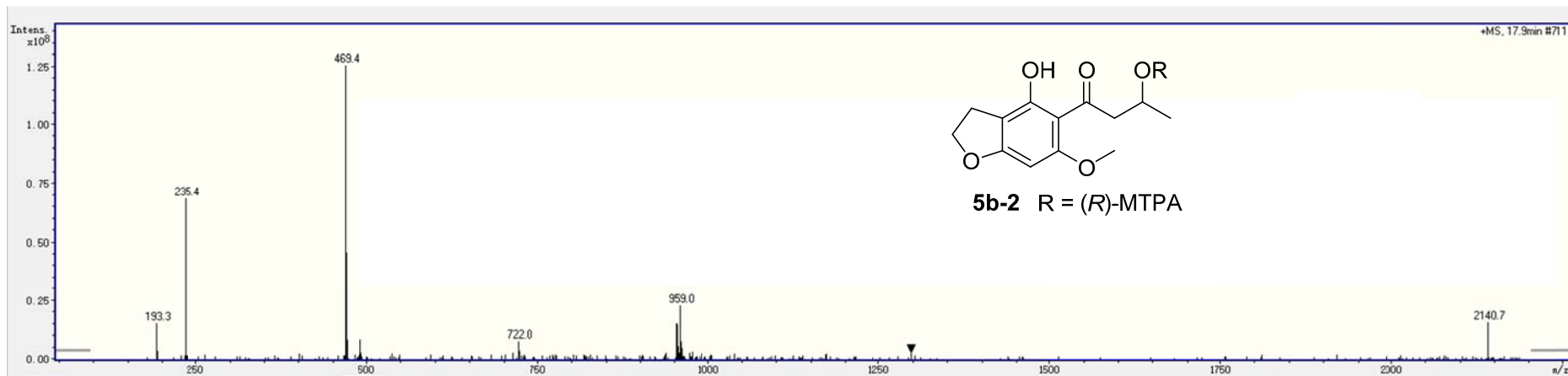
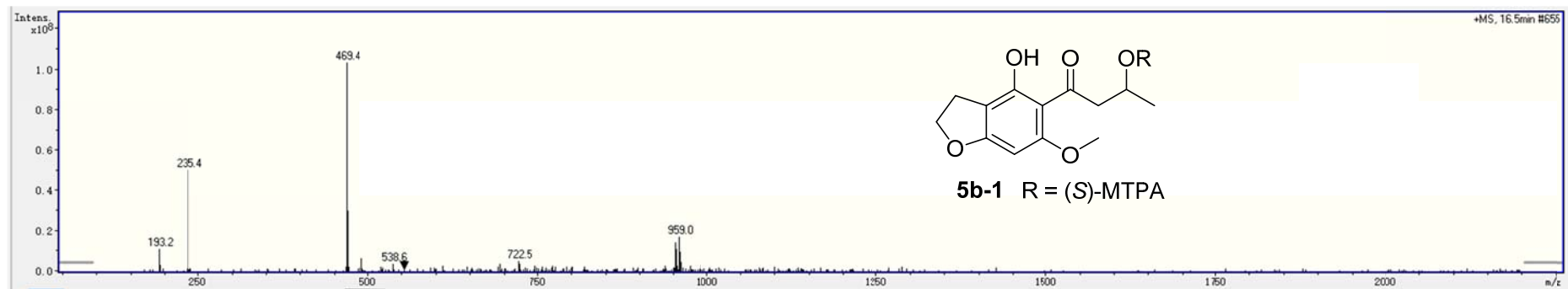


Figure S11. Spectroscopic data for *S*- and *R*-MTPA esters of **5b**. (Continued)

(B) The ^1H NMR (700MHz) spectrum of *S*- and *R*-MTPA esters of **5b** in methanol- d_4 .

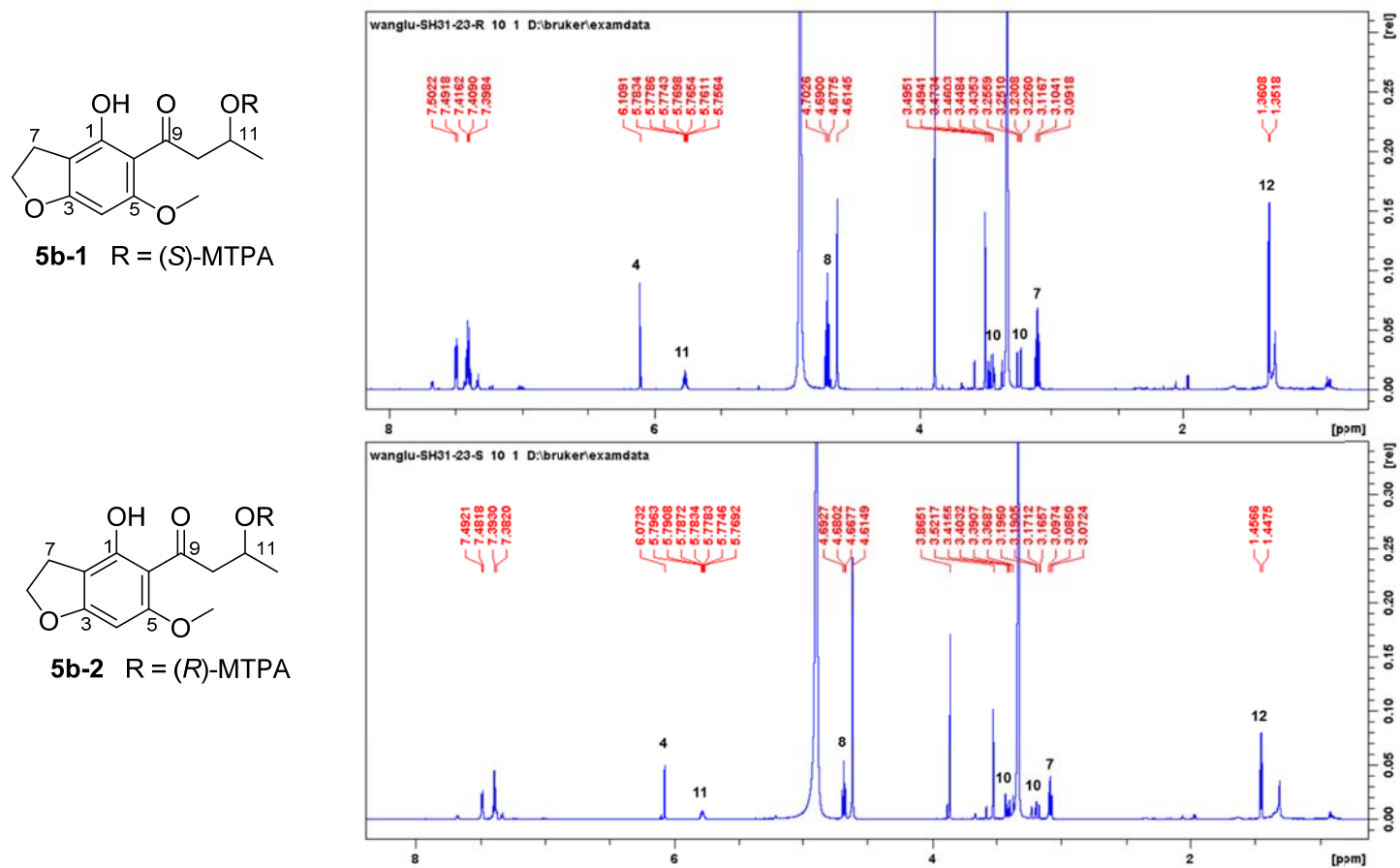
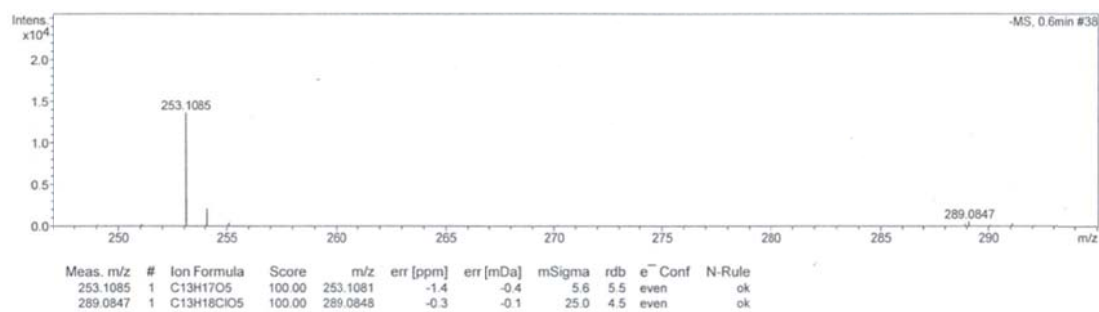


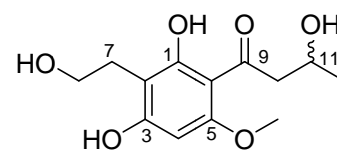
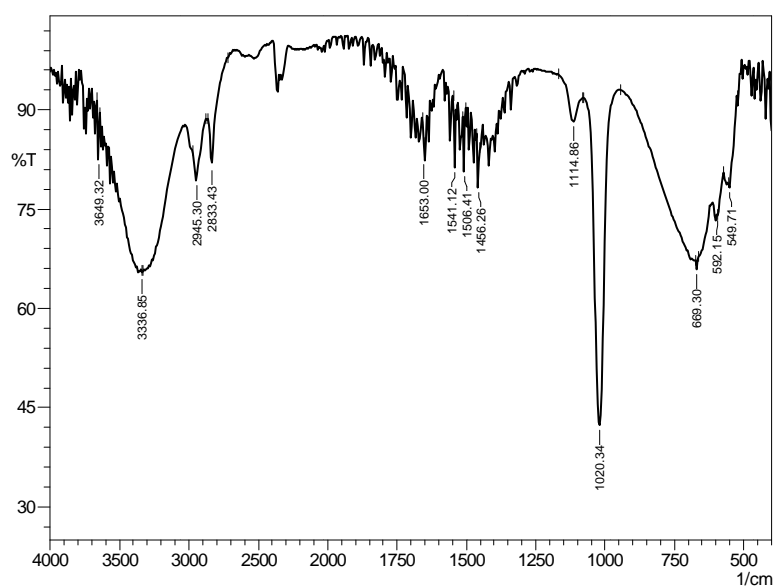
Figure S12. Spectroscopic data for **6**.

(A) HR-ESI-MS (a), IR (b), and UV (c) spectra of **6**.

(a). HR-ESI-MS



(b). IR



6a 11*R*

6b 11*S*

Chemical Formula:

$C_{13}H_{18}O_6$

Exact Mass: 270.11

(c). UV

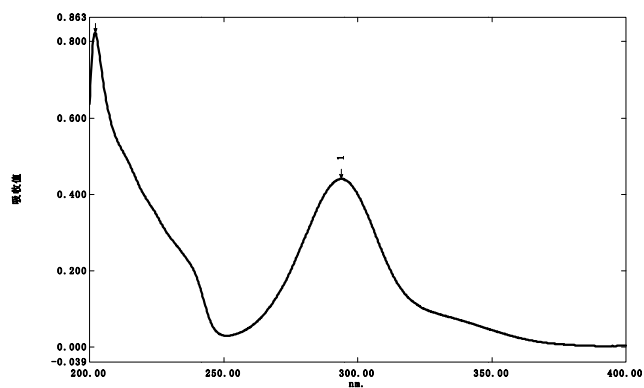


Figure S12. Spectroscopic data for **6** (Continued)

(B) The ^1H NMR spectrum of **6** in methanol- d_4 .

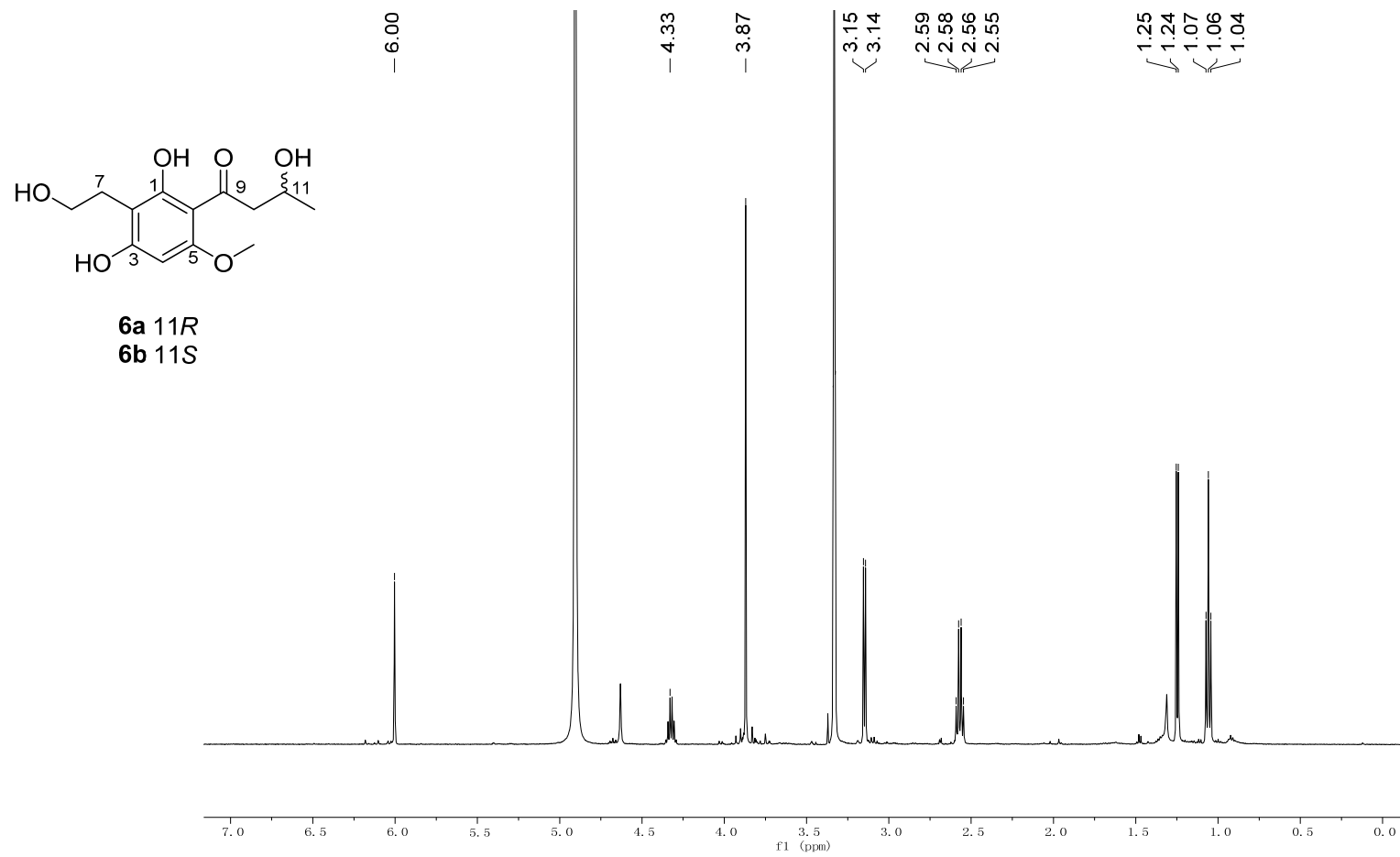


Figure S12. Spectroscopic data for **6**. (Continued)

(C) The ^{13}C and DEPT 135 NMR spectrum of **6** in methanol- d_4 .

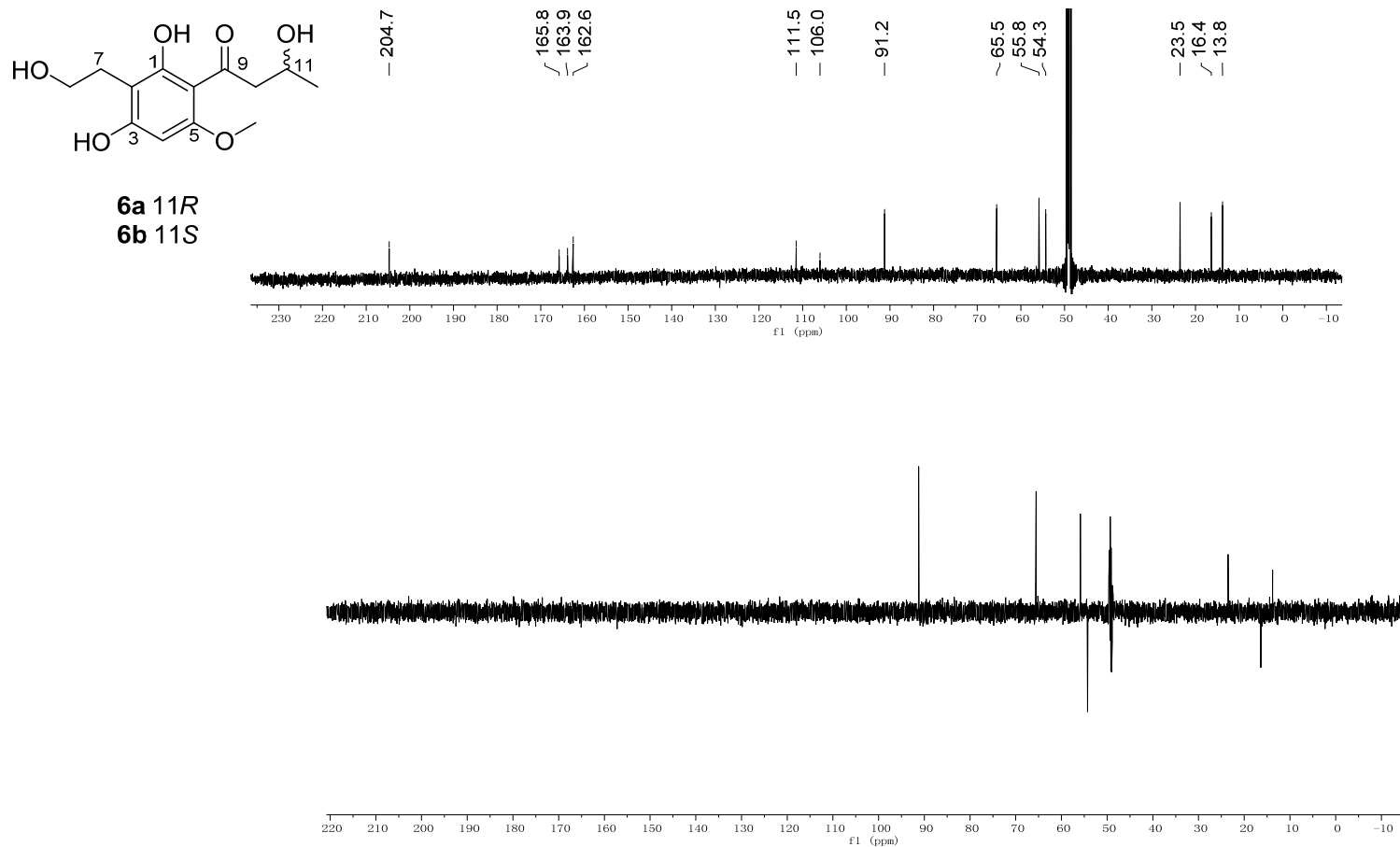


Figure S12. Spectroscopic data for **6**. (Continued)

(D) The HSQC spectrum of **6** in methanol-*d*₄.

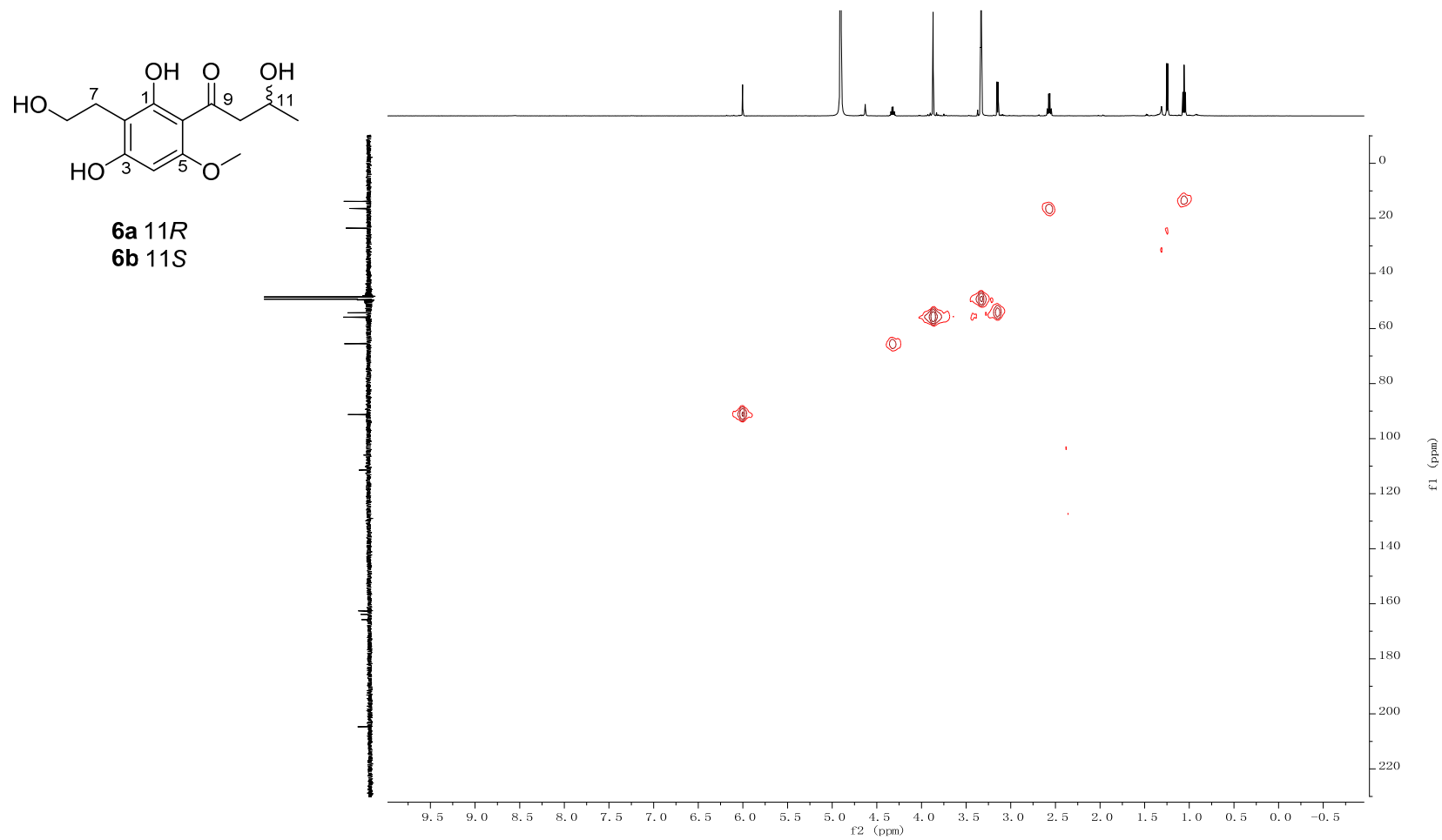


Figure S12. Spectroscopic data for **6**. (Continued)

(E) The COSY spectrum of **6** in methanol- d_4 .

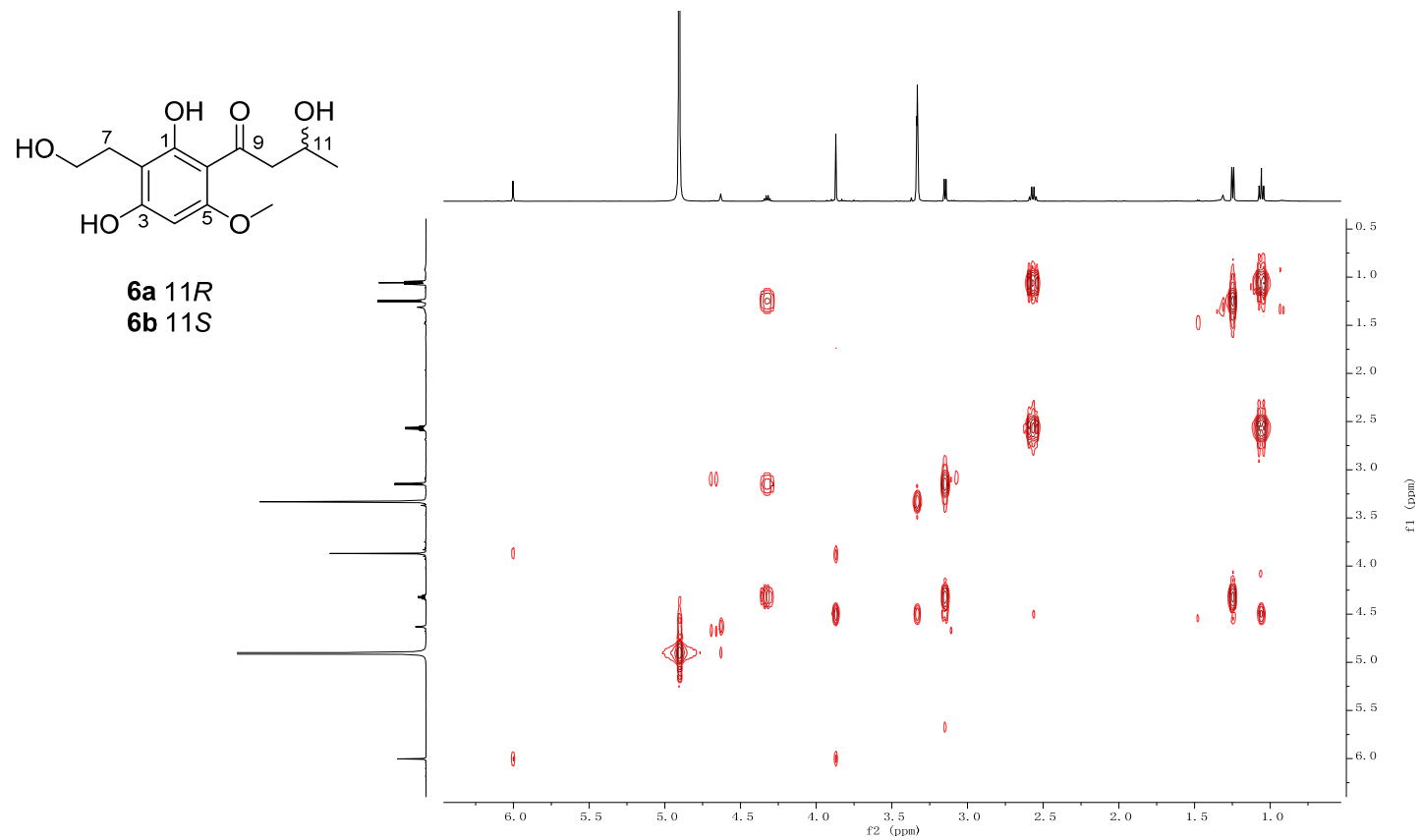


Figure S12. Spectroscopic data for **6**. (Continued)

(F) The HMBC spectrum of **6** in methanol- d_4 .

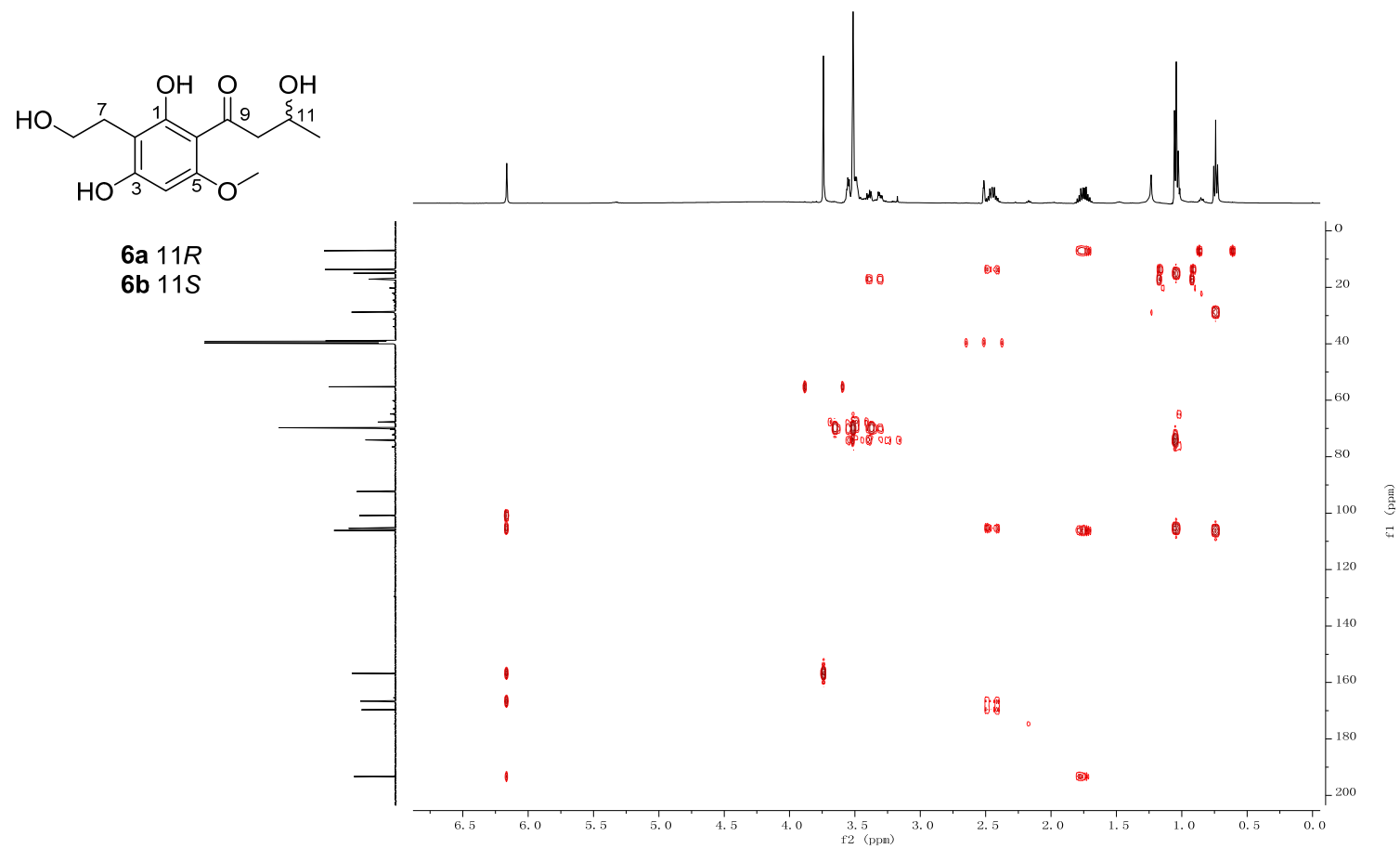
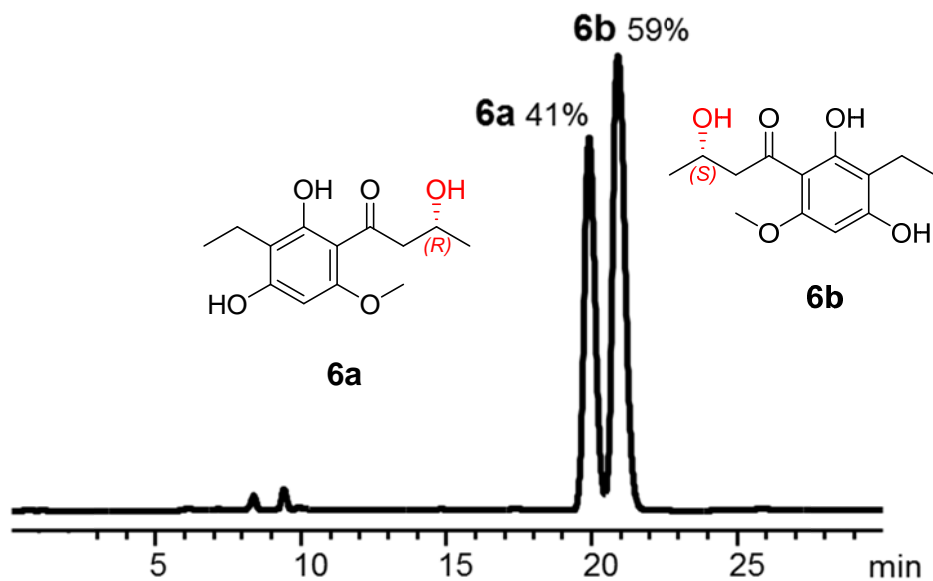


Figure S13. Chiral-phase HPLC analyses of compound **6**.



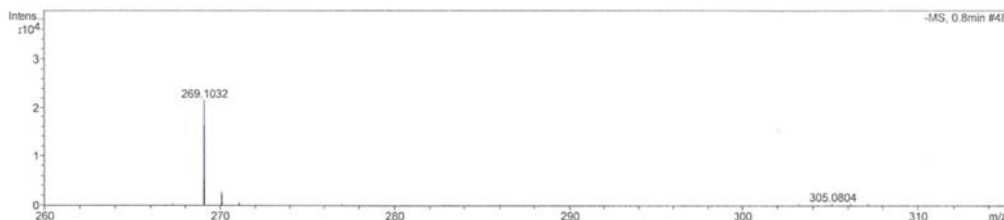
Chiral analysis of **6**, Isocratic elution: 0-30 min, A: 26%, B: 74%; Area of Peak-1 = 42974 (11*R*, t_{R1} = 19.9min), Area of Peak-2 = 60840 (11*S*, t_{R2} = 20.9min); 11*R* : 11*S* = 1 : 1.4

Column: Phenomenex Lux Cellulose-5 column, 4.6 × 250 mm, 5μM. Phenomenex instrument Co., LTD. Solvents: water; B, Acetonitrile. Detection wavelength 300 nm. Flow rate 0.5 mL min⁻¹.

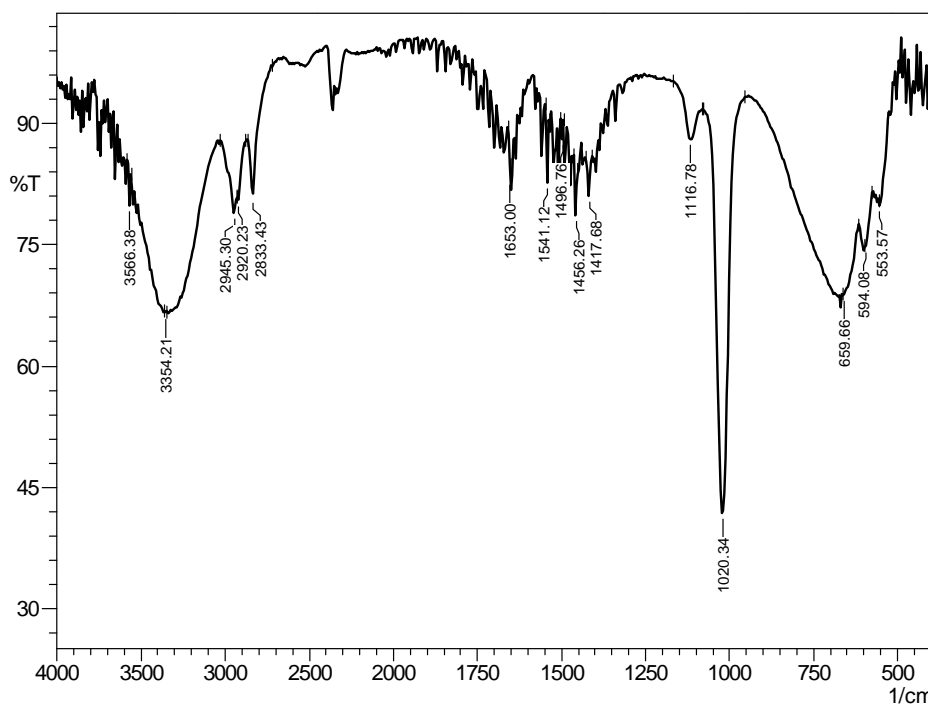
Figure S14. Spectroscopic data for **7**.

(A) HR-ESI-MS (a), IR (b), and UV (c) spectra of **7**.

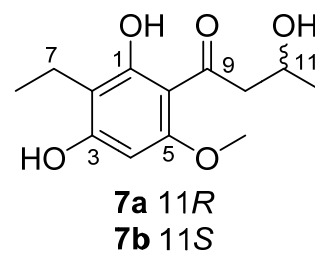
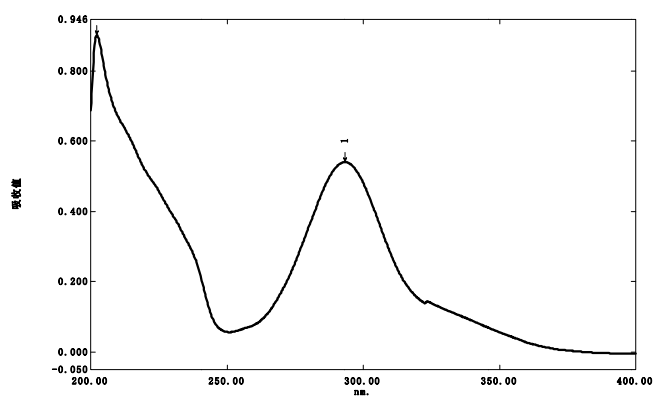
(a). HR-ESI-MS



(b). IR



(c). UV



Chemical Formula: C₁₃H₁₈O₅
Exact Mass: 254.12

Figure S14. Spectroscopic data for **7** (Continued)

(B) The ^1H NMR spectrum of **7** in $\text{DMSO-}d_6$.

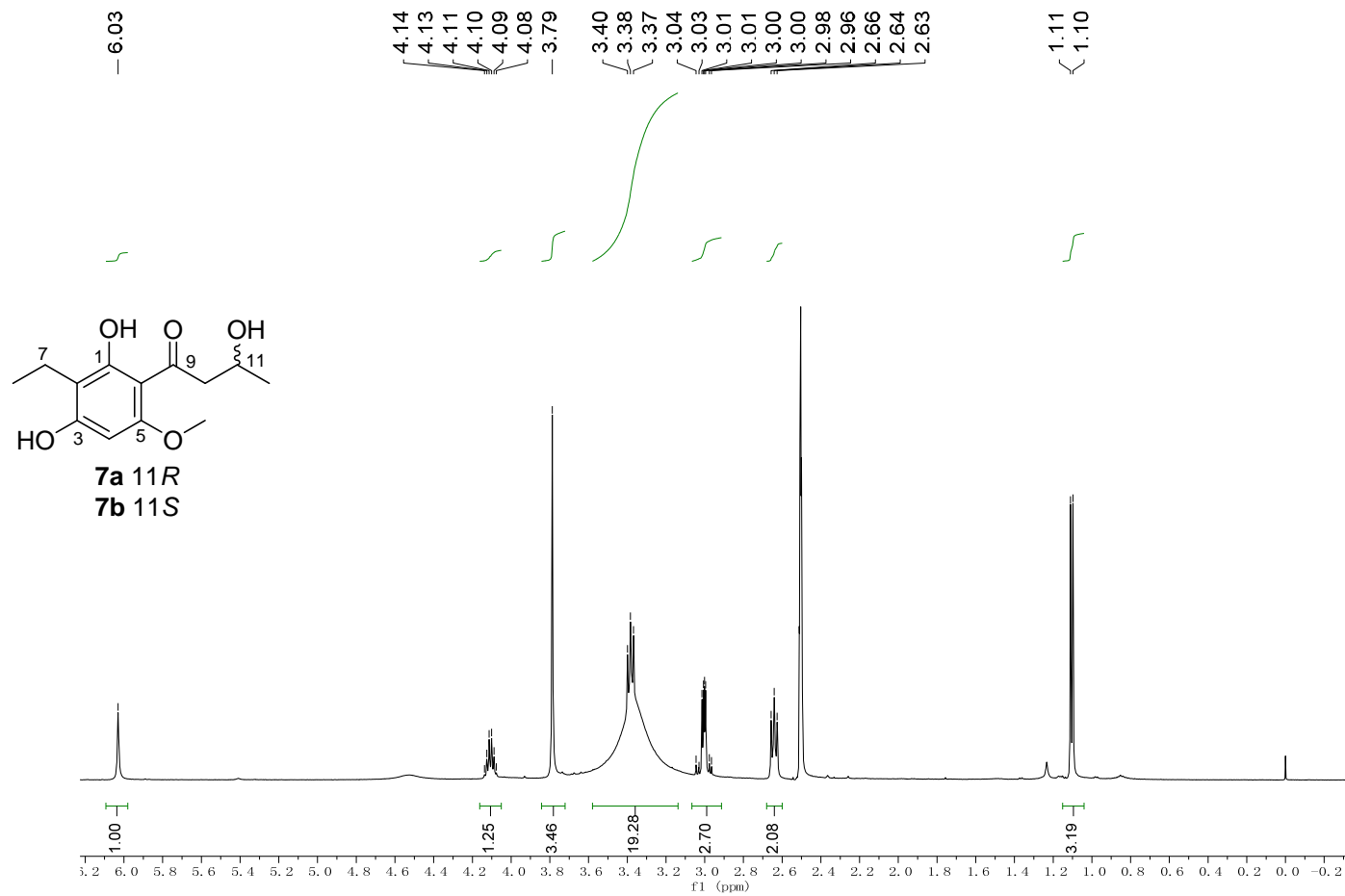


Figure S14. Spectroscopic data for **7**. (Continued)

(C) The ^{13}C spectrum of **7** in $\text{DMSO-}d_6$.

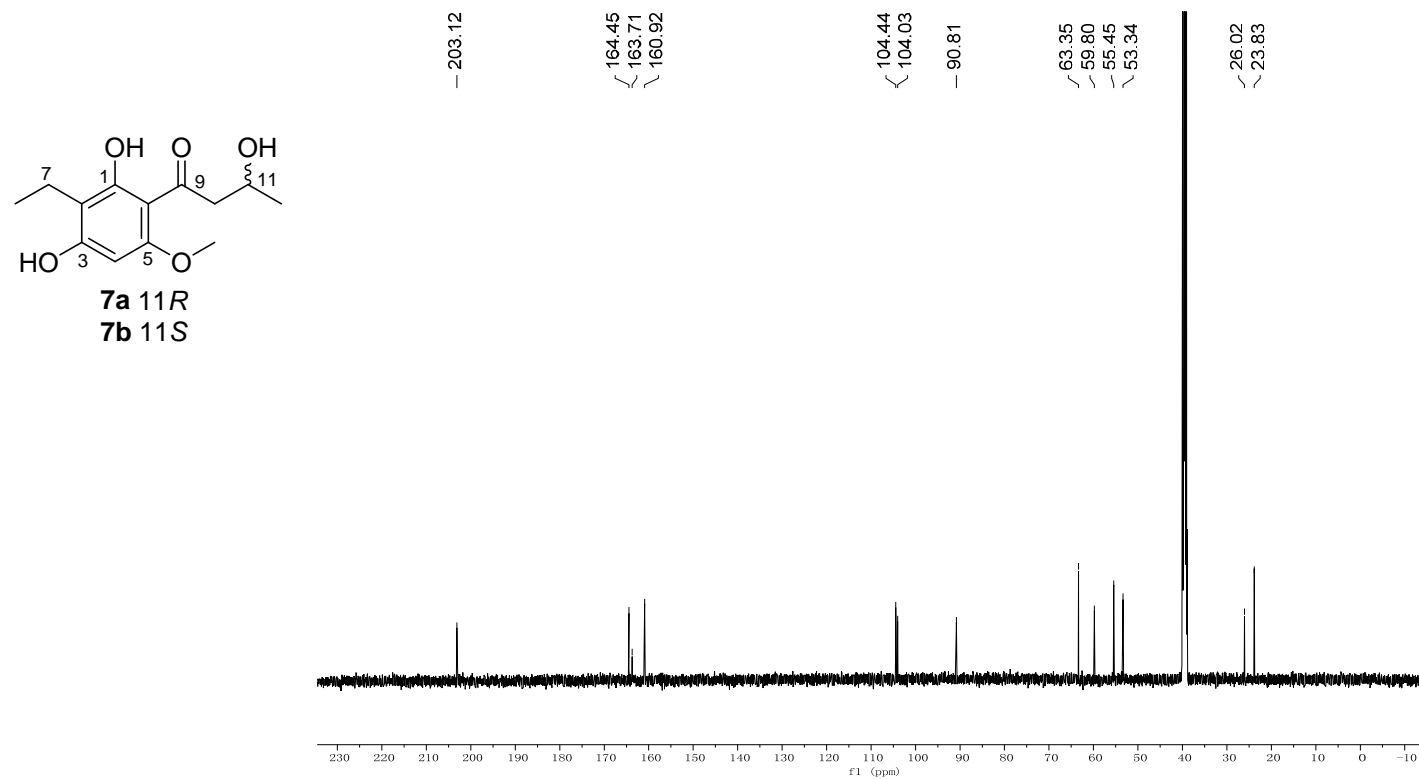


Figure S14. Spectroscopic data for **7**. (Continued)

(D) The HSQC spectrum of **7** in DMSO- d_6 .

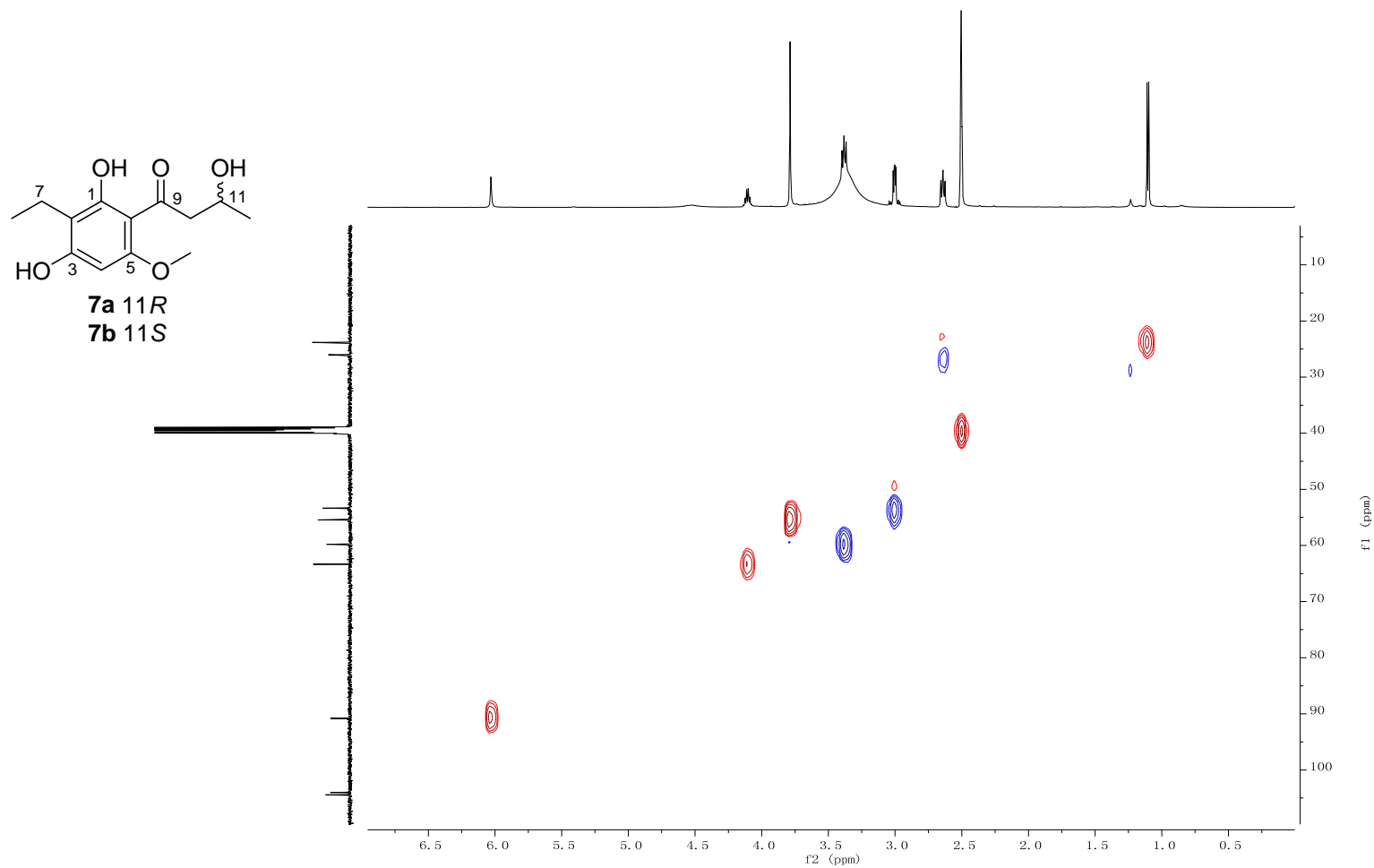


Figure S14. Spectroscopic data for **7**. (Continued)

(E) The COSY spectrum of **7** in DMSO- d_6 .

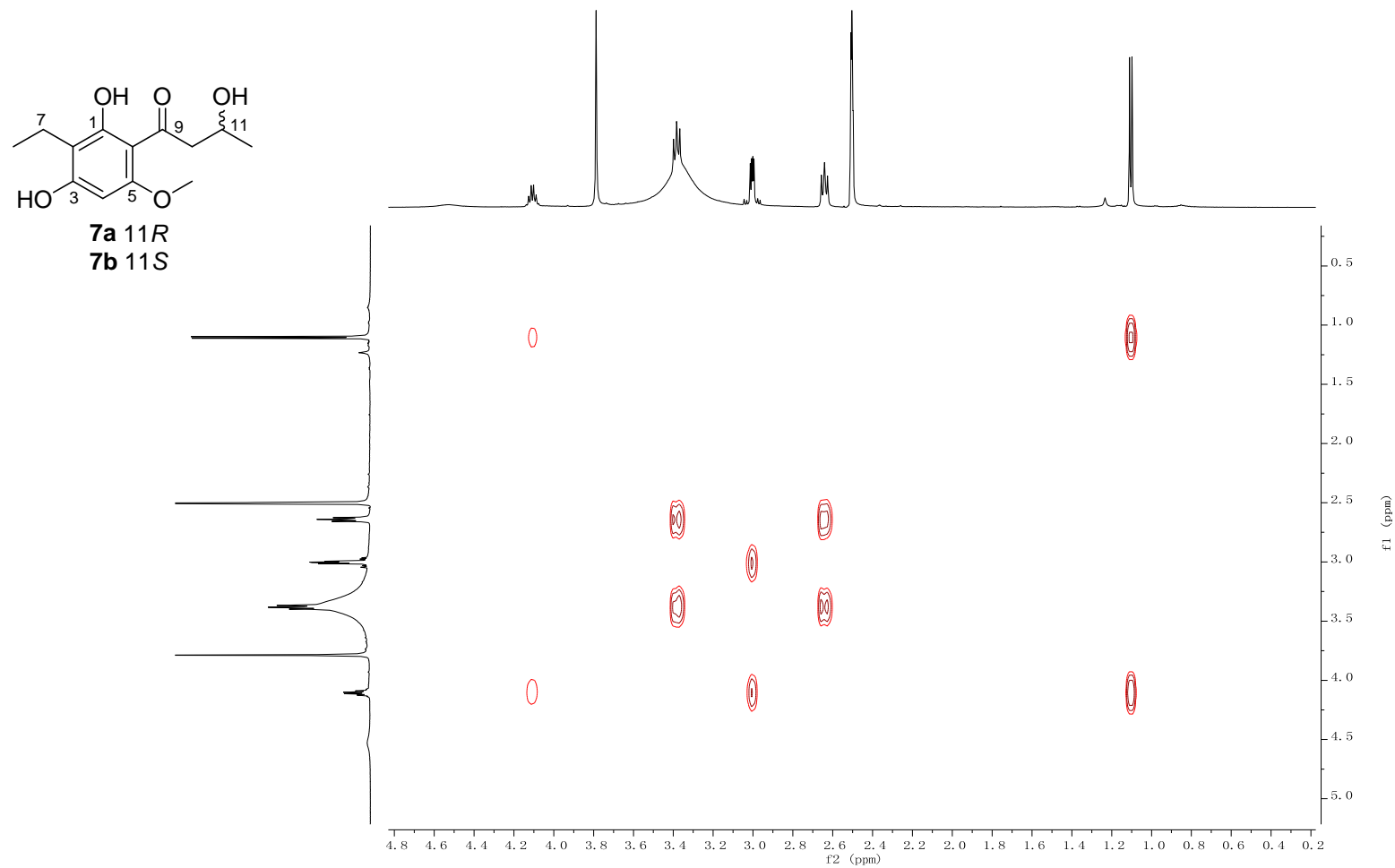


Figure S14. Spectroscopic data for **7**. (Continued)

(E) The HMBC spectrum of **7** in DMSO-*d*₆.

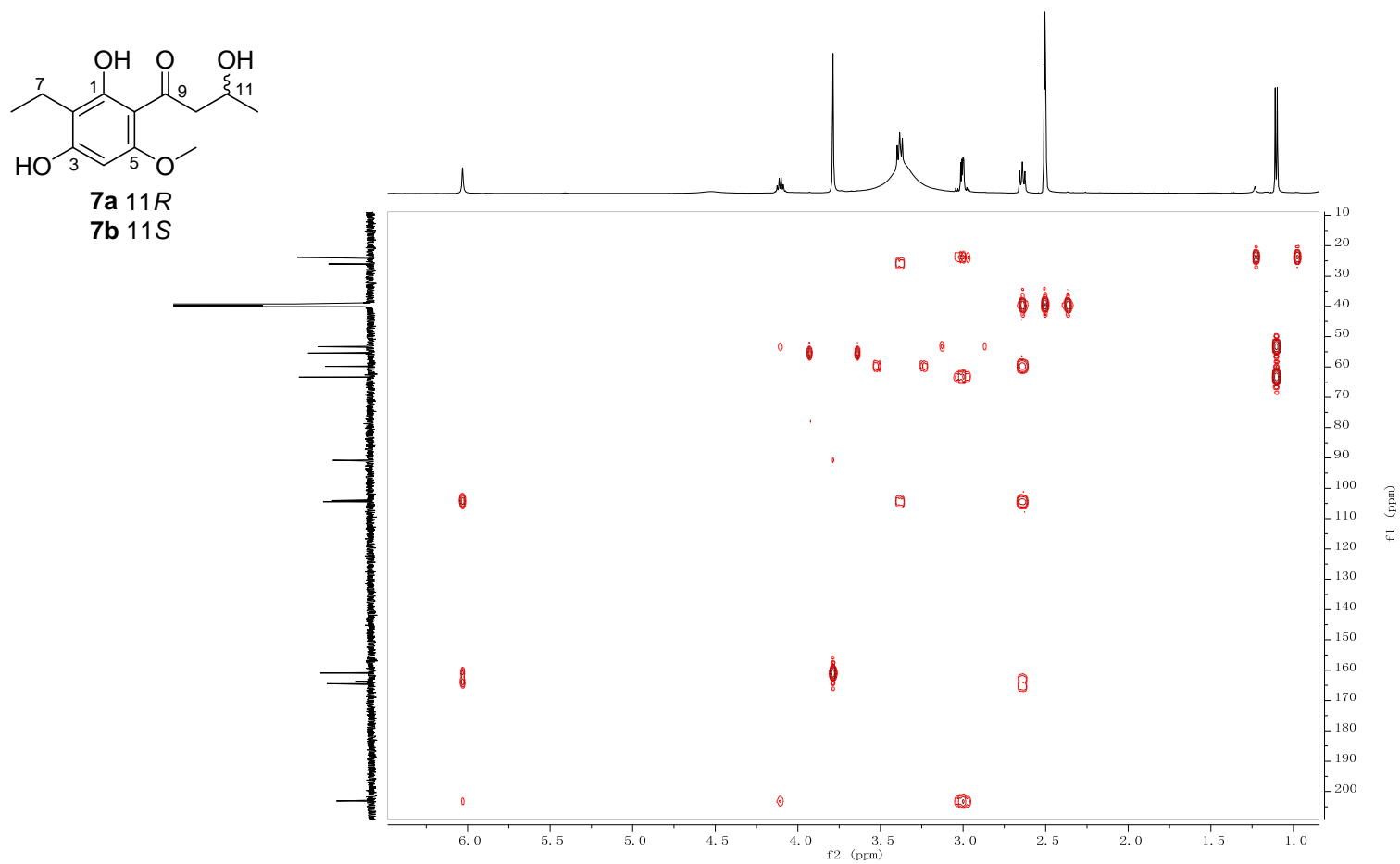
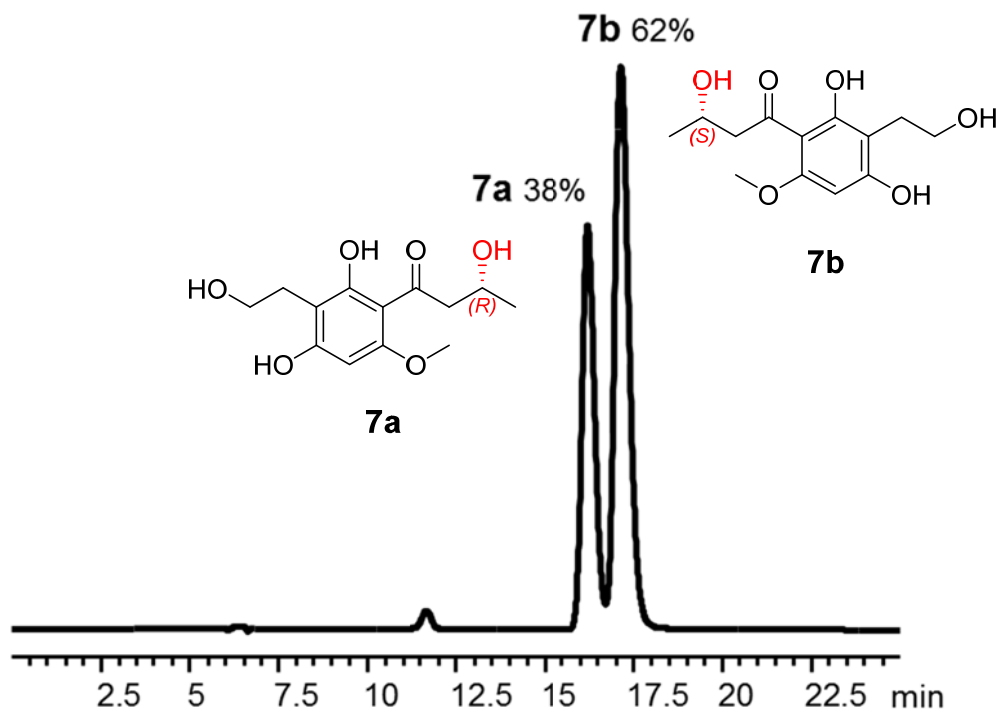


Figure S15. Chiral-phase HPLC analyses of compound **7**.

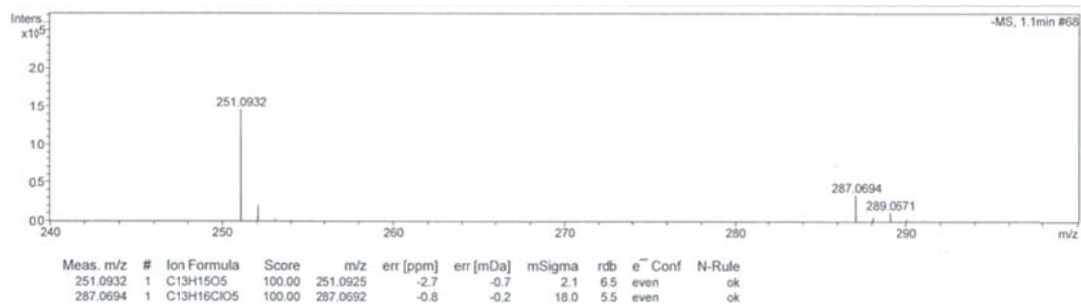


Chiral analysis of **7**, Isocratic elution: 0-25 min, A: 28%; B: 72%; Area of Peak-1 = 27786 (11*R*, t_{R1} = 16.2min), Area of Peak-2 = 45100 (11*S*, t_{R2} = 17.1min); 11*R* : 11*S* = 1 : 1.6.
Column: Phenomenex Lux Cellulose-5 column, 4.6 × 250 mm, 5μM. Phenomenex instrument Co., LTD. Solvents: A, water; B, Acetonitrile. Detection wavelength 300 nm. Flow rate 0.5 mL min⁻¹.

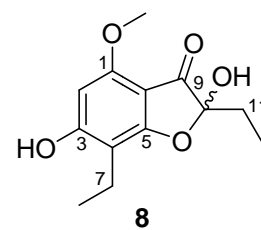
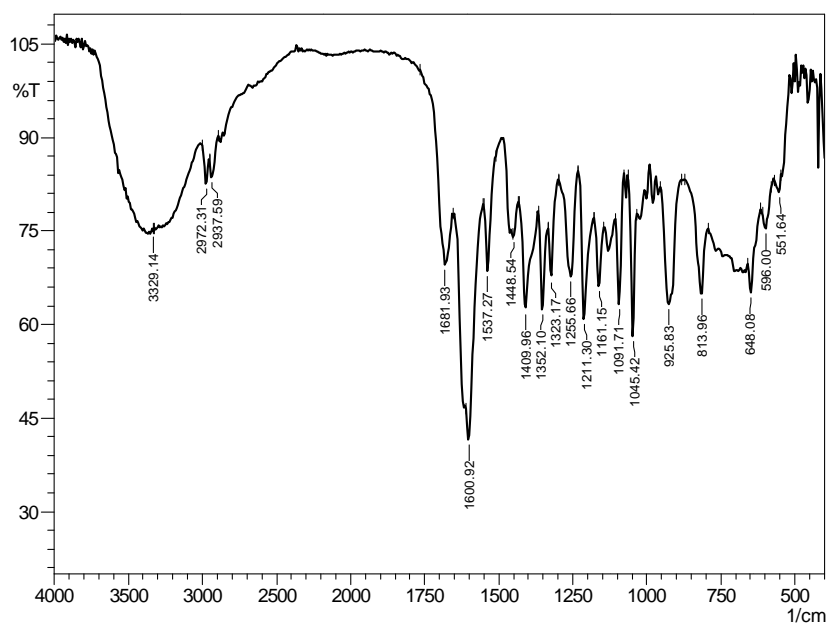
Figure S16. Spectroscopic data for **8**.

(A) HR-ESI-MS (a), IR (b), and UV (c) spectra of **8**.

(a). HR-ESI-MS



(b). IR



Chemical Formula: C₁₃H₁₆O₅
Exact Mass: 252.10

(c). UV

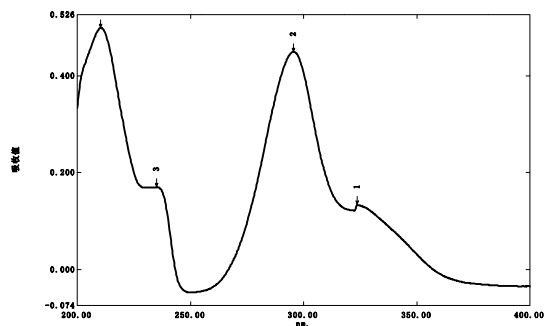


Figure S16. Spectroscopic data for **8** (Continued)

(B) The ^1H NMR spectrum of **8** in $\text{DMSO-}d_6$.

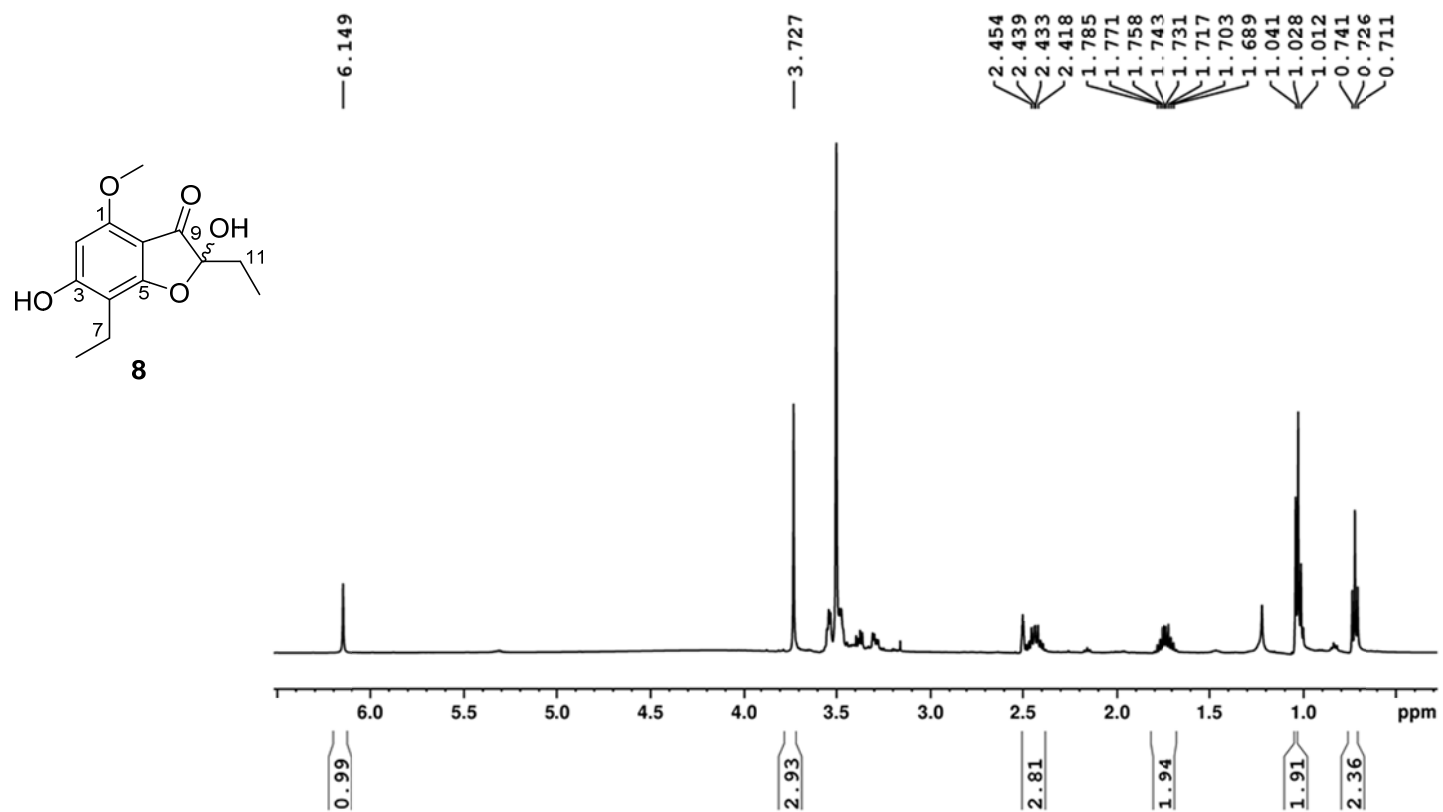


Figure S16. Spectroscopic data for **8**. (Continued)

(C) The ^{13}C and DEPT 135 NMR spectrum of **8** in $\text{DMSO-}d_6$.

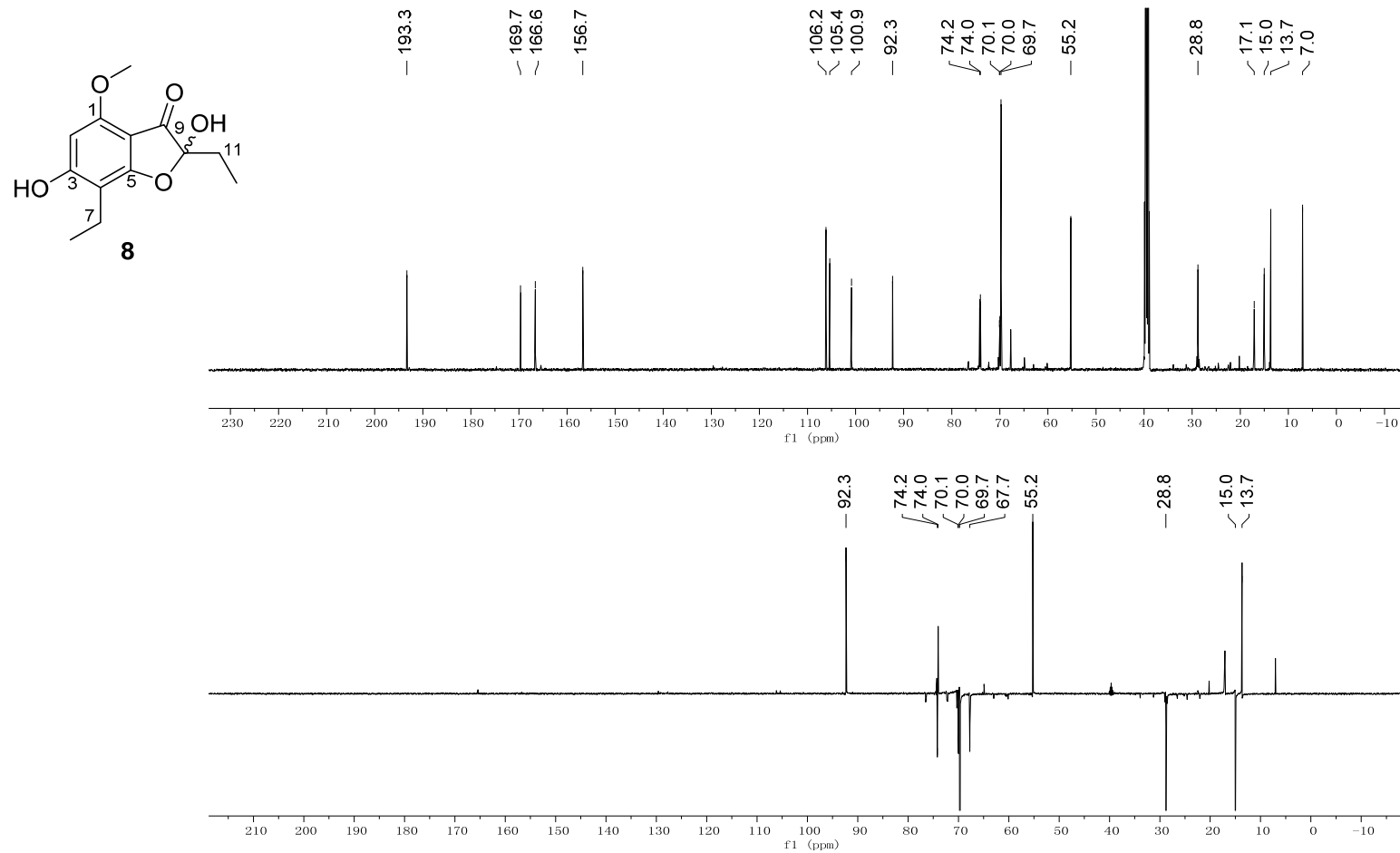


Figure S16. Spectroscopic data for **8** . (Continued)

(D) The HSQC spectrum of **8** in DMSO-*d*₆.

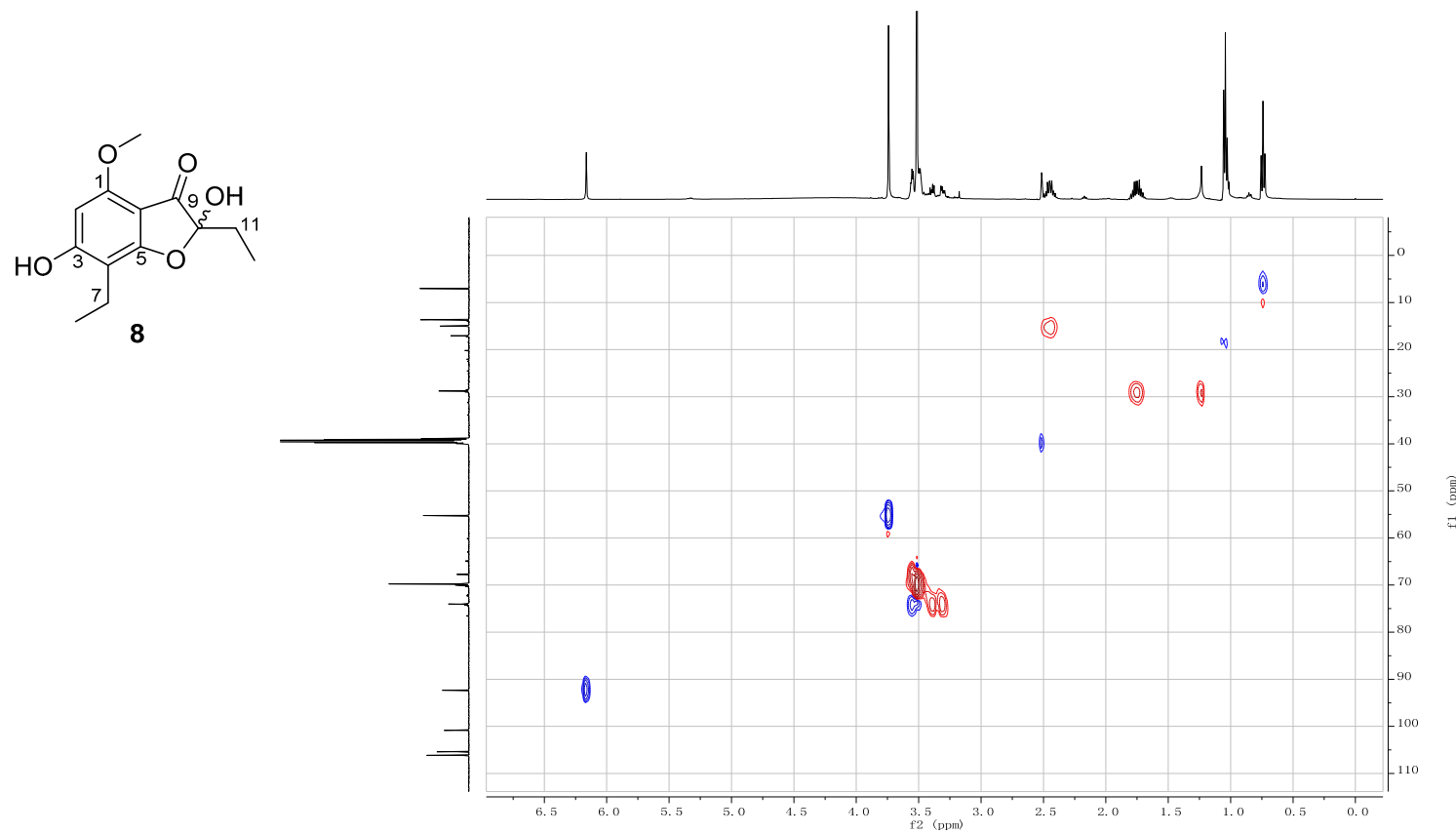


Figure S16. Spectroscopic data for **8**. (Continued)

(E) The COSY spectrum of **8** in DMSO-*d*₆.

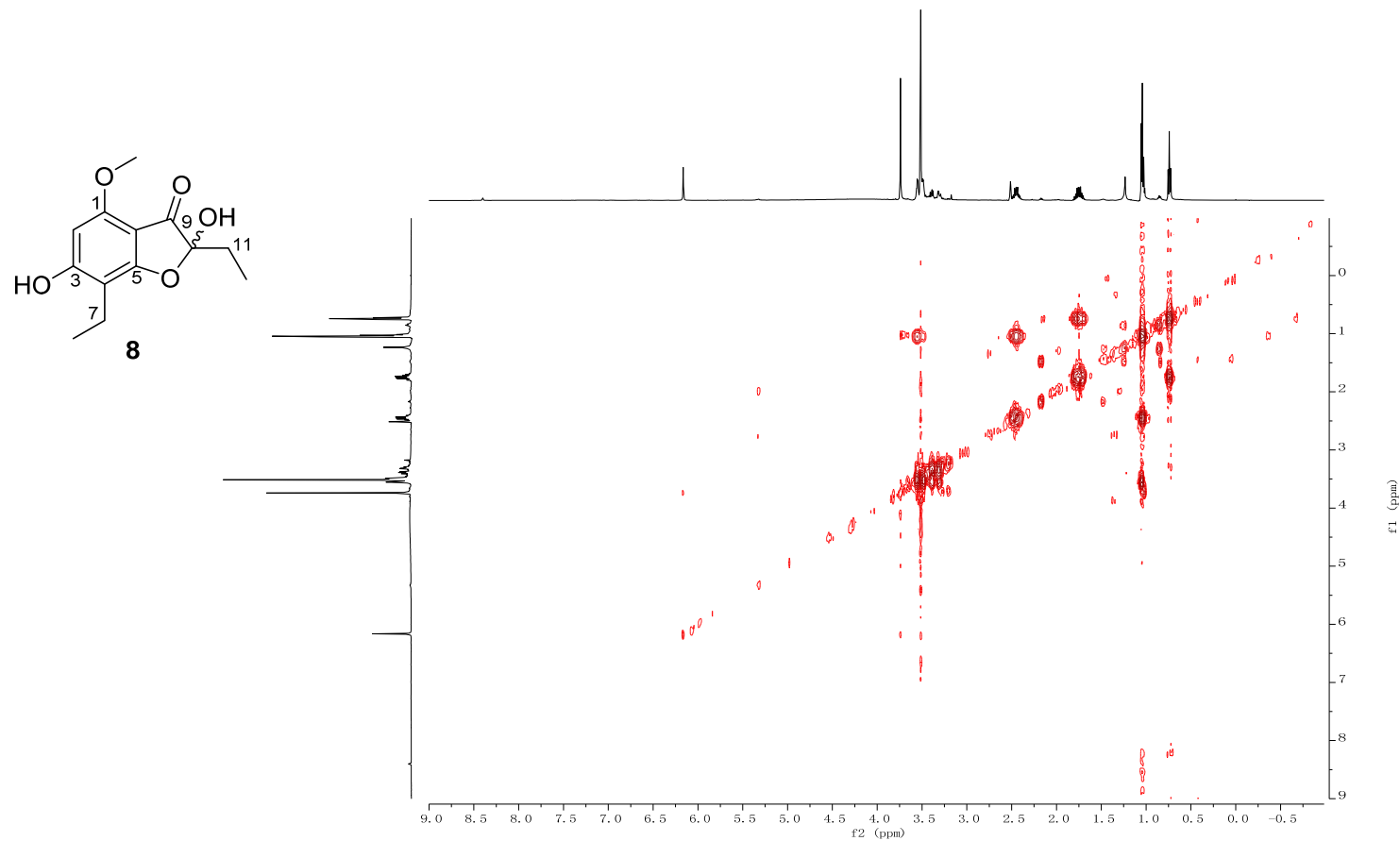


Figure S16. Spectroscopic data for **8**. (Continued)

(F) The HMBC spectrum of **8** in DMSO-*d*₆.

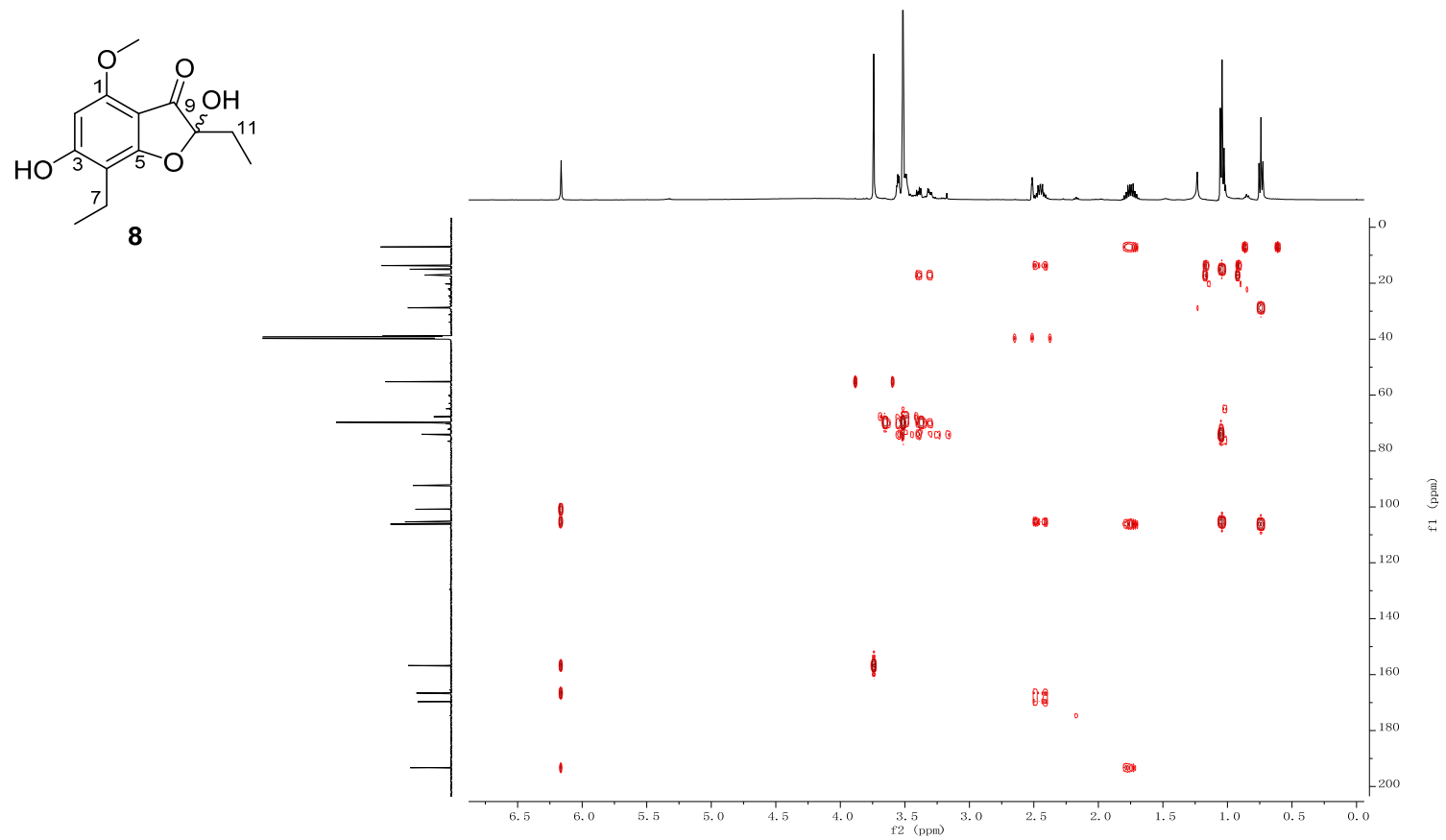
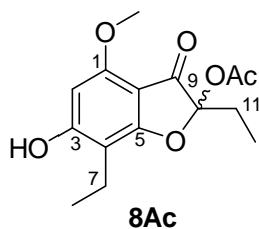
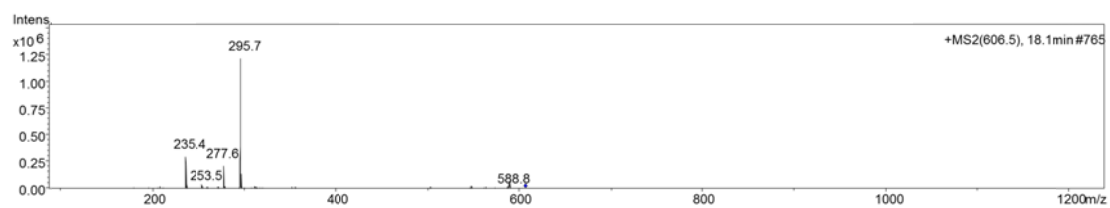


Figure S17. Spectroscopic data for **8Ac**.

(A) LRESIMS



Chemical Formula: $C_{15}H_{18}O_6$

Exact Mass: 294.11

Figure S17. Spectroscopic data for **8Ac**. (Continued)

(B) The ^1H NMR (700MHz) spectrum of **8Ac** in $\text{DMSO-}d_6$.

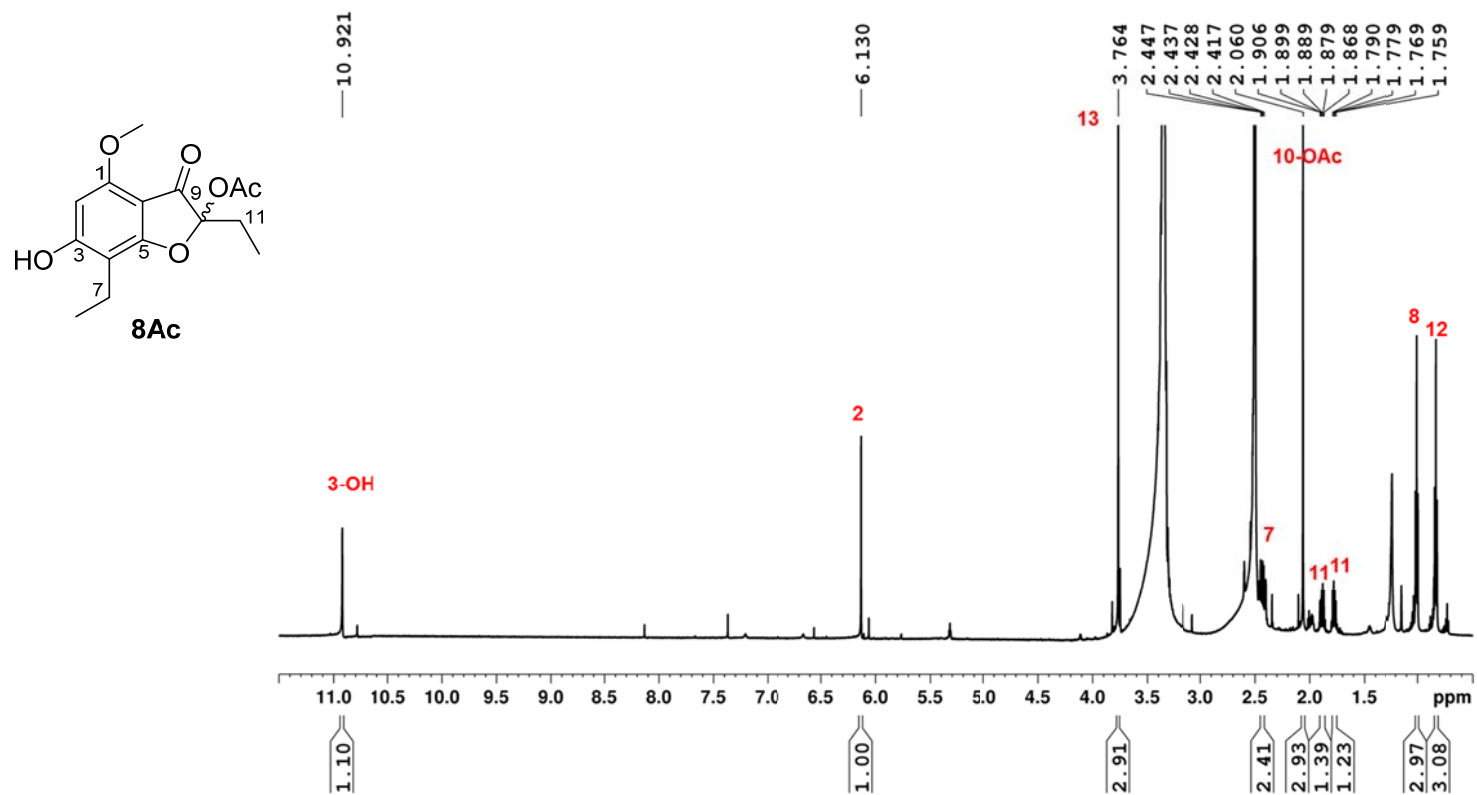


Figure S17. Spectroscopic data for **8Ac**. (Continued)

(C) The ^1H NMR (700MHz) spectrum of **8** and **8Ac** in $\text{DMSO-}d_6$.

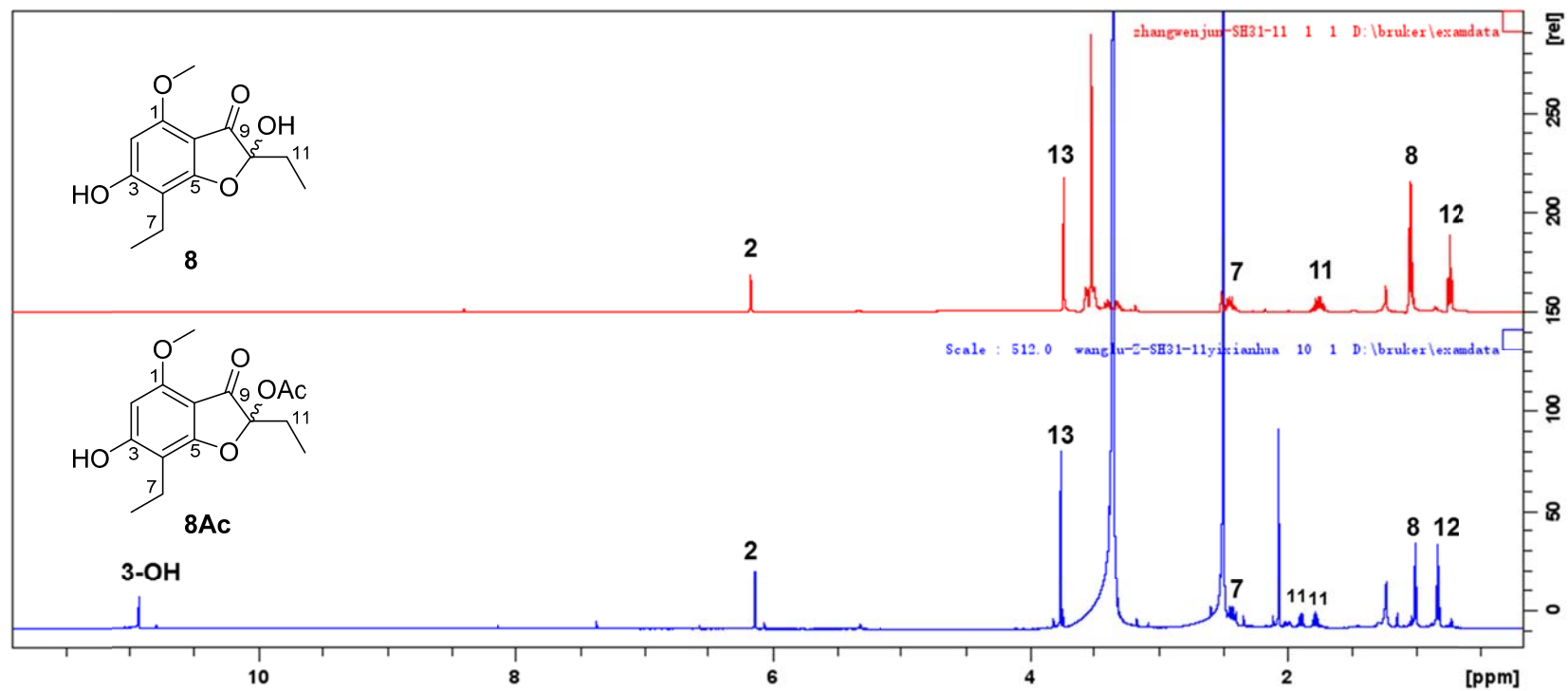
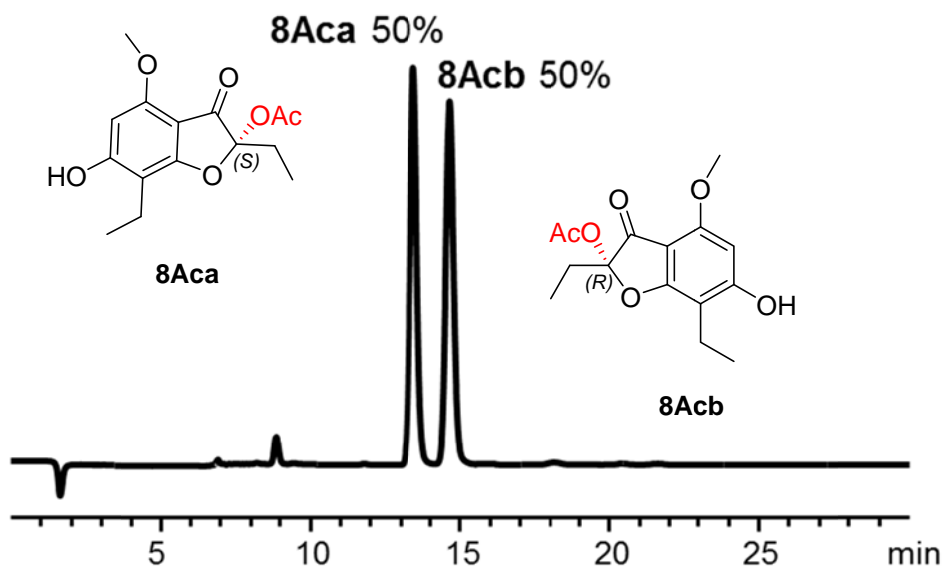
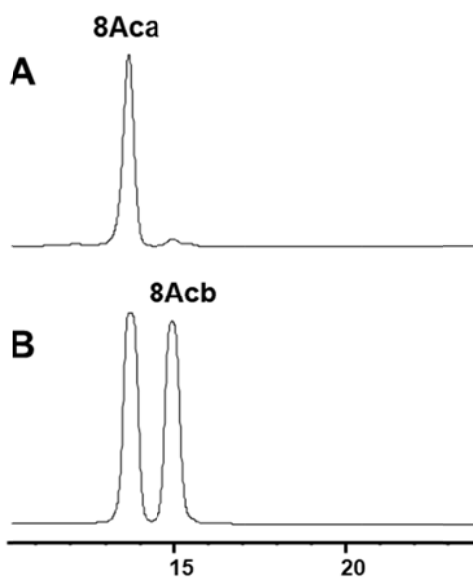


Figure S18. Chiral-phase HPLC analyses of compound **8Ac**.



Chiral analysis of **8Ac**, Isocratic elution: 0-30 min, A: 48%; B: 52%; Area of Peak-1 = 3541 (11*S*, t_{R1} = 13.4min), Area of Peak-2 = 3602 (11*R*, t_{R2} = 14.7min); 11*S* : 11*R* = 1 : 1.

Column: Phenomenex Lux Cellulose-5 column, 4.6 × 250 mm, 5μM. Phenomenex instrument Co., LTD. Solvents: A, water; B, Acetonitrile. Detection wavelength 300 nm. Flow rate 0.5 mL min⁻¹



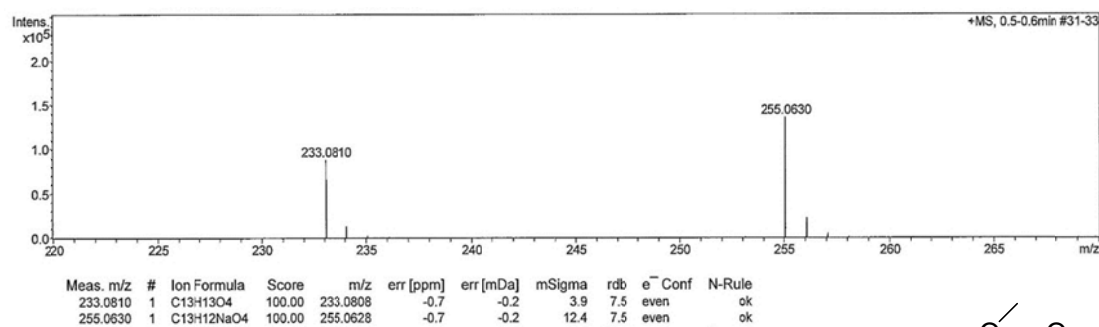
A: **8Aca**

B: **8Acb** can spontaneously convert to **8Aca** and **8Acb** quickly after separated from **8Ac**.

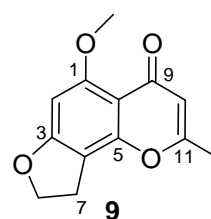
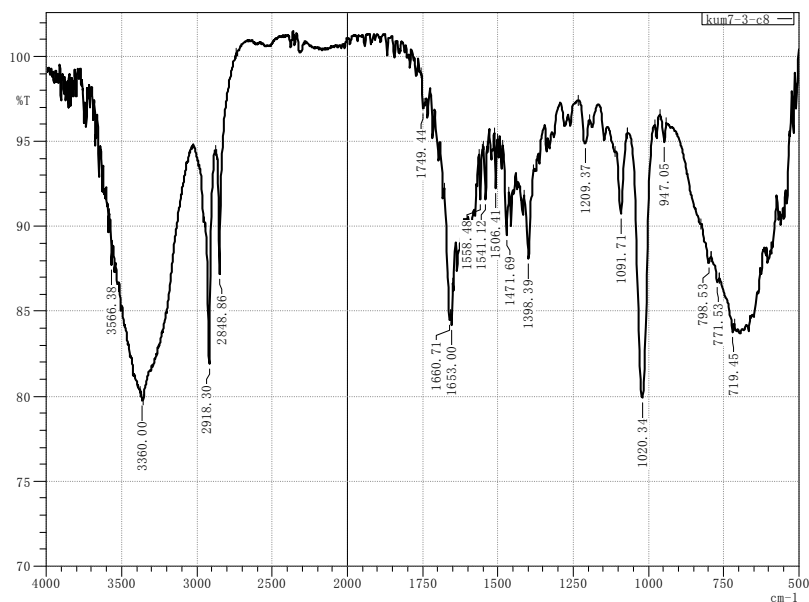
Figure S19. Spectroscopic data for **9**.

(A) HR-ESI-MS (a), IR (b), and UV (c) spectra of **9**.

(a). HR-ESI-MS



(b). IR



(c). UV

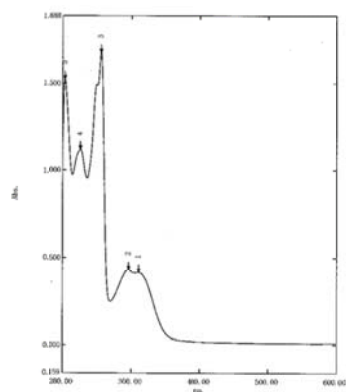


Figure S19. Spectroscopic data for **9**. (Continued)

(B) The ^1H NMR (500MHz) spectrum of **9** in CDCl_3 .

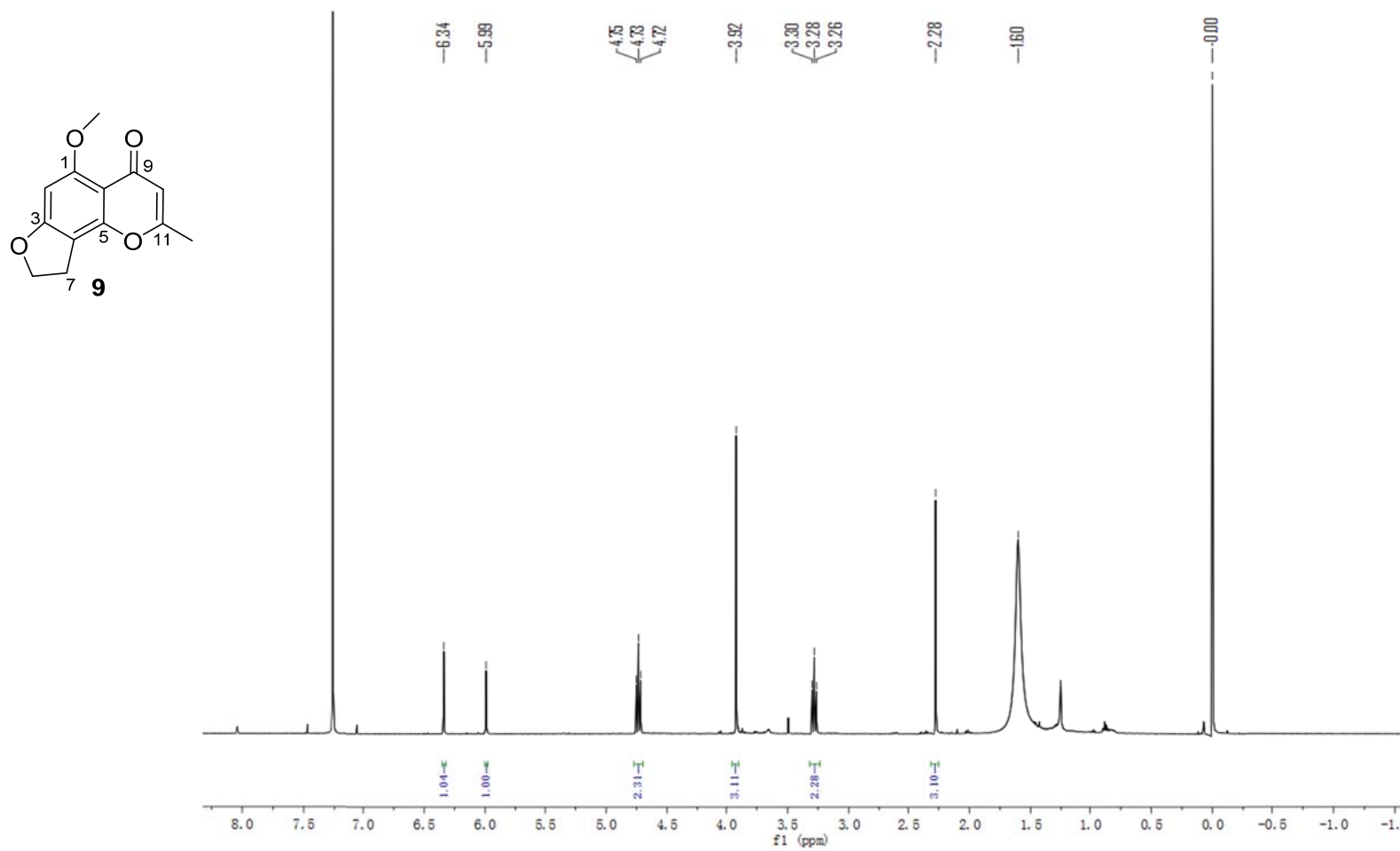


Figure S19. Spectroscopic data for **9**. (Continued)

(C) The ^{13}C and DEPT 135 NMR spectrum of **9** in CDCl_3 .

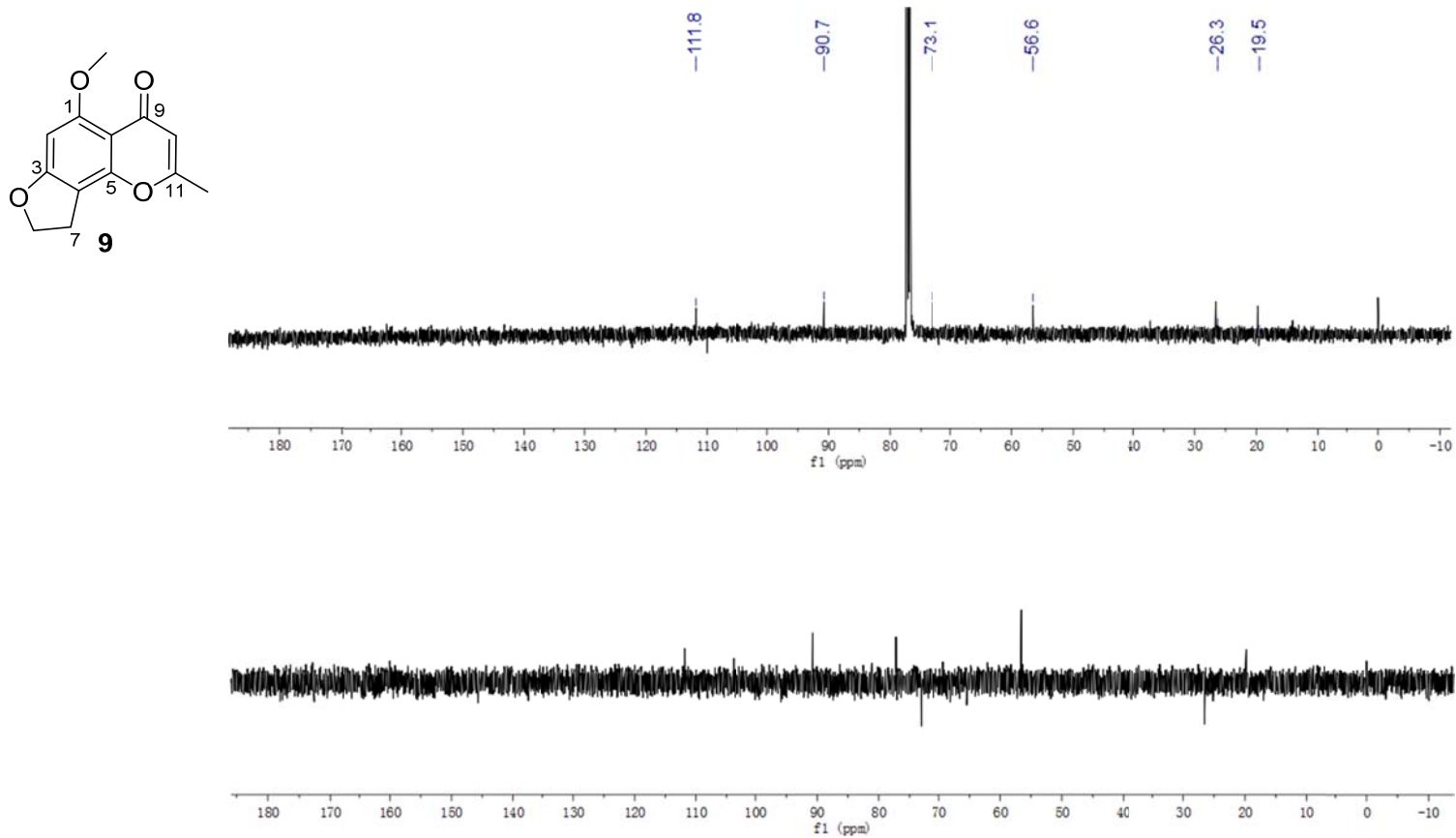


Figure S19. Spectroscopic data for **9**. (Continued)

(D) The HSQC (500MHz) spectrum of compound **9** in CDCl₃.

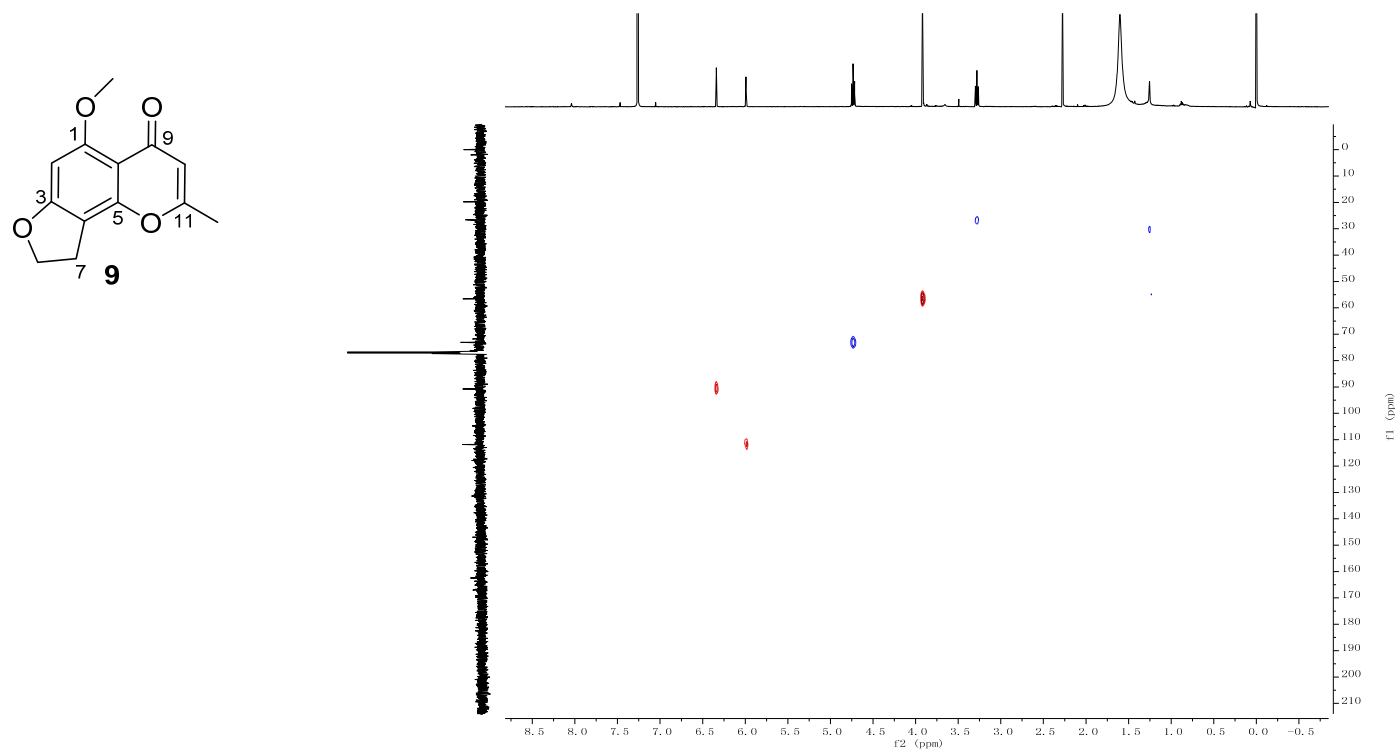


Figure S19. Spectroscopic data for **9**. (Continued)

(E) The COSY (500MHz) spectrum of **9** in CDCl₃.

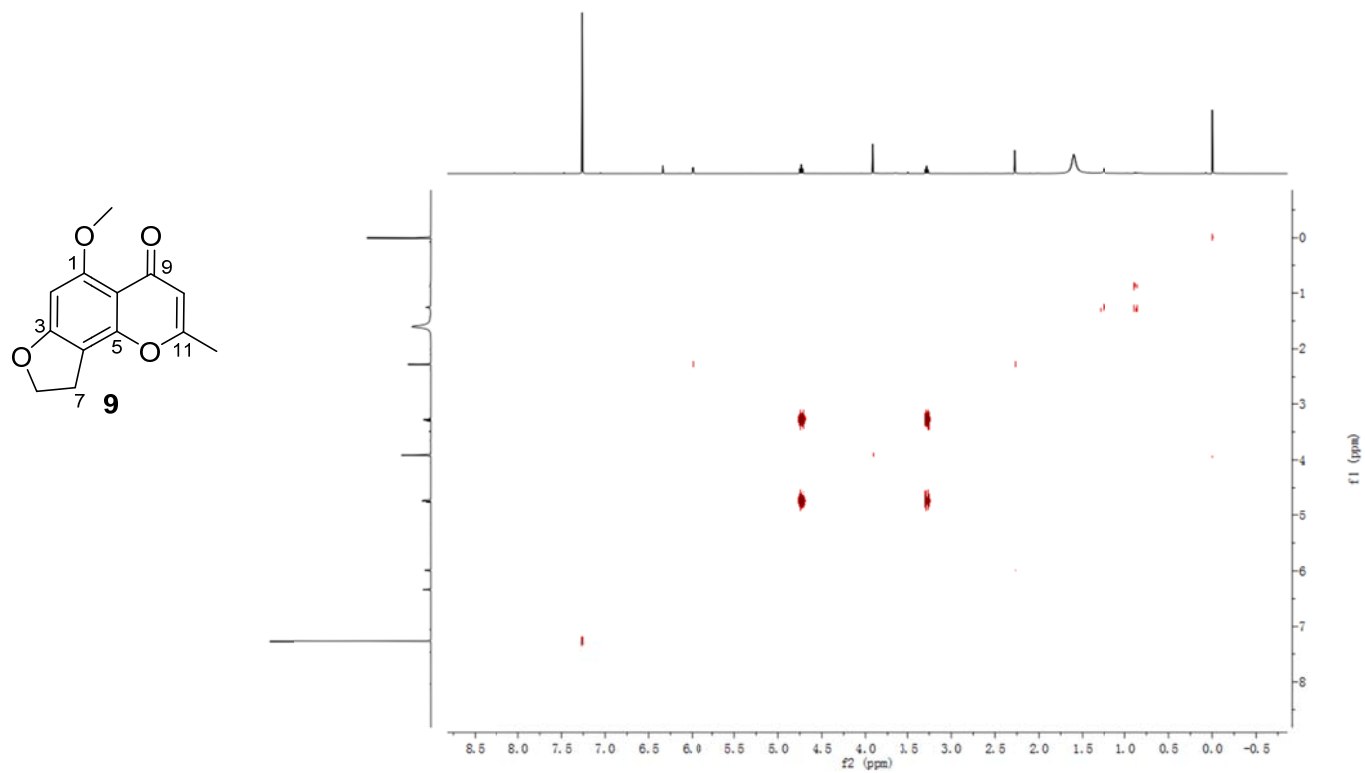


Figure S19. Spectroscopic data for **9**. (Continued)

(F) The HMBC (500MHz) spectrum of **9** in CDCl₃.

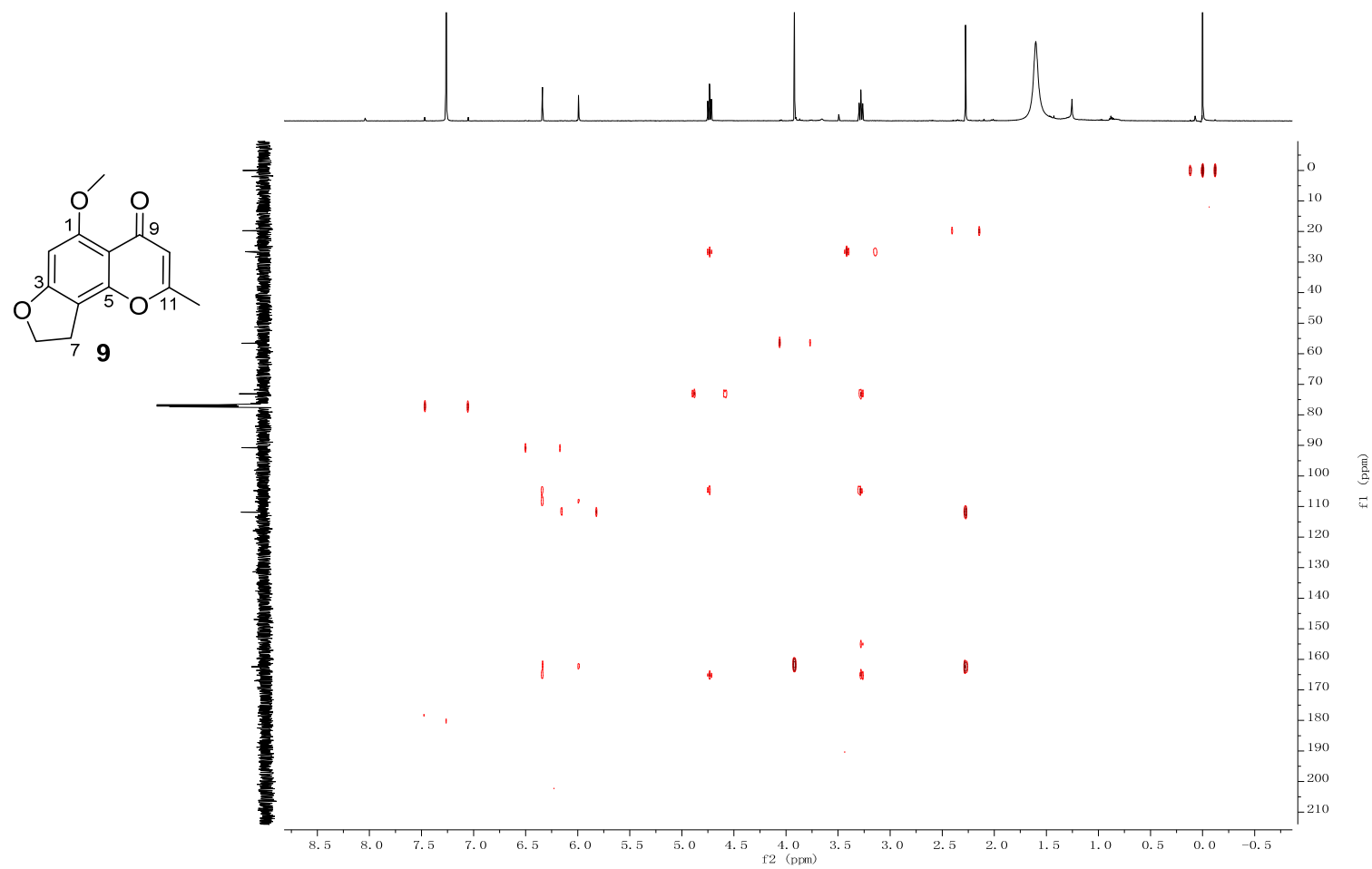
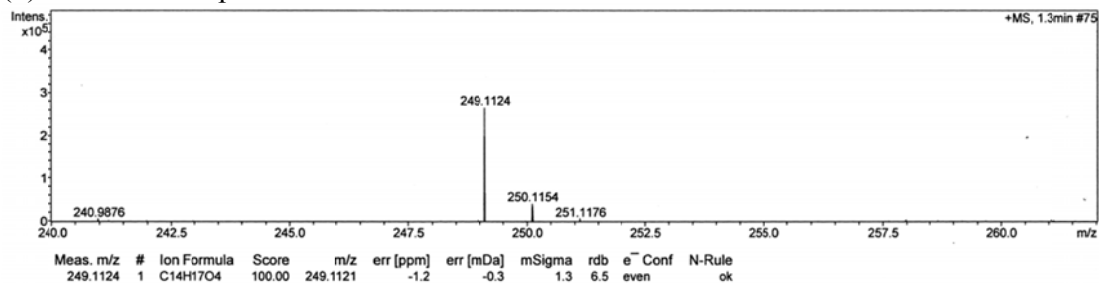


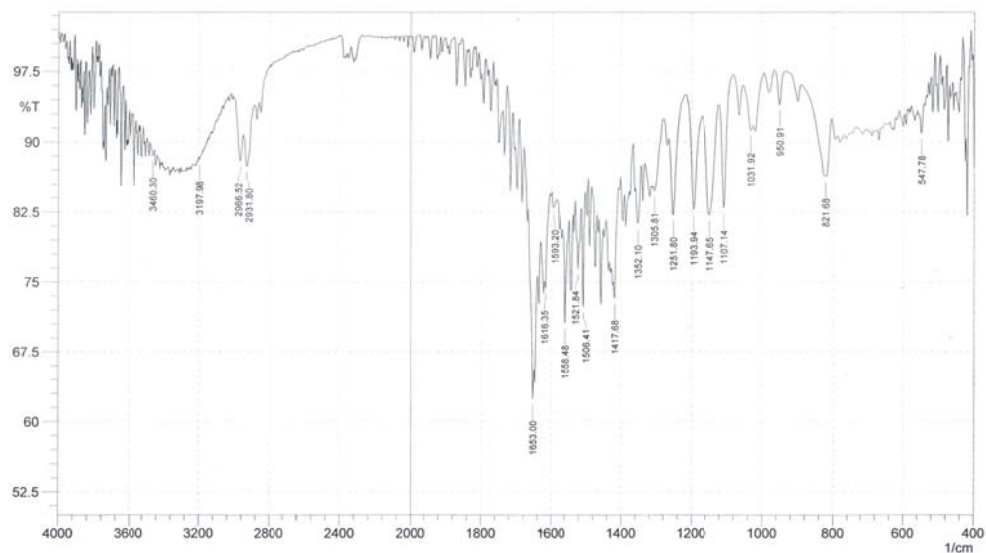
Figure S20. Spectroscopic data for **10** and **11**.

(A) HR-ESI-MS (a), IR (b), and UV (c) spectra of **10** and **11**.

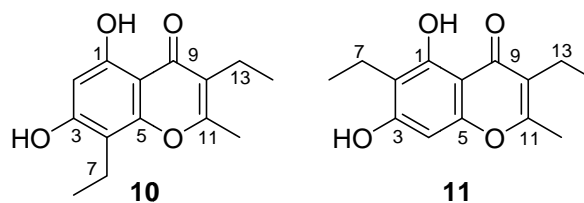
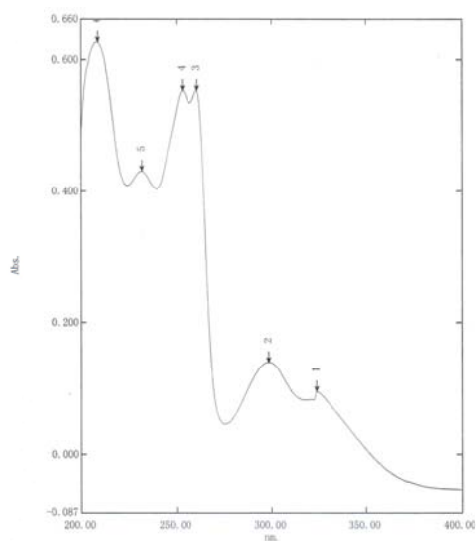
(a) HR-ESI-MS spectra of **10** and **11**.



(b) IR



(c) UV



Chemical Formula: C₁₄H₁₆O₄
Exact Mass: 248.10

Figure S20. Spectroscopic data for **10** and **11**.(Continued)

(B) The ^1H NMR spectrum of **10** and **11**.in methanol- d_4 .

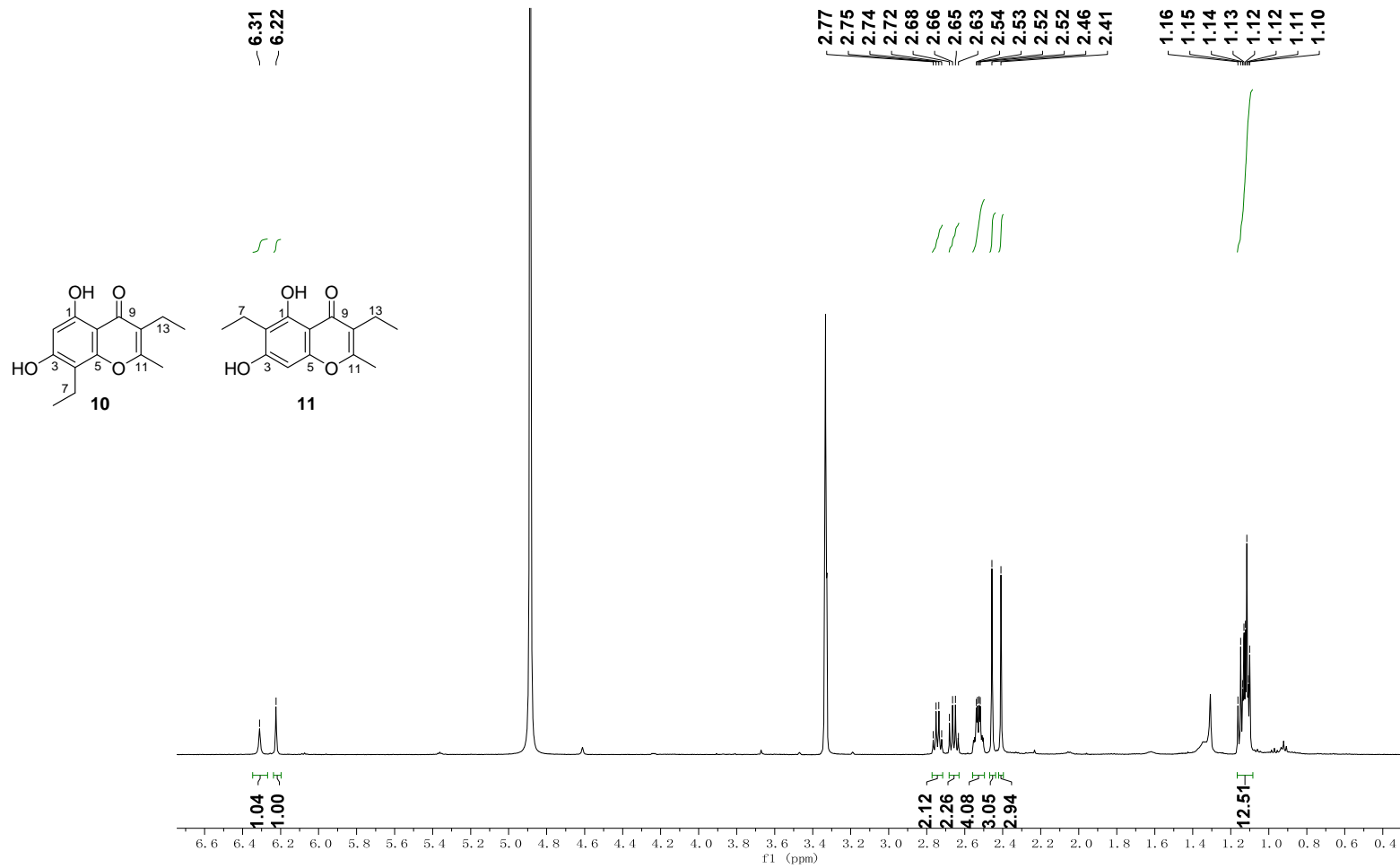


Figure S20. Spectroscopic data for **10** and **11**. (Continued)

(C) The ^{13}C NMR spectrum of **10** and **11** in methanol- d_4 .

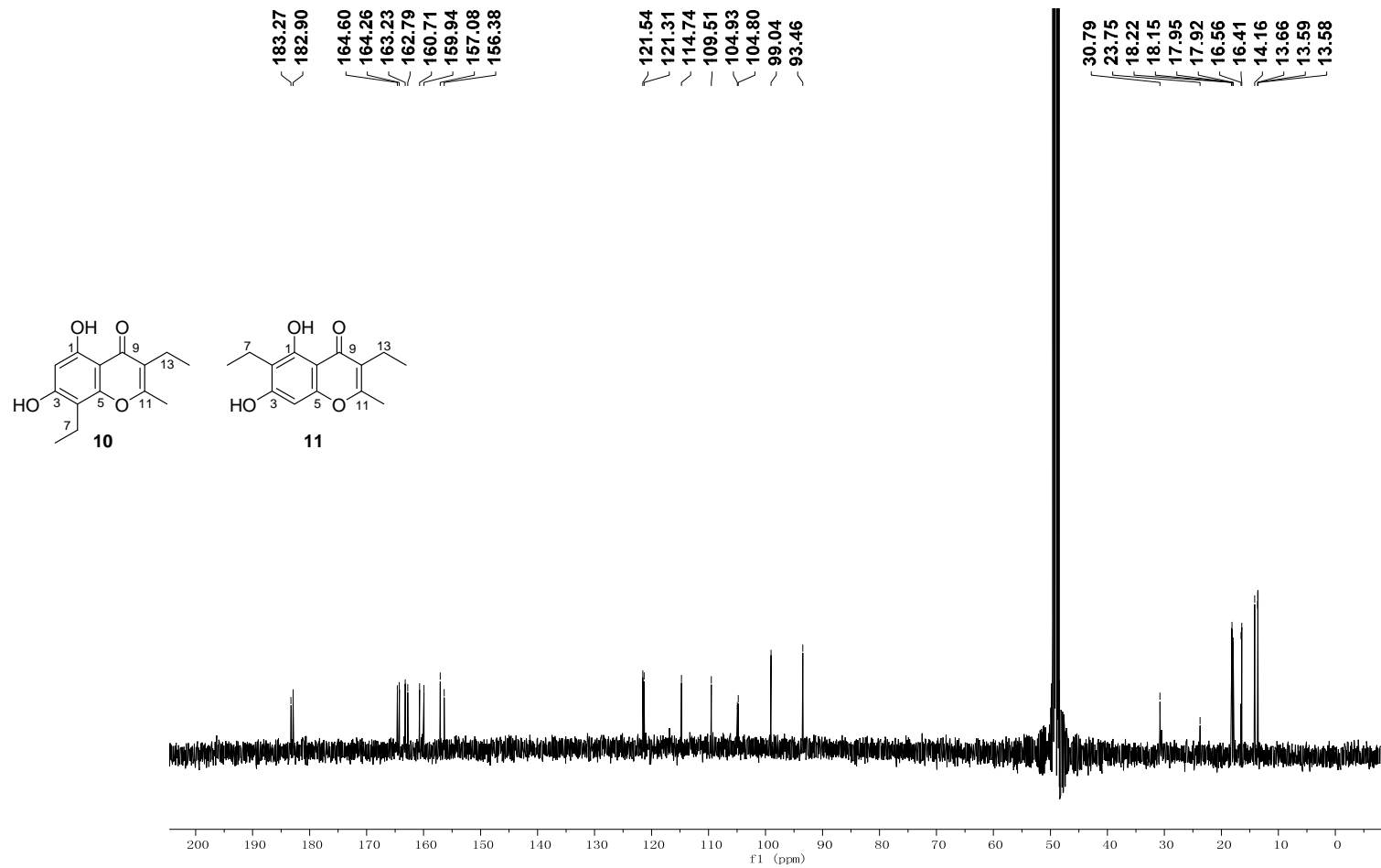


Figure S20. Spectroscopic data for **10** and **11**. (Continued)

(D) The HSQC spectrum of **10** and **11**. in methanol-*d*₄.

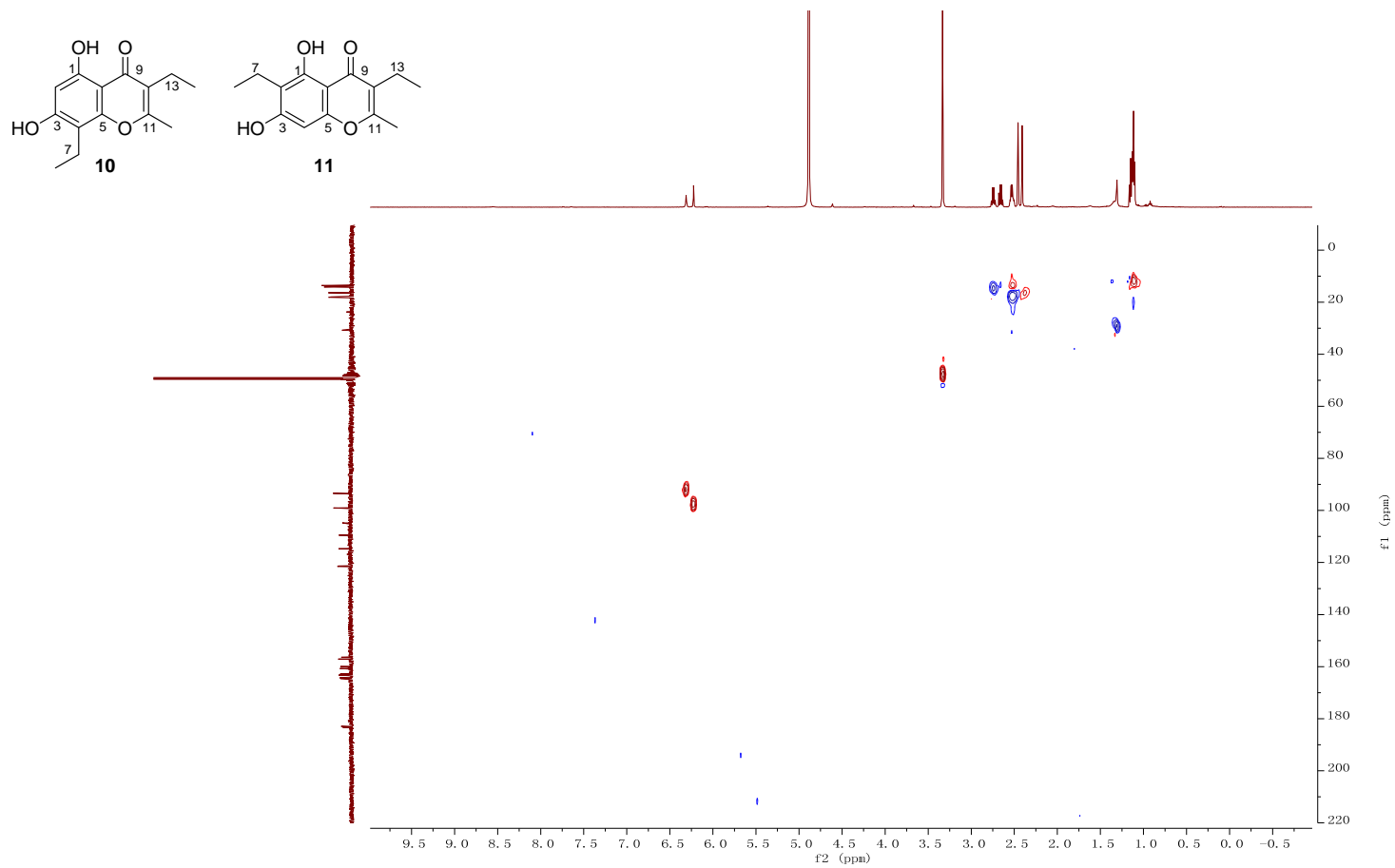


Figure S20. Spectroscopic data for **10** and **11**. (Continued)

(E) The COSY spectrum of **10** and **11**. in methanol-*d*₄.

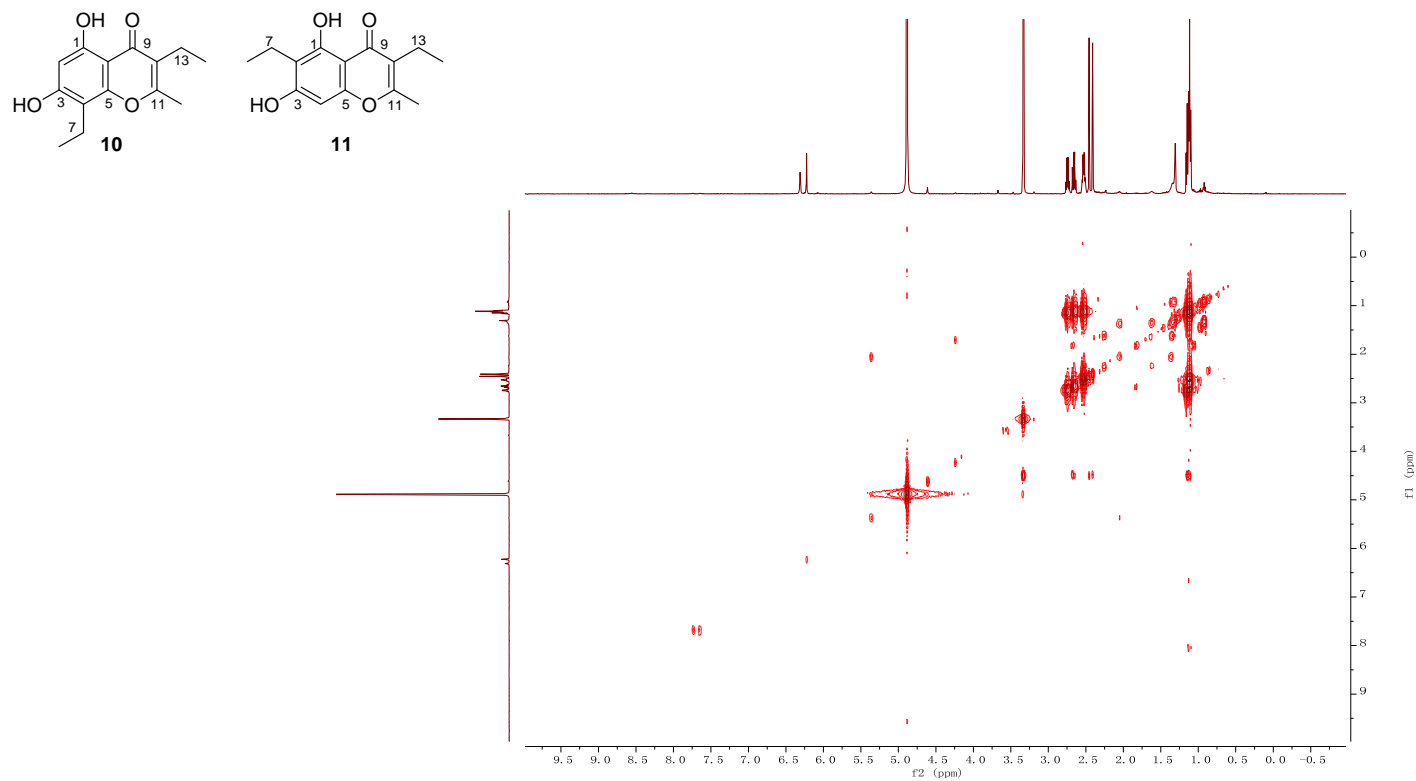


Figure S20. Spectroscopic data for **10** and **11**. (Continued)

(F) The HMBC spectrum of **10** and **11**. in methanol- d_4 .

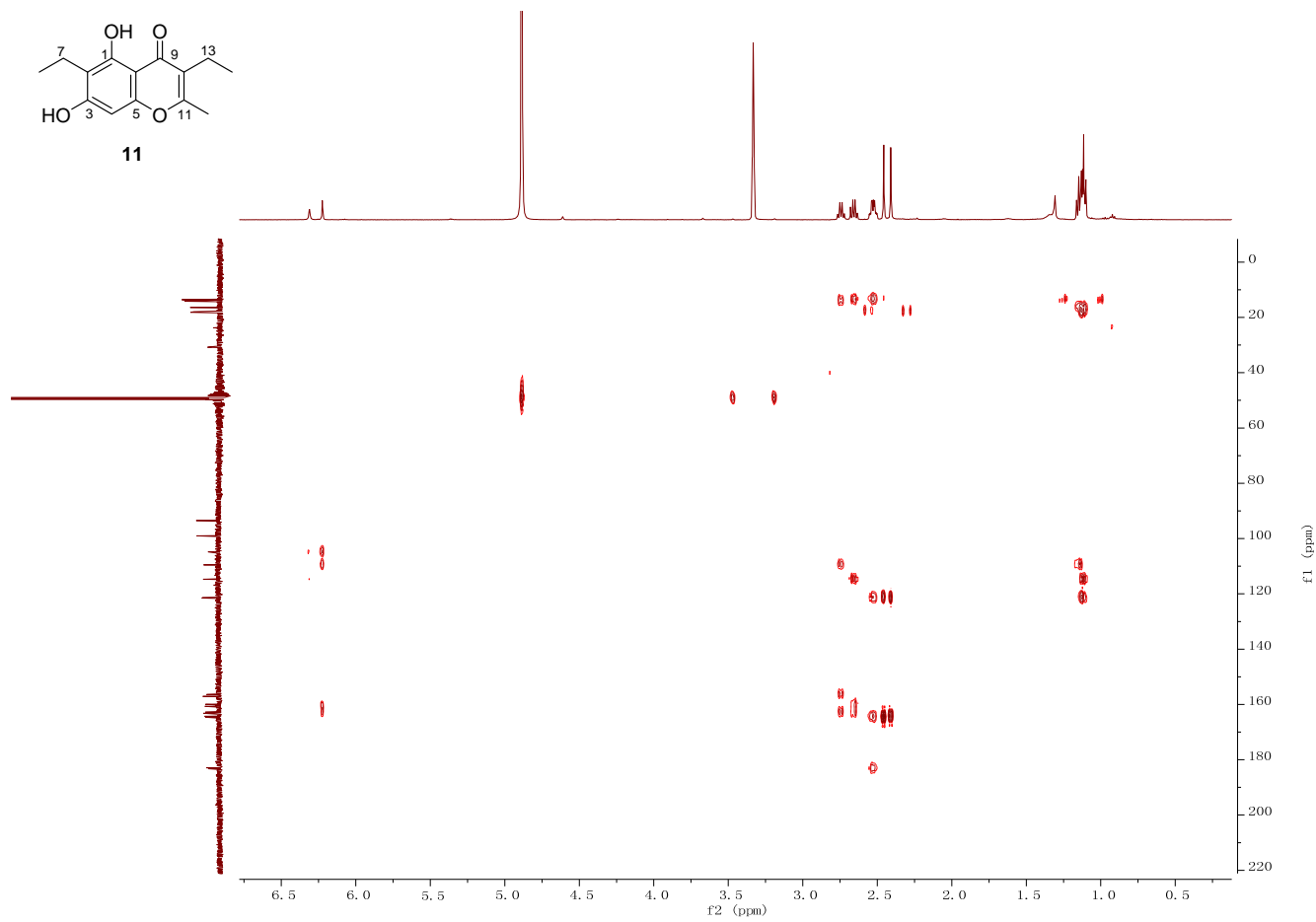
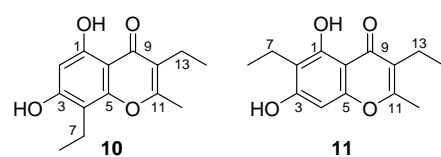
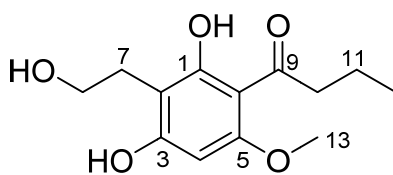
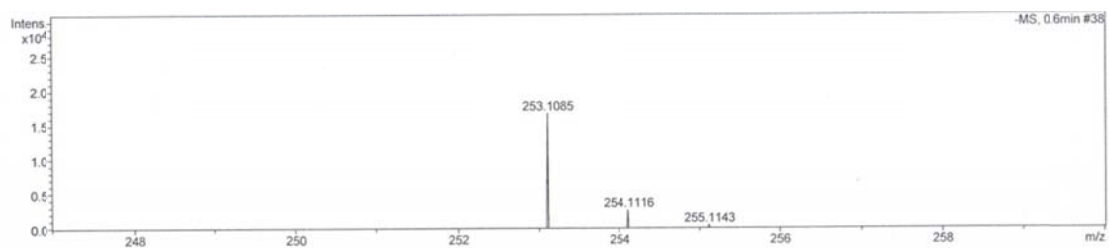


Figure S21. Spectroscopic data for **12**.

(A) HR-ESI-MS spectra of **12**.



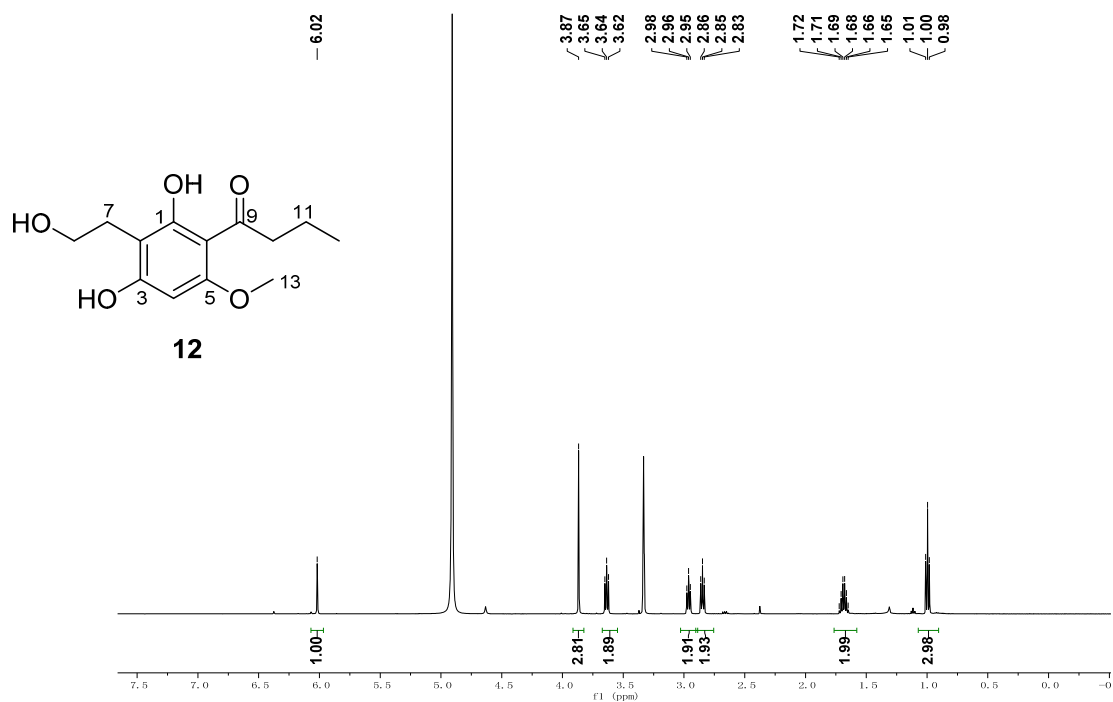
12

Chemical Formula: C₁₃H₁₈O₅

Exact Mass: 254.12

Figure S21. Spectroscopic data for **12** (Continued)

(B) The ^1H NMR spectrum of **12** in methanol- d_4 .



(C) The ^{13}C and spectrum of **12** in methanol- d_4 .

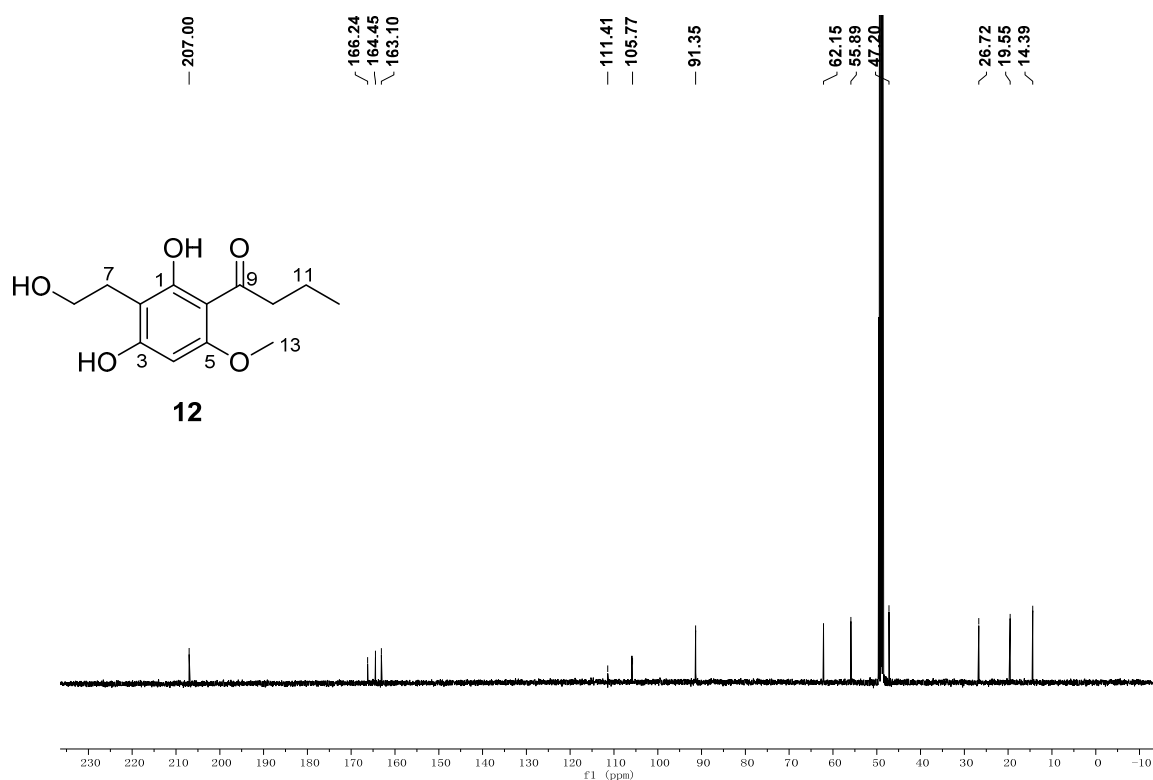
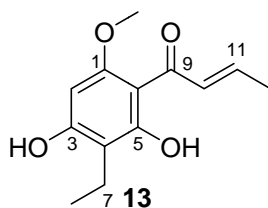
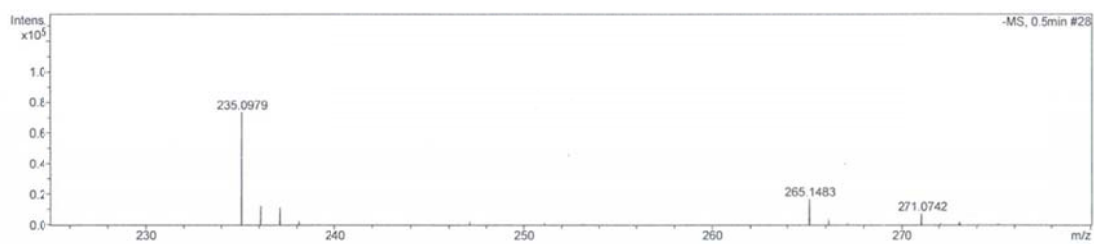


Figure S22. Spectroscopic data for **13**.

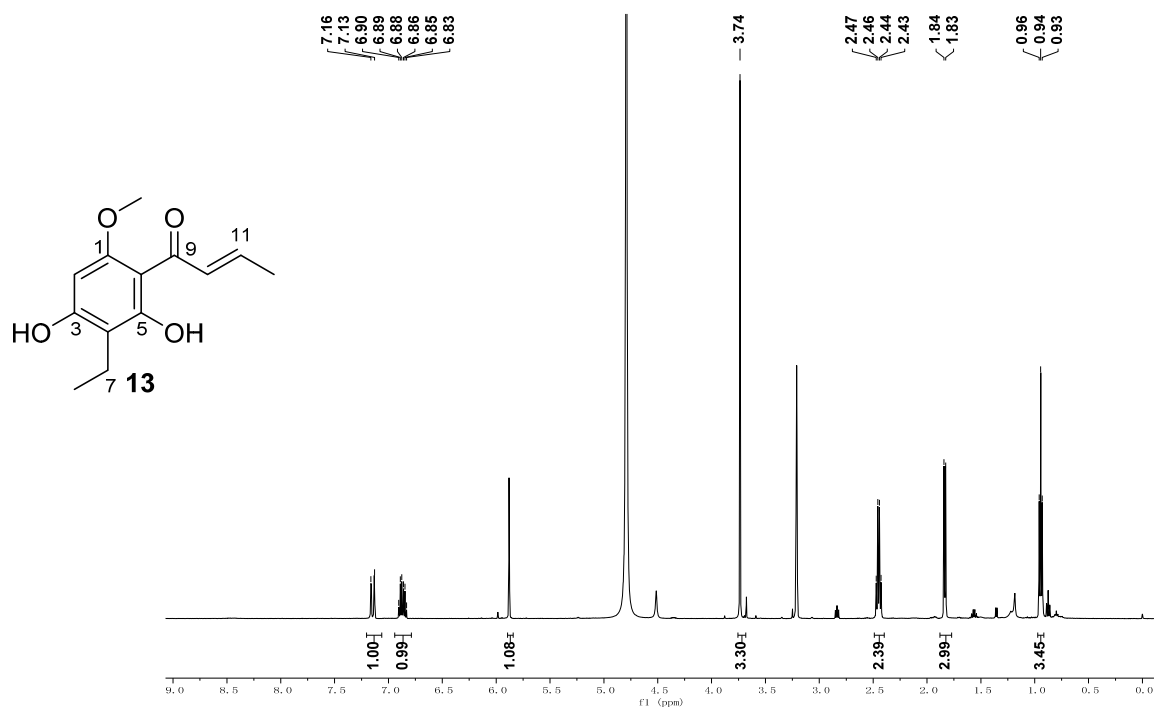
(A) HR-ESI-MS spectra of **13**.



Chemical Formula: $C_{13}H_{16}O_4$
Exact Mass: 236.10

Figure S22. Spectroscopic data for **13** (Continued)

(B) The ^1H NMR spectrum of **13** in methanol- d_4 .



(C) The ^{13}C spectrum of **13** in methanol- d_4 .

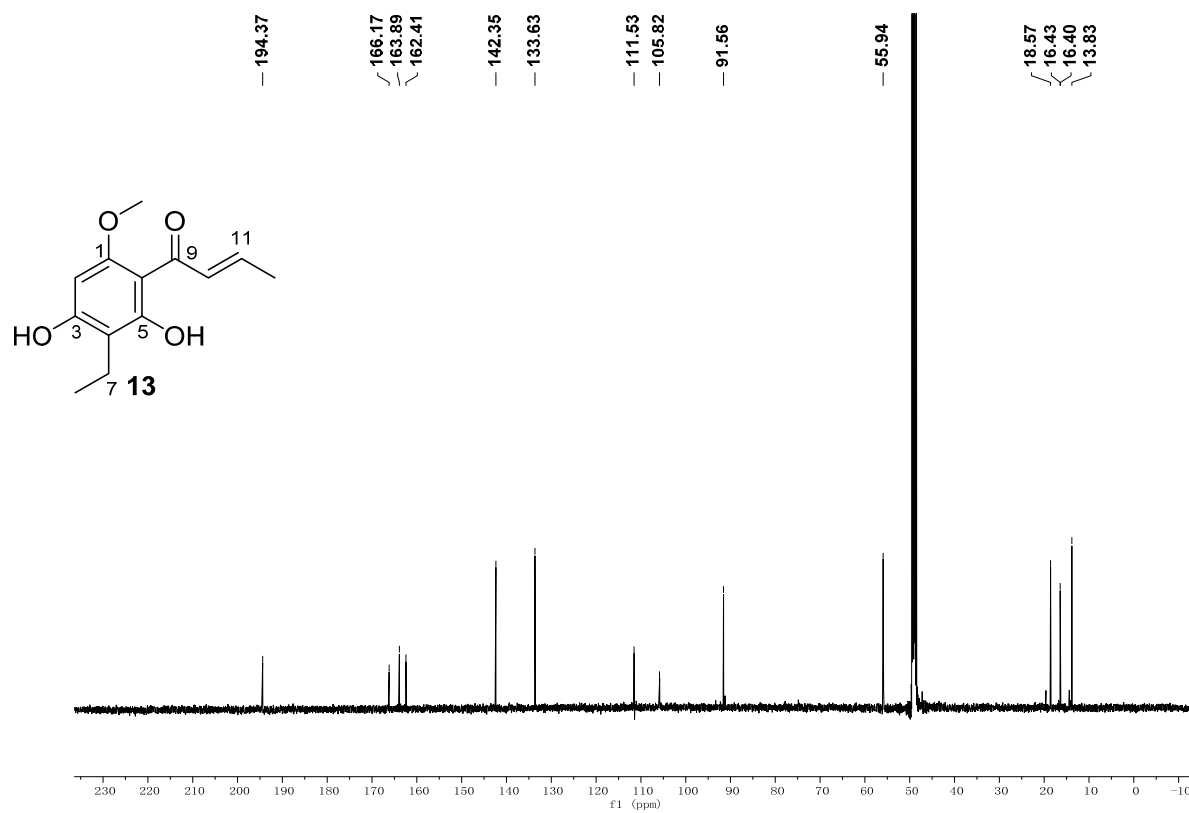
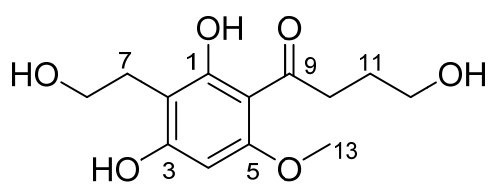
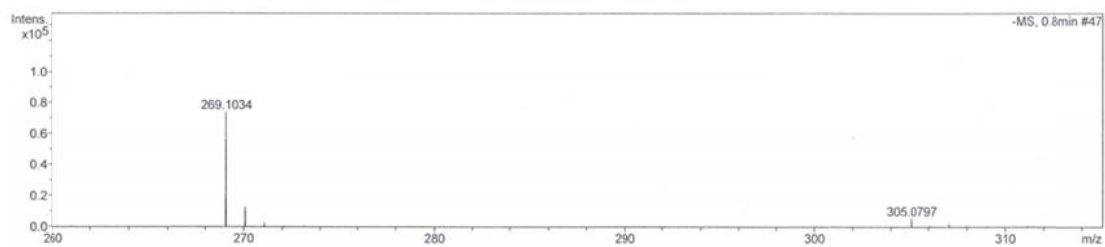


Figure S23. Spectroscopic data for **14**.

(A) HR-ESI-MS spectra of **14**.



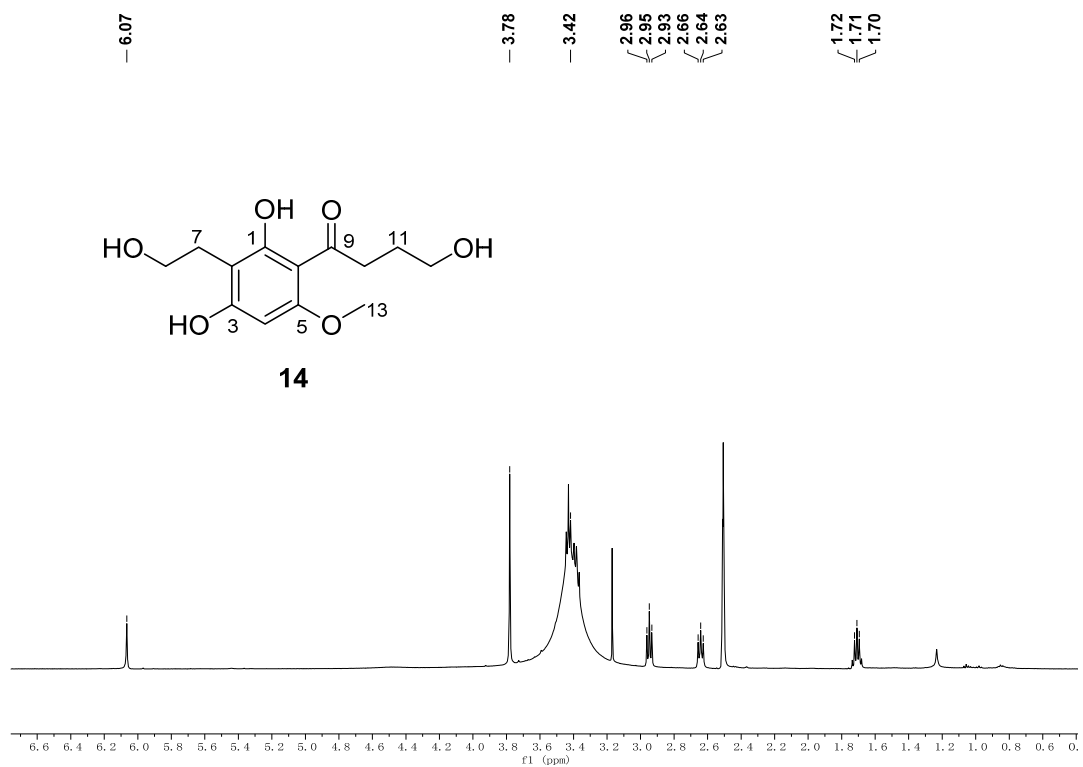
14

Chemical Formula: C₁₃H₁₈O₆

Exact Mass: 270.11

Figure S23. Spectroscopic data for **14** (Continued)

(B) The ^1H NMR spectrum of **14** in methanol- d_4 .

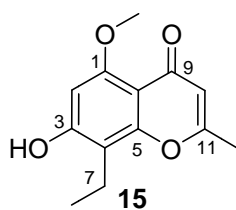
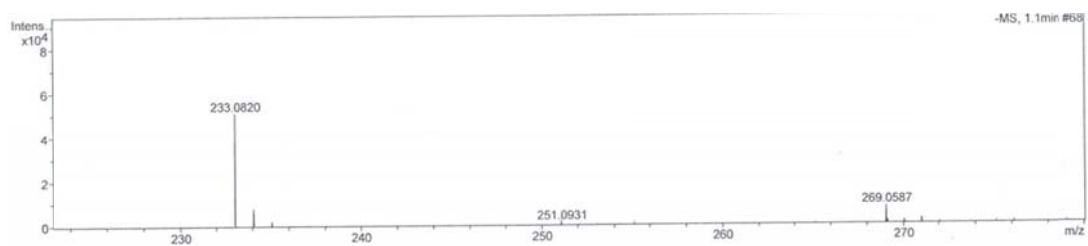


(C) The ^{13}C and spectrum of **14** in methanol- d_4 .



Figure S24. Spectroscopic data for **15**.

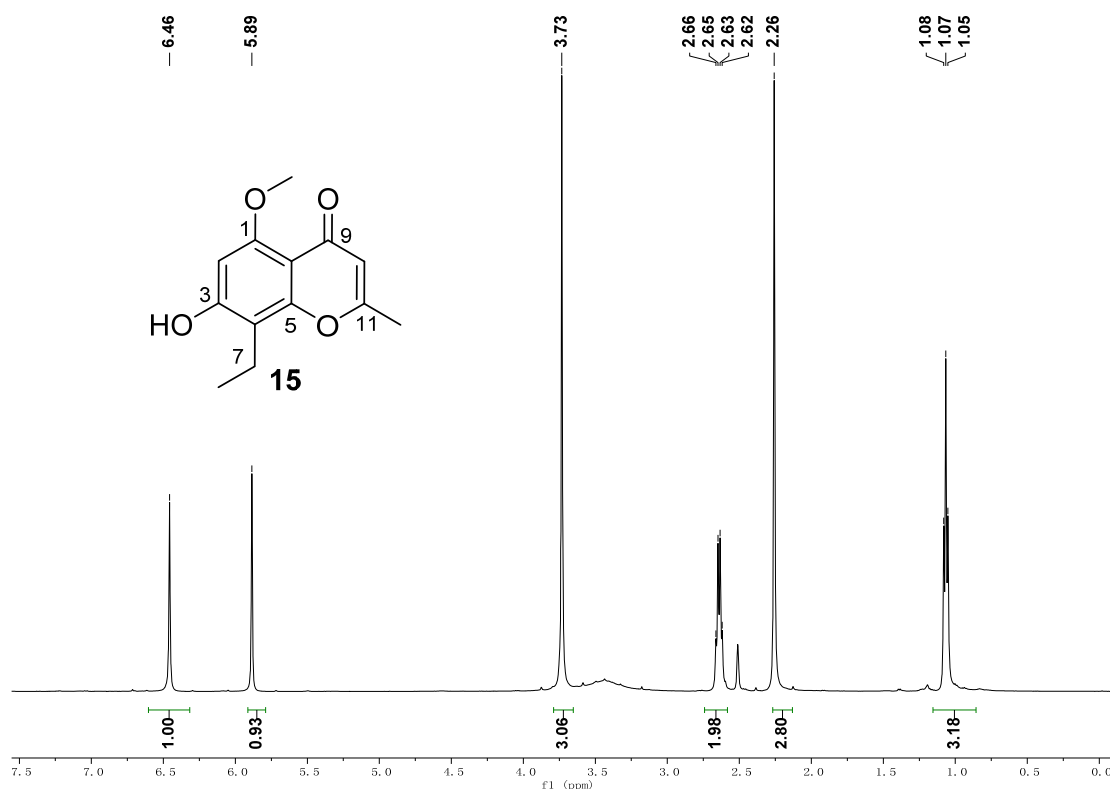
(A) HR-ESI-MS spectra of **15**.



Chemical Formula: C₁₃H₁₄O₄
Exact Mass: 234.09

Figure S24. Spectroscopic data for **15** (Continued)

(B) The ^1H NMR spectrum of **15** in methanol- d_4 .



(C) The ^{13}C and spectrum of **15** in methanol- d_4 .

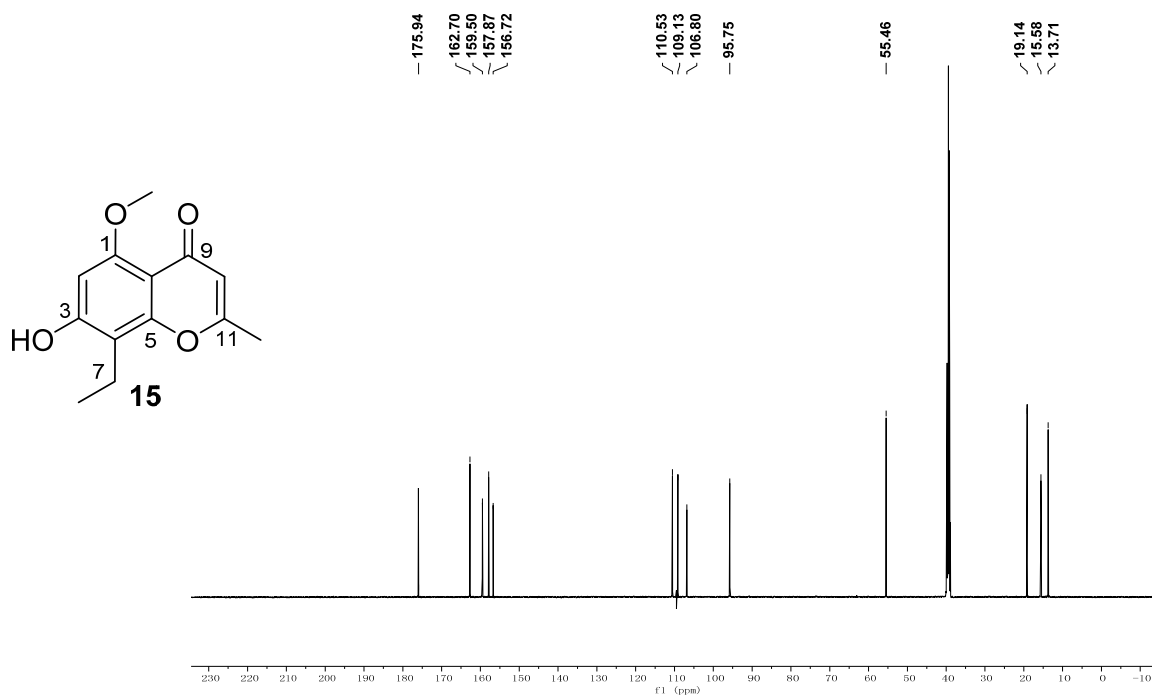
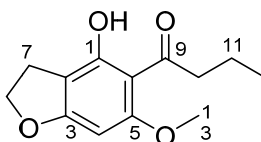
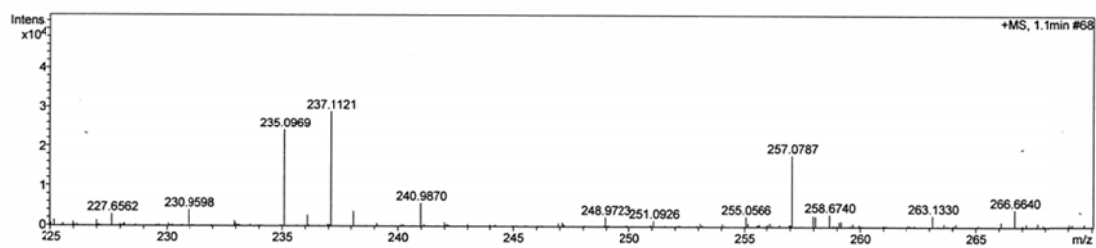


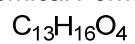
Figure S25. Spectroscopic data for **16**.

(A) HR-ESI-MS spectra of **16**.



16

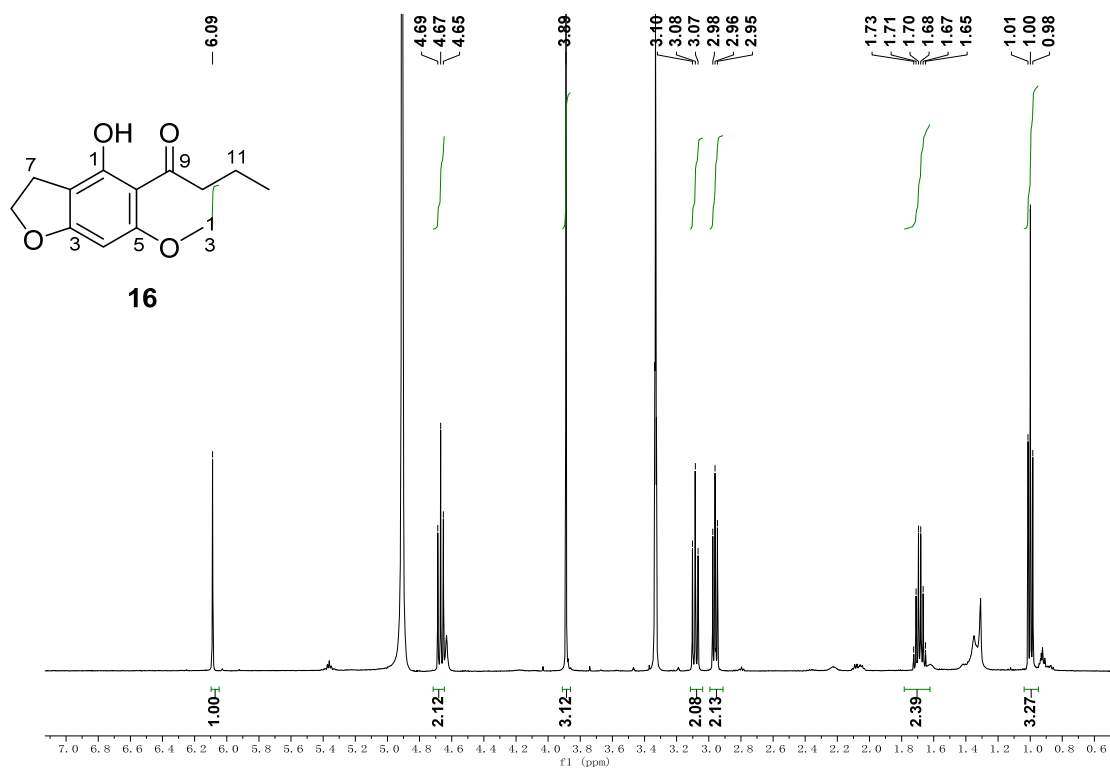
Chemical Formula:



Exact Mass: 236.10

Figure S25. Spectroscopic data for **16** (Continued)

(B) The ^1H NMR spectrum of **16** in methanol- d_4 .



(C) The ^{13}C spectrum of **16** in methanol- d_4 .

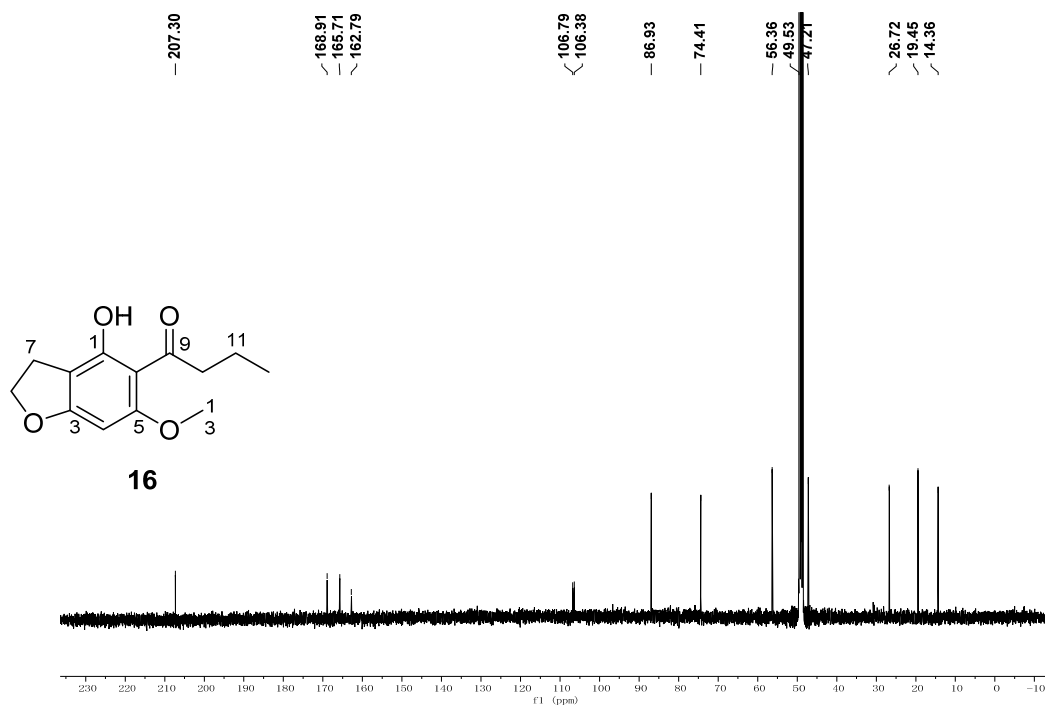
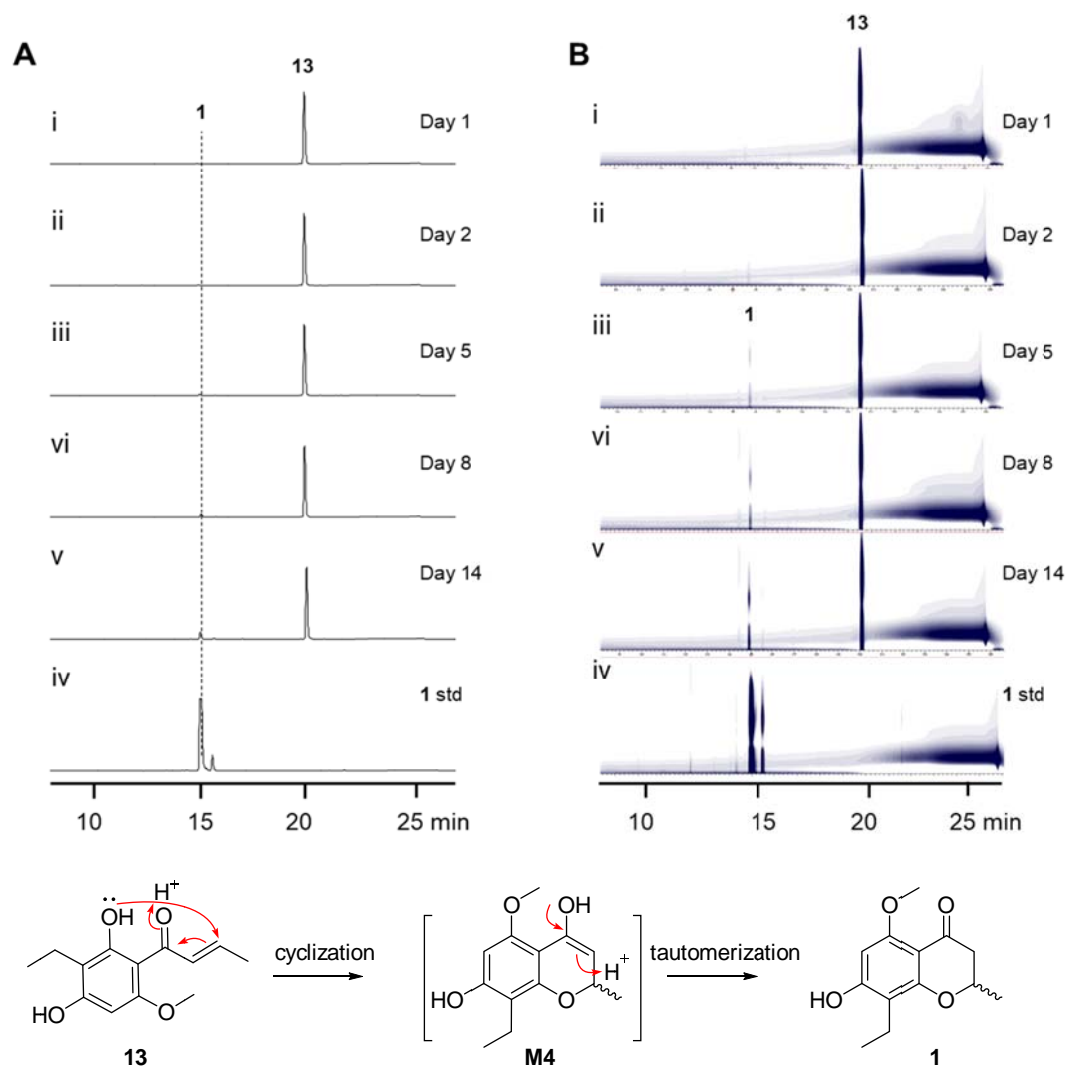


Figure S26. Spontaneous reaction observed from **13** to **1**.



HPLC analysis for determination the stability of **13** in DMSO. The sample was placed under room temperature for 14 days. UV absorptions at (A) 288 nm and (B) 200-400 nm are illustrated.

Reference

1. Y. Huang, X. Jiang, W. Liu, C. Huang, L. Zhang, H. Zhu, C. Zhang and W. Zhang, *Microbiol. Chin*, 2018, **45**, 1881-1888.
2. T. Bruhn, A. Schaumlöffel, Y. Hemberger and G. Bringmann, *Chirality*, 2013, **25**, 243-249.
3. C. Sun, Z. Liu, X. Zhu, Z. Fan, X. Huang, Q. Wu, X. Zheng, X. Qin, T. Zhang, H. Zhang, J. Ju and J. Ma, *J. Nat. Prod.*, 2020, **83**, 1646-1657.
4. Y. Xiao, S. Li, S. Niu, L. Ma, G. Zhang, H. Zhang, J. Ju and C. Zhang, *J Am Chem Soc*, 2011, **133**, 1092-1105.
5. W. A. Ayer and L. D. Jimenez, *Can. J. Chem.*, 1994, **72**, 2326-2332.
6. J. W. Kim, W. Ko, E. Kim, G. S. Kim, G. J. Hwang, S. Son, M.-H. Jeong, J.-S. Hur, H. Oh, S.-K. Ko, J.-H. Jang and J. S. Ahn, *J. Antibiot.* , 2018, **71**, 753-756.
7. C. Yang, S. Xiao, S. Yan, M. Zhang, Q. Cai, S. Fu and Q. Meng, *J. Chin. Chem. Soc*, 2019, **66**, 325-329.
8. W. A. Ayer and L. D. Jimenez, *Can. J. Chem*, 1994, **72**, 2326-2332.